

AD-A197 022

AFWAL-TR-86-2119

Volume II

DTIC FILE COPY

(2)



AN EFFICIENT METHOD FOR PREDICTING THE VIBRATORY
RESPONSE OF LINEAR STRUCTURES WITH FRICTION INTERFACES

VOLUME II - Steady-State Vibrations of a Two-Body
System with a Frictional Interface

Enrique Bazan-Zurita, Jacobo Bielak, and Jerry H. Griffin
Carnegie Institute of Technology
Carnegie Mellon University
Pittsburgh, Pennsylvania 15213

4 April 1988

Final Report for Period May 83 - October 86

Approved for public release; distribution unlimited.

AERO PROPULSION LABORATORY
AIR FORCE WRIGHT AERONAUTICAL LABORATORIES
AIR FORCE SYSTEMS COMMAND
WRIGHT-PATTERSON AIR FORCE BASE, OHIO 45433-6563

DTIC
ELECTE
S AUG 01 1988 D
aH

NOTICE

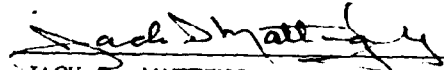
When Government drawings, specifications, or other data are used for any purpose other than in connection with a definitely Government-related procurement, the United States Government incurs no responsibility or any obligation whatsoever. The fact that the government may have formulated or in any way supplied the said drawings, specifications, or other data, is not to be regarded by implication, or otherwise in any manner construed, as licensing the holder, or any other person or corporation; or as conveying any rights or permission to manufacture, use, or sell any patented invention that may in any way be related thereto.

This report is releasable to the National Technical Information Service (NTIS). At NTIS, it will be available to the general public, including foreign nations.

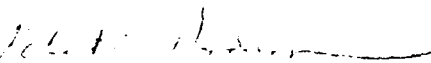
This technical report has been reviewed and is approved for publication.



WILLIAM A. STANGE
Project Engineer
Components Branch
Turbine Engine Division
FOR THE COMMANDER



JACK D. MATTINGLY, Lt Col, USAF
Chief, Components Branch
Turbine Engine Division



ROBERT E. HENDERSON
Deputy for Technology
Turbine Engine Division
Aero Propulsion Laboratory

If your address has changed, if you wish to be removed from our mailing list, or if the addressee is no longer employed by your organization please notify AFWAL/POTA WPAFB, OH 45433-6563 to help us maintain a current mailing list.

Copies of this report should not be returned unless return is required by security considerations, contractual obligations, or notice on a specific document.

UNCLASSIFIED

SECURITY CLASSIFICATION OF THIS PAGE

ADA197022

REPORT DOCUMENTATION PAGE					
1a. REPORT SECURITY CLASSIFICATION UNCLASSIFIED		1b. RESTRICTIVE MARKINGS			
2a. SECURITY CLASSIFICATION AUTHORITY		3. DISTRIBUTION/AVAILABILITY OF REPORT Approved for Public Release, distribution unlimited.			
2b. DECLASSIFICATION/DOWNGRADING SCHEDULE					
4. PERFORMING ORGANIZATION REPORT NUMBER(S) R-86-158, R-86-159, R-86-160		5. MONITORING ORGANIZATION REPORT NUMBER(S) AFWAL-TR-86-2119, Volume II			
6a. NAME OF PERFORMING ORGANIZATION Carnegie Mellon University	6b. OFFICE SYMBOL (If applicable)	7a. NAME OF MONITORING ORGANIZATION Aero Propulsion Laboratory (AFWAL/POTA) Air Force Wright Aeronautical Laboratories			
6c. ADDRESS (City, State and ZIP Code) Carnegie Mellon University Pittsburgh PA 15213		7b. ADDRESS (City, State and ZIP Code) AFWAL/POTA Wright-Patterson AFB OH 45433-6563			
8a. NAME OF FUNDING/SPONSORING ORGANIZATION	8b. OFFICE SYMBOL (If applicable)	9. PROCUREMENT INSTRUMENT IDENTIFICATION NUMBER F-33615-83-K-2316			
8c. ADDRESS (City, State and ZIP Code)		10. SOURCE OF FUNDING NOS.			
		PROGRAM ELEMENT NO.	PROJECT NO.	TASK NO.	WORK UNIT NO.
		61102F	2307	S2	12
11. TITLE (Include Security Classification) An efficient method for predicting the (OVER)					
12. PERSONAL AUTHOR(S) Bazan-Zurita, E., Bielak, J., and Griffin, J.H.					
13a. TYPE OF REPORT FINAL	13b. TIME COVERED FROM May 83 TO Oct 86	14. DATE OF REPORT (Yr., Mo., Day) 88 APRIL 04		15. PAGE COUNT 68	
16. SUPPLEMENTARY NOTATION					
17. COSATI CODES			18. SUBJECT TERMS (Continue on reverse if necessary and identify by block number)		
FIELD	GROUP	SUB. GR.			
19. ABSTRACT (Continue on reverse if necessary and identify by block number) In recent years it has become increasingly clear that friction damping in joints can affect significantly the dynamic response of structures with friction interfaces. In this report, we analyze the steady-state harmonic response of a system consisting of two spring masses connected by a Coulomb-type friction joint, as the simplest example of structures of this type. Two reasons motivate this work: (1) the simple system can serve as a basis for gaining physical insight into the behavior of more complex systems, and (2) inasmuch as this problem can be solved exactly, the solution can be used to assess the accuracy of approximate methods developed for more general systems. The differential equations governing the motion of the system during slip, partial-slip or stuck conditions of the joint are formulated in dimensionless form in order to identify the parameters controlling the dynamic response and to obtain results that are applicable to a large number of cases. An efficient analytical solution method (OVER)					
20. DISTRIBUTION/AVAILABILITY OF ABSTRACT UNCLASSIFIED/UNLIMITED <input checked="" type="checkbox"/> SAME AS RPT. <input type="checkbox"/> DTIC USERS <input type="checkbox"/>			21. ABSTRACT SECURITY CLASSIFICATION UNCLASSIFIED		
22a. NAME OF RESPONSIBLE INDIVIDUAL WILLIAM A. STANGE			22b. TELEPHONE NUMBER (Include Area Code) (513) 255-2081	22c. OFFICE SYMBOL AFWAL/POTA	

DD FORM 1473, 83 APR

EDITION OF 1 JAN 73 IS OBSOLETE.

UNCLASSIFIED

SECURITY CLASSIFICATION OF THIS PAGE

Key words: Gas TURBINE ENGINES. (JES) ←

UNCLASSIFIED

SECURITY CLASSIFICATION OF THIS PAGE

11. vibratory response of linear structures with friction interfaces. Volume II - Steady-State Vibrations of a Two-Body System with a Frictional Interface.
19. is then presented, in which the mathematical problem is reduced to a system of linear algebraic equations. Exact solutions for selected systems are obtained, and the role of various parameters in the dynamic behavior of the system is examined in light of these results. In particular, the determination of optimum design values for the joint parameters is illustrated.

An approximate method of solution also is presented; it is based on the assumption that only the first Fourier component of the friction force in the joint has a significant contribution on system response. This method constitutes a complex variable generalized version of the harmonic balance method, that requires only the solution of a real quadratic equation for the relative displacements. The method provides, as well, a criterion for determining the slip-to-stuck transition in the joint as a function of force excitation. The advantages and limitations of the method are assessed by comparing a large number of exact and approximate solutions. From this comparison, several modifications are proposed to improve the accuracy of the approximate method for the case of partial slipping in the joint. The possibility of extending the various approaches to more complex structures also is discussed.

UNCLASSIFIED

SECURITY CLASSIFICATION OF THIS PAGE

ACKNOWLEDGEMENTS

This work was supported by the Aero Propulsion Laboratory, Wright-Patterson Air Force Base, Contract No. F33615-K-2316, under the direction of Dr. James C. MacBain and Mr. William Stange.

Table of Contents

1. Introduction	1
2. Equations of Motion	2
3. Exact Analytical Solution	4
3.1 One Slip-to-Stuck Change in a Semiperiod	4
3.2 Friction Joint Always Sliding	8
3.3 Some Limiting Cases	9
3.4 Numerical Integration	10
3.5 Numerical Results	10
4. Approximate Methods of Solution	13
4.1 Harmonic Balance Method	13
4.2 Modified Harmonic Balance Methods	16
5. Comparison of Results of Different Methods	19
6. Concluding Remarks	20
Appendix A - Definition of Algebraic Functions	65
Appendix B - Derivation of Equations 22 to 24	68



Accession For					
NTIS GRA&I	<input checked="" type="checkbox"/>				
DTIC TAB	<input type="checkbox"/>				
Unannounced	<input type="checkbox"/>				
Justification					
By _____					
Distribution/					
Availability Codes					
Dist	<table style="width: 100%; border-collapse: collapse;"> <tr> <td style="width: 50%; padding: 2px;">Avail and/or</td> <td style="width: 50%; padding: 2px;">Special</td> </tr> <tr> <td style="height: 40px; vertical-align: bottom; padding: 2px;">A-1</td> <td style="height: 40px; vertical-align: bottom; padding: 2px;"></td> </tr> </table>	Avail and/or	Special	A-1	
Avail and/or	Special				
A-1					

1 INTRODUCTION

One of the most important considerations in the design of components of gas turbine engines is the reduction of the amplitudes of steady-state vibrations of some components of the engine during operation. Large repetitions of high-amplitude vibrations can result in catastrophic fatigue failures of such components. This problem has become more critical with the current tendency to design engines to avoid material inelastic behavior, because this practice produces also a significant reduction of the amount of energy dissipated by means of viscous or hysteretic damping. Therefore, to keep the vibration amplitudes within acceptable limits, the designers of gas turbine engines are using alternative sources of energy dissipation. The most widely accepted solution is the inclusion of especially designed friction interfaces, which have shown good performance in laboratory tests as well as in airplane operation.

The study of steady-state vibrations of structures with so-called frictional dampers has attracted the attention of many researchers. The first analytical solution for a single-degree-of-freedom system with a Coulomb frictional joint was presented by Den Hartog in 1931 [1,2]. The most relevant contributions until 1979 are discussed by Plunkett [3]. More recently, further analytical and experimental research has been reported by, among others Griffin and coworkers, [4,5,6] Muzynska et al, [7] Srinivasan et al, [8] Dominic et al, [9] and Soni and Bogner [10].

Most analytical studies are limited to cases with only one friction joint, mainly due to the difficulties of solving the nonlinear differential equations which result from the mathematical models. The available mathematical models and methods of solution cannot be easily extended to problems with several friction joints, and their results do not explain completely all the experimentally observed phenomena. For these reasons, a more efficient and rational utilization of friction dampers still requires additional experimental and analytical research.

This report is the result of initial work aiming at the development of a simple, approximate, yet accurate, methodology to study the steady-state response of multi-degree-of-freedom structures containing friction interfaces, but which are otherwise linear. As a first step in pursuing this goal we consider the steady-state vibrations of the two-body system shown in Fig. 1, which is the simplest case of linear substructures connected by friction joints. The springs and the dampers are considered to be linear, and the friction joint connecting the bodies is of Coulomb type.

In studying this problem our main objectives are: a) to find an exact analytical solution; b) to assess the accuracy and applicability of some approximate methods of solution; and c) to understand the role of the friction joint in the dynamic behavior of the system.

The first part of the report deals with the formulation of the differential equations governing the motion of the system. Then, an exact analytical method of solution for these equations is presented. Exact results for selected systems are included, to understand the role of different parameters in the steady-state response.

In a subsequent section a complex variable version of the harmonic balance method to obtain approximate solutions is presented. The advantages and limitations of this solution method are discussed. In particular, some modifications to improve the accuracy of the method when the joint is only partially sliding are proposed.

Selected numerical results are obtained to compare exact and approximate solutions. The possibility of extending the different mathematical models and methods to more general problems is also examined.

2 EQUATIONS OF MOTION

The system under study is depicted in Fig. 1. M_1 and M_2 are the masses of the bodies; K_1 and K_2 are the stiffnesses of the linear springs; C_1 and C_2 are the constants of the viscous (or if it is the case, structural) dampers; μ and N are the friction coefficient and the constant normal force in the Coulomb friction joint. The forces applied on M_1 and M_2 are harmonic with the same frequency W and with amplitudes Q_1 and Q_2 , respectively; β is a prescribed phase angle of the second force with respect to the first one.

We will first formulate the equations of motion of the system for the two possible states of the friction joint (slipping and stuck), and the mathematical representation of the conditions producing changes from one to the other.

Let X_1 and X_2 be the displacements of the corresponding masses, and F the tangential force in the joint. Then, Newton's second law yields the following equations of motion for the masses:

$$M_1 \ddot{X}_1 + C_1 \dot{X}_1 + K_1 X_1 = Q_1 \cos WT - F \quad (1)$$

$$M_2 \ddot{X}_2 + C_2 \dot{X}_2 + K_2 X_2 = Q_2 \cos(WT + \beta) + F \quad (2)$$

where dots denote derivatives with respect to time.

When the joint is sliding, F must satisfy the following conditions:

- a) $|F| = \mu N$
- b) Its sign is opposite to that of the relative velocity, $\dot{X}_1 - \dot{X}_2$.

These conditions reflect the nonlinear nature of the problem, because both X_1 and X_2 depend on F , which, in turn, depends on their derivatives.

In order to identify the parameters governing the dynamic response of the system and to obtain results applicable to a wider range of cases, it is convenient to express the above equations in a dimensionless form.

For this purpose, define the following constants:

$$\begin{aligned}
 m &= M_2/(M_1 + M_2) \\
 k &= K_2/(K_1 + K_2) \\
 T_0 &= [(M_1 + M_2)/(K_1 + K_2)]^{1/2} \\
 \omega &= WT_0 \\
 X_s &= Q_1/(K_1 + K_2) \\
 f &= F/Q_1 \\
 f_0 &= \mu N/Q_1 \\
 \zeta_j &= C_j/[2 (K_j M_j)^{1/2}] \quad , j = 1, 2 \\
 \Omega_j &= (K_j / M_j)^{1/2} \quad , j = 1, 2 \\
 \alpha &= Q_2/Q_1
 \end{aligned} \tag{3}$$

and the following dimensionless variables:

$$\begin{aligned}
 x_j &= X_j/X_s \quad , j = 1, 2 \\
 t &= T/T_0
 \end{aligned} \tag{4}$$

With the above definitions simple algebraic manipulations transform (1) and (2) into

$$(1-m) \ddot{x}_1 + 2\zeta_1\Omega_1\dot{x}_1 + (1-k) x_1 = -f_0 + \cos\omega t \tag{5}$$

$$m \ddot{x}_2 + 2\zeta_2\Omega_2\dot{x}_2 + k x_2 = f_0 + \alpha\cos(\omega t + \beta) \tag{6}$$

These are the nondimensional equations for the system of Fig. 1. The conditions to be fulfilled by the force f when the joint is sliding become

$$|f| = f_0$$

$$\text{sign}(f) = -\text{sign}(\dot{x}_1 - \dot{x}_2)$$

When the joint is stuck the difference between the displacements of the masses is equal to some constant value d , i. e.

$$x_1 = x_2 + d \tag{7}$$

As a consequence, the time derivatives of x_1 and x_2 are the same and equations (5) and (6) reduce to

$$x_1 + 2(\zeta_1\Omega_1 + \zeta_2\Omega_2)\dot{x}_1 + x_1 = \cos(\omega t) + \alpha\cos(\omega t + \beta) + kd \tag{8}$$

This equation holds while the amplitude of the tangential force in the joint remains below f_0 .

3 EXACT ANALYTICAL SOLUTION

Exact analytical solutions for the differential equations of motion are desirable because they describe all the characteristics of the system response. Hence, the significance of all the physical parameters can be precisely determined. This eventually will provide a basis for proposing approximate methods of solution and also the means to assess the accuracy and limitations of those methods.

In our case, the difficulties to obtain analytical solutions arise from the fact that it is necessary to know at any time whether the friction joint is stuck or sliding in order to use the corresponding equation of motion. However, this information is part of the solution rather than part of the data. In general, an unknown number of incursions in both conditions can take place in a semiperiod of vibration.

In the analytical method presented in this section it is assumed that the joint is either always sliding or it only experiences one slip-to-stuck change during a semiperiod. The first step of the method is to obtain solutions of the equations of motion as algebraic expressions with unknown constant coefficients, for both the slipping and the stuck states of the joint. Then, to calculate those coefficients, two types of conditions are imposed: a) continuity conditions of displacements and velocities when the joint passes from a sliding situation to a stuck one, and b) periodicity conditions relating the values of the response at the beginning and at the end of a semiperiod. By taking advantage of the form of the resulting equations, the mathematical problem is eventually reduced to the solution of a system of algebraic linear equations.

3.1 One Slip-to-Stuck Change in a Semiperiod.

Without any loss of generality we can define the initial time, $t = 0$, as exactly the instant at which the joint passes from a stuck to a sliding condition, i. e., the instant at which f reaches the value f_0 . This definition implies the introduction of an unknown phase angle, ϕ , in the terms describing the excitation forces in the equations of motion, to take into account that such forces are not known at this initial time. Hence, in equations (5), (6) and (8), $\cos(\omega t)$ and $\cos(\omega t + \beta)$ must be replaced by $\cos(\omega t + \phi)$ and $\cos(\omega t + \beta + \phi)$, respectively; only in some very particular cases will ϕ be zero.

The tangential force f while the joint is sliding is equal to the constant value f_0 . Under this condition equations (6) and (7) are linear, and their solutions are

$$x_1(t) = A_1 f_1(t) + A_2 f_2(t) + g_1(t, \phi) - f_0/(1-m) \quad (9)$$

$$x_2(t) = A_3 f_3(t) + A_4 f_4(t) + g_2(t, \phi) + f_0/m \quad (10)$$

where A_j ($j=1,2,3,4$) are unknown constants, $f_j(t)$ ($j=1,2,3,4$) are known functions of time depending on the system parameters m , k , ζ_1 and ζ_2 , and $g_j(t, \phi)$ ($j=1,2$) are known harmonic functions of time depending on the mentioned parameters and those defining the excitation (α , β , and ω). Functions $f_j(t)$ represent the

complementary solutions of the equations, and functions $g_j(t, \phi)$ are the particular solutions due the harmonic excitation. All of them are given in Appendix A.

Differentiation of (9) and (10) with respect to time yields the following expressions for the velocities:

$$\dot{x}_1(t) = A_1 \dot{f}_1(t) + A_2 \dot{f}_2(t) + \dot{g}_1(t, \phi) \quad (11)$$

$$\dot{x}_2(t) = A_3 \dot{f}_3(t) + A_4 \dot{f}_4(t) + \dot{g}_2(t, \phi) \quad (12)$$

The first condition to be satisfied by this solution is that at $t = 0$ the relative velocity between the two bodies $\dot{x}_1(0) - \dot{x}_2(0)$ is zero, in agreement with the definition that $t = 0$ is the time at which the joint is passing from a stuck to a sliding condition. Hence,

$$A_1 \dot{f}_1(0) + A_2 \dot{f}_2(0) - A_3 \dot{f}_3(0) - A_4 \dot{f}_4(0) = \dot{g}_1(0, \phi) - \dot{g}_2(0, \phi) \quad (13)$$

Simple algebraic operations yield

$$b_{11}A_1 + b_{12}A_2 + b_{13}A_3 + b_{14}A_4 = p_1 \sin \phi + q_1 \cos \phi \quad (14)$$

The coefficients b_{ij} , p_1 and q_1 are defined in Appendix A. Note that these are time independent quantities.

We will now assume that the joint remains sliding during some time interval $t_1 > 0$ at the end of which the relative velocity becomes zero again and the joint returns to a stuck state. This is expressed by

$$A_1 \dot{f}_1(t_1) + A_2 \dot{f}_2(t_1) - A_3 \dot{f}_3(t_1) - A_4 \dot{f}_4(t_1) = \dot{g}_1(t_1, \phi) - \dot{g}_2(t_1, \phi) \quad (15)$$

that can be also written in the form:

$$b_{21}A_1 + b_{22}A_2 + b_{23}A_3 + b_{24}A_4 = p_2 \sin \phi + q_2 \cos \phi \quad (16)$$

In addition, we assume that between t_1 and the end of the semiperiod t_2 ($t_2 = \pi/\omega$) the joint remains stuck. During this second time interval the motion of the system is described by the linear ordinary differential equation (8), whose solution is

$$x_1(t) = E_1 f_5(t) + E_2 f_6(t) + g_3(t, \phi) + kd \quad (17)$$

As before, $f_5(t)$ and $f_6(t)$ are known complementary solutions of the differential equation which depend on the system parameters, and $g_3(t, \phi)$ is the particular solution due to the harmonic external forces which is determined by both the system and the excitation parameters. These functions are also described in Appendix A.

The expression for the common velocity of the two bodies is now

$$\dot{x}_1(t) = E_1 \dot{f}_5(t) + E_2 \dot{f}_6(t) + \dot{g}_3(t, \phi) \quad (18)$$

The constants d , E_1 and E_2 can be found from the continuity conditions of the displacements and velocities at $t = t_1$, which require these quantities to have respectively the same values just before and just after t_1 . In the

case of $x_1(t)$, replacing t by t_1 into (9) and (17) and equating the results we obtain

$$E_1 f_5(t_1) + E_2 f_6(t_1) + g_3(t_1, \phi) + kd = A_1 f_1(t_1) + A_2 f_2(t_1) + g_1(t_1, \phi) - f_0/(1-m) \quad (19)$$

Similarly, for $x_2(t)$, from (7), (12) and (17) we have

$$E_1 f_5(t_1) + E_2 f_6(t_1) + g_3(t_1, \phi) + kd - d = A_3 f_3(t_1) + A_4 f_4(t_1) + g_2(t_1, \phi) + f_0/m \quad (20)$$

and for $\dot{x}_1(t)$,

$$E_1 \dot{f}_5(t_1) + E_2 \dot{f}_6(t_1) + \dot{g}_3(t_1, \phi) = A_2 \dot{f}_1(t_1) + A_2 \dot{f}_2(t_1) + \dot{g}_1(t_1, \phi) \quad (21)$$

The continuity condition for $x_2(t)$ is automatically satisfied by imposing it to $x_1(t)$, since t_1 is, by definition, a time at which both velocities have the same value.

The last three equations constitute a linear system in d , E_1 and E_2 , whose solution (Appendix B) is

$$d = A_1 f_1(t_1) + A_2 f_2(t_1) + g_1(t_1, \phi) - f_0/(1-m) - A_3 f_3(t_1) - A_4 f_4(t_1) - g_2(t_1, \phi) - f_0/m \quad (22)$$

$$E_1 = A_1 f_7(t_1) + A_2 f_8(t_1) + A_3 f_9(t_1) + A_4 f_{10}(t_1) + g_4(t_1, \phi) + c_1 f_0 \quad (23)$$

$$E_2 = A_1 f_{11}(t_1) + A_2 f_{12}(t_1) + A_3 f_{13}(t_1) + A_4 f_{14}(t_1) + g_5(t_1, \phi) + c_2(t_1) f_0 \quad (24)$$

As the excitation is harmonic, the steady-state response at a time t has to have the same magnitude, but opposite sign, than at t plus or minus a semiperiod, t_2 . This requirement is referred as the periodicity condition and can be expressed as

$$x_1(t_2) = -x_1(0) \quad (25)$$

$$x_2(t_2) = -x_2(0) \quad (26)$$

$$\dot{x}_1(t_2) = -\dot{x}_1(0) \quad (27)$$

$$f(t_2) = -f(0) \quad (28)$$

The last condition is feasible because at $t = 0$, and as a consequence at $t = t_2$, the force in the joint is a continuous function of time. Later on, we will see that this is not the case at $t = t_1$. The periodicity condition for $\dot{x}_2(t)$ coincides with the one for $\dot{x}_1(t)$ because both velocities are identical at $t=0$ and also at $t = t_2$.

Equation (25) can be expanded as

$$A_1 f_1(0) + A_2 f_2(0) + g_1(0, \phi) - f_0/(1-m) + E_1 f_5(t_2) + E_2 f_6(t_2) + g_3(t_2, \phi) + kd = 0$$

Using the expressions previously obtained for d , E_1 , and E_2 we arrive at

$$b_{31} A_1 + b_{32} A_2 + b_{33} A_3 + b_{34} A_4 + b_{35} f_0 = p_3 \sin \phi + q_3 \cos \phi \quad (29)$$

Similarly, (26) and (27) can be written as

$$b_{41}A_1 + b_{42}A_2 + b_{43}A_3 + b_{44}A_4 + b_{45}f_0 = p_4 \sin \phi + q_4 \cos \phi \quad (30)$$

$$b_{51}A_1 + b_{52}A_2 + b_{53}A_3 + b_{54}A_4 + b_{55}f_0 = p_5 \sin \phi + q_5 \cos \phi \quad (31)$$

The last periodicity condition, equation (28), says that at the end of the semiperiod the tangential force in the joint is equal to $-f_0$. In fact, at exactly this time another change from the stuck to the sliding condition occurs, as it happens at $t = 0$. The mentioned force is computed by replacing $x_1(t)$ from (17) into the proper terms of the differential equations (5) or (6), with $t = t_2$. The result can be written as:

$$b_{61}A_1 + b_{62}A_2 + b_{63}A_3 + p_6 \sin \phi + q_6 \cos \phi = 0 \quad (32)$$

In summary, we have formulated the conditions to find an analytical solution for the steady-state vibrations of the system under study when only one slip-to-stuck change occurs in the friction joint in a semiperiod of vibration. The result is a set of six coupled algebraic equations ((14), (16) and (29) to (32)) with six unknowns (A_1 to A_4 , t_1 and ϕ). Although it is mathematically possible to solve directly this system of equations, this is a complicated task because most of the coefficients b_{ij} are strongly nonlinear functions of the unknown t_1 and some iterative numerical procedure would have to be used.

An indirect, simpler approach is used here taking into account that the first five equations of the system are linear in f_0 . We consider f_0 as one of the unknowns and, in exchange, t_1 as an independent variable. In this way, the coefficients b_{ij} become constants and the first five equations can be written as

$$B A = P \sin \phi + Q \cos \phi \quad (33)$$

where

$$A^T = \langle A_1 \ A_2 \ A_3 \ A_4 \ f_0 \rangle$$

$$B = \begin{bmatrix} b_{11} & b_{12} & \dots & b_{15} \\ b_{21} & b_{22} & \dots & b_{25} \\ \dots & \dots & \dots & \dots \\ \dots & \dots & \dots & \dots \\ b_{51} & b_{52} & \dots & b_{55} \end{bmatrix}$$

$$P^T = \langle p_1 \ p_2 \ p_3 \ p_4 \ p_5 \rangle$$

$$Q^T = \langle q_1 \ q_2 \ q_3 \ q_4 \ q_5 \rangle$$

Solving this linear system of equations we obtain

$$A = B^{-1}P \sin \phi + B^{-1}Q \cos \phi \quad (34)$$

in particular,

$$A_1 = p_7 \sin \phi + q_7 \cos \phi$$

$$A_2 = p_8 \sin \phi + q_8 \cos \phi$$

$$A_3 = p_9 \sin \phi + q_9 \cos \phi$$

Replacing these values into (32), we arrive at

$$(b_{61}p_7 + b_{62}p_8 + b_{63}p_9 + p_6)\sin \phi + (b_{61}q_7 + b_{62}q_8 + b_{63}q_9 + q_6)\cos \phi = 0$$

or

$$-\tan \phi = \frac{b_{61}p_7 + b_{62}p_8 + b_{63}p_9 + p_6}{b_{61}q_7 + b_{62}q_8 + b_{63}q_9 + q_6} \quad (35)$$

This equation yields two values of ϕ . For each of them a set of values for the elements of vector A is obtained with (33). Each of these sets is the negative of the other, reflecting the periodicity condition. We are interested in the solution with a positive f_0 , because we have assumed that this is the case at $t=0$. The other solution is equally valid and corresponds to the other semiperiod of vibration.

It should be pointed out that the above solution is valid only if the relative velocity $\dot{x}_1(t) - \dot{x}_2(t)$ does not have any change of sign between 0 and t_1 ; otherwise, there will be several changes from the sliding to the stuck condition and viceversa, contradicting the assumption of only one of such changes in a semiperiod. This requirement was not imposed when formulating the equations; therefore, it has to be verified separately. For the same reasons, it also has to be verified that the magnitude of the tangential force in the friction joint between t_1 and t_2 is smaller than f_0 .

3.2 Friction Joint Always Sliding

When the normal load is smaller than some limit value the friction joint is always sliding. In this case $t_1 = t_2$ and the differential equations (5) and (6), as well as their solutions (9) and (10), are valid all the time. Assuming that a change of sign in the relative velocity and, as a consequence, in the friction force, occurs at $t=0$, which requires the introduction of the unknown phase angle ϕ in the excitation force, we have now five unknowns, namely A_1 , A_2 , A_3 , A_4 and ϕ . This assumption leads again to equation (14).

The periodicity conditions are also expressed by equations (25) to (27) and by

$$\dot{x}_2(t_2) = -\dot{x}_2(0) \quad (36)$$

which this time is not automatically satisfied because we have not enforced the condition that the velocities are the same at $t = t_2$ (this is an equivalent requirement).

Equations (25) and (27) can be written again in the form of (29) and (31). However, an additional simplification can be done considering that $g_j(t, \phi)$ are harmonic functions with period $2t_2$ and, as a consequence, $g_j(t_2, \phi) = -g_j(0, \phi)$. The same is true for any time derivatives of $g_j(t, \phi)$. Therefore, instead of (29) and (31), we now have

$$A_1 f_1(0) + A_2 f_2(0) - 2f_0/(1-m) + A_1 f_1(t_2) + A_2 f_2(t_2) = 0 \quad (37)$$

$$A_1 \dot{f}_1(0) + A_2 \dot{f}_2(0) + A_1 \dot{f}_1(t_2) + A_2 \dot{f}_2(t_2) = 0 \quad (38)$$

This constitutes a system of two linear equations with two unknowns, A_1 and A_2 , that can be solved explicitly.

Following the same procedure with (26) and (36), a similar system of equations for A_3 and A_4 is obtained. After all the A_j are known ϕ can be calculated with (14). As in the previous case, the condition that no change in the relative velocity occurs between $t=0$ and $t=t_2$ has to be verified separately.

3.3 Some Limiting Cases

The analytical solutions presented in this section provide the tools for computing the values of the parameter f_0 corresponding to three limiting situations. First, recalling that t_1 was defined as the time at which slip occurs in a semiperiod of vibration, when $t_1=0$, there is no slip at all, and equation (8) with $d = 0$ always governs the motion of the system. Therefore, the solution for this case, gives for $\mu N/Q_1$ a limit r_1 such that when $\mu N/Q_1 > r_1$ the joint remains always stuck.

The second limiting case is that of no normal force in the joint, i.e., $f_0 = 0$. The joint is always sliding and the two masses vibrate separately. The solution can be obtained introducing $f_0 = 0$ in equations (9) and (10).

Finally, we can obtain the maximum value, r_2 , of $\mu N/Q_1$ for which the joint will be always sliding. This limit can be calculated by considering t_1 equal to the semiperiod of vibration ($t_1 = \pi/\omega$) in the equations of section 3.1. The same result is obtained solving the equations for the case of pure slip (section 3.2) with the additional restriction that the initial value of the relative acceleration is zero. The reason is that our solutions are valid only if the relative velocity is positive during the first semiperiod of vibration, and since the initial velocity is nil, zero is the lower value of the relative acceleration at $t = 0$ that can satisfy this condition.

3.4 Numerical Integration

Theoretically, the analytical method of solution can be easily extended to cases with more slip-to-stuck and stuck-to-slip changes in the friction interface, by using in each situation the analytical solution of the corresponding differential equations, and by imposing similar continuity and periodicity conditions. However, the size and complexity of the resulting algebraic problem increase very rapidly, and numerical step-by-step integration of the differential equations becomes a more practical method to obtain an exact solution.

Several well known time step-by-step schemes can be used to integrate the equations of motion, for instance, the Runge-Kuta or the Newmark families of methods. Efficient algorithms to apply these methods, as well as discussions of their mathematical characteristics (stability, convergency and accuracy), are presented in a number of books on numerical methods and on structural dynamics [11,12]. More recently, Dickens and Wilson [13], Sinha and Griffin [4], Hilber et al [14], Bazzi and Anderheggen [15], and Zienkiewicz et al [16] have presented improved versions of these type of methods.

For the problem considered in this paper almost all the available methods could be used with more or less the same levels of efficiency and accuracy, because we are dealing with only two ordinary differential equations. Obviously, this remark is not true for problems involving more degrees of freedom and more friction joints.

The main advantage of using step-by-step procedures is that any number of slip-to-stick changes and vice versa can be considered without difficulty. In fact that number is a result of the solution procedure. On the other hand, the main disadvantage arises from the fact that for nonlinear steady-state problems the integration has to be carried out for a sufficiently long time to reach the periodic state, i.e., until the effect of the initial disturbances becomes negligible. For this reason the numerical integration can be impractical even for systems with a moderate number of degrees of freedom. In this work this approach was used mainly to verify the analytical exact method and to assess the accuracy of approximate methods in cases with several slip-stick changes in the friction interface (Fig.2).

3.5 Numerical Results

In order to understand the role of the different parameters defining the system depicted in Fig. 1 in its dynamic behavior, we have computed the response for particular values of those parameters. Of special interest is the influence of the friction joint in the response. We also want to gain insight about the usefulness of analytical results in designing structures with friction interfaces.

The selected values of the parameters are presented in Table 1. Detailed exact results for the first case of this table are presented in this section. We have verified that all the relevant characteristics of the steady-

state response of the system under study can be appreciated in the results corresponding to this case.

The values of the ratio, r_1 , of the maximum frictional force, μN , to the amplitude, Q_1 , of the the load applied to M_1 that prevent slipping are presented in Fig. 3 as a function of the excitation frequency. For a prescribed frequency, any $\mu N/Q_1$ ratio equal or greater than the value in the curve will not allow any slipping in the joint. On the other hand, a prescribed value of $\mu N/Q_1$, can be represented by a horizontal line whose intersections with the curve of limiting values provide the range of frequencies for which there will be some slipping in the joint. The peak value (12.96) of this curve occurs for the resonant frequency of the system when the joint remains locked ($\omega=1$). The maximum value, r_2 , of $\mu N/Q_1$ that allows the joint to be sliding all the time is also presented in Fig. 3. For a given frequency, the joint will be always sliding if $\mu N/Q_1$ is equal or lower than the limiting value in the curve; and for a prescribed $\mu N/Q_1$ we can determine the range of frequencies for which the joint is always slipping.

The effects of $\mu N/Q_1$ on the amplitude of the system response are illustrated in Figs. 4, 5 and 6, in which frequency response curves have been plotted for several values of $\mu N/Q_1$. Fig. 4 shows that the amplitude, x_1 , of the normalized displacement of M_1 , has two sets of peak values. The first one corresponds to the normalized natural frequency of the M_1 - K_1 system, on which the external load is applied. The maximum, resonant, response occurs when there is no friction force ($\mu N/Q_1=0$) and M_1 - K_1 is vibrating without any interaction with the other mass and spring. For small values of $\mu N/Q_1$ the friction joint is always slipping and the peak values occur for the same resonant frequency. However, the presence of these small friction forces produces appreciable reductions of the maximum response.

As $\mu N/Q_1$ increases, the peak values move to an excitation frequency close to unity, the dimensionless resonance frequency of the system when the joint remains locked. In such cases, slipping occurs during one part of a cycle only. Eventually, if $\mu N/Q_1$ equals or exceeds the limiting value presented in Fig. 3 (12.96 for $\omega=1$), the two masses will vibrate together without any relative slipping (compare Figs. 5 and 6 for $\mu N/Q_1=12.96$). This process can be appreciated by examining the detailed time histories depicted in Figs. 7 and 8. In Fig. 7, $\mu N/Q_1$ is large enough to prevent slipping. Thus x_1 and x_2 coincide, and both have the maximum value 51.7. This is an elastic case and all the steady-state responses are harmonic. In Fig. 8, with a lower value of $\mu N/Q_1$, there is a small difference between x_1 and x_2 , resulting from a small slip between the two masses (shown by a dashed line). This slip, however, is sufficient to produce a significant reduction in the maximum values, which are now 30.5 and 31.3, respectively. Even though in this case the displacements are not strictly harmonic, it is obvious that they can be accurately approximated by harmonic functions with the same frequency as the excitation.

In the case of Fig. 9 the value of $\mu N/Q_1$ is very small and consequently the joint is always sliding. The

friction force varies as an alternating square wave. As in the previous case, the variations of the displacements are essentially, although not exactly, harmonic waves.

The main purpose of including a friction element in a vibrating system is to dissipate some of the energy imparted to the system. Since energy dissipation is a function of the slip load μN and the fraction of the period of oscillation during which slip occurs it is of interest to examine how this fraction, denoted as τ in Fig. 10, varies with the frequency of excitation ω and the normalized slip load $\mu N/Q_1$. τ is shown in Fig. 11. Note that for most values of $\mu N/Q_1$ and ω the friction element either slips during the entire period of oscillation ($\tau=1$) or remains stuck ($\tau=0$). The transition generally occurs over a narrow frequency band. In particular, for small values of $\mu N/Q_1$ and frequencies greater than unity a sudden change from a totally sliding condition to one of no slip can be appreciated. This effect may be of significance in design.

For cases of pure slip, as that of Fig. 9, the tangential force in the friction element changes abruptly from $+\mu N$ to $-\mu N$ as the relative velocity between the end points of the element changes sign. Clearly, no jump occurs if the element is stuck (Fig. 7). For partial slip the jump takes a value that lies between those corresponding to the extreme cases (Fig. 8). The values, q , of this jump in the slip force, normalized with respect to μN (see Fig. 11) are presented in Fig. 12. Note the similarity between the τ and q curves.

It can be shown that the energy dissipated in each cycle of vibration is equal to 4 times the product of $\mu N/Q_1$ and the initial relative displacement $x_1(0)-x_2(0)$. Obviously, the energy is zero when either the relative displacement or the normal force in the joint are nil, and it will have a maximum value for some intermediate value of $\mu N/Q_1$. This can be appreciated in Fig. 13 for $\omega=0.7071$ and in Fig. 14 for $\omega=1$. The variation of energy with the excitation frequency, for prescribed values of $\mu N/Q_1$, is shown in Fig. 15.

The phase angles ψ_1 and ψ_2 , of the displacements x_1 and x_2 with respect to the exciting force are shown in figures 16 and 17 as a fraction of π . Two elastic limiting cases are included, namely the case of no friction ($\mu N/Q_1=0$) and that of no slip ($\mu N/Q_1=12.96$). Fig. 16 shows that ψ_1 is always positive, indicating that the response always lags behind the excitation, as in the elastic case. For frequencies between the resonant ones (i.e., between the almost vertical slopes of the limiting cases) ψ_1 lies between the two elastic values corresponding to that frequency. For ψ_2 we have only one limiting elastic case because there is no force acting on mass M_2 .

Fig. 18 shows the maximum values, $x_{1\max}$, of the normalized displacement of mass M_1 , as a function of $\mu N/Q_1$. All the possible values of the excitation frequency were considered in obtaining each point of this curve. For low values of $\mu N/Q_1$, $x_{1\max}$ decreases very rapidly, until a minimum value is reached ($x_{1\max} = 6.36$). Then, for further increments of $\mu N/Q_1$, $x_{1\max}$ also increases, until a constant value is obtained when

$\mu N/Q_1$ is large enough to maintain the joint always locked. The value of $\mu N/Q_1$ corresponding to the minimum response is defined as the optimum value of such a ratio (in this case, $\mu N/Q_1$ optimum = 1.0). Similar optimization curves can be constructed for any other response of interest. Naturally, it is highly desirable to design the friction joint to have parameters close to the optimum ones.

In order to evaluate the accuracy that can be expected from approximate methods, we have computed the coefficient of the first Fourier component of the tangential force in the joint. Results for $\omega=0.7071$ and $\omega=1$ are presented in Figs. 19 and 20. As expected, these coefficients have a maximum value of $4/\pi$ corresponding to cases in which the joint is always sliding. The minimum value is 1.0 and occurs when the joint is locked.

Exact results have been also computed for other cases included in Table 1. As pointed out earlier, they present characteristics similar to those discussed in the case covered in this section. These exact results are later used in comparisons with results of approximate methods.

4 APPROXIMATE METHODS OF SOLUTION

In view of the difficulties of obtaining analytical or numerical exact solutions, approximate methods have been used by several researchers [4, 6, 7]. The most widely used method is the so-called harmonic balance method which finds the best approximation of the response in the space of the harmonic functions with the same frequency as the excitation. This method is completely equivalent to the linearization technique proposed by Caughey [17]. Its theoretical foundations have been thoroughly studied by Spanos and Iwan [18].

In this section a complex variable version of the method is presented for the system under study; then, some modifications are proposed to improve its accuracy when the joint is not always sliding. A comparison of exact and approximate results is also presented to illustrate the accuracy and applicability of the various methods.

4.1 Harmonic Balance Method

The following assumptions are made in this method:

- a) The response is harmonic with the same frequency as the excitation forces;
- b) The friction force has the same direction as the relative velocity in the joint, but opposite sign;
- c) The friction joint is always sliding, i.e., no lock condition is considered;
- d) Only the first Fourier component of the friction force has a significant participation in the response of the system, i.e., the effect of higher components is negligible.

In order to present a complex variable approach of the method the excitation forces are defined as

$$Q_j(t) = \bar{Q}_j \exp(i\omega T), j=1,2$$

where an overbar denotes a complex quantity, and $i=\sqrt{-1}$

According to assumptions a) and d) we can also write

$$X_j(T) = \bar{X}_j \exp(i\omega T) \quad (40)$$

$$F(T) = \bar{F} \exp(i\omega T) \quad (41)$$

thus,

$$\dot{X}_j(T) = i\omega \bar{X}_j \exp(i\omega T) \quad (42)$$

$$\ddot{X}_j(T) = -\omega^2 \bar{X}_j \exp(i\omega T) \quad (43)$$

By substituting these expressions into (1) and (2) and dropping the factor $\exp(i\omega T)$ the following complex algebraic equations are obtained:

$$(K_1 - \omega^2 M_1 + i\omega C_1) \bar{X}_1 = \bar{Q}_1 - \bar{F} \quad (44)$$

$$(K_2 - \omega^2 M_2 + i\omega C_2) \bar{X}_2 = \bar{Q}_2 + \bar{F} \quad (45)$$

solving for \bar{X}_1 and \bar{X}_2

$$\bar{X}_1 = h_1(\omega) \bar{Q}_1 - h_1(\omega) \bar{F} \quad (46)$$

$$\bar{X}_2 = h_2(\omega) \bar{Q}_2 + h_2(\omega) \bar{F} \quad (47)$$

where

$$h_j(\omega) = (K_j - \omega^2 M_j + i\omega C_j)^{-1} \quad (48)$$

The relative displacement can be now written as

$$\bar{X}_1 - \bar{X}_2 = [h_1(\omega) \bar{Q}_1 - h_2(\omega) \bar{Q}_2] - [h_1(\omega) + h_2(\omega)] \bar{F} \quad (49)$$

define

$$\bar{D} = D \exp(i\theta) = \bar{X}_1 - \bar{X}_2 \quad (50)$$

$$P = [h_1(\omega) \bar{Q}_1 - h_2(\omega) \bar{Q}_2] \quad (51)$$

$$\bar{R} = [h_1(\omega) + h_2(\omega)] \quad (52)$$

where D is the amplitude and θ is the phase angle of the relative displacement in the friction joint. This allows us to write

$$\bar{D} + \bar{R}\bar{F} = \bar{P} \quad (53)$$

which is an equation relating the relative displacement with the tangential force in the friction joint.

From (42), the relative velocity is

$$\dot{X}_1(T) - \dot{X}_2(T) = iW(\bar{X}_1 - \bar{X}_2)\exp(iWT) = iW\bar{D}\exp(iWT)$$

Taking into account that W is a positive real constant, the definition of θ in (50), and that $i = \exp(\pi/2)$, we conclude that the phase angle of the relative velocity in the joint is $(\theta + \pi/2)$. According to assumption b) this is also the phase angle of the friction force (the proper sign was already considered when formulating the equations of motion). Therefore,

$$\bar{F} = iF \exp(i\theta) \quad (54)$$

Besides, according to assumptions c) and d) this force has the shape of an alternating square wave in time (see Fig. 4), and only the first Fourier coefficient of such a wave has to be considered. Hence,

$$F = (4/\pi)\mu N$$

Then, for a prescribed value of μN , the only unknowns in (53) are D and θ .

The traditional application of the harmonic balance method consists in equating the real and the imaginary parts of both members of (53) obtaining two real nonlinear equations in D and θ . The equation resulting from the real parts corresponds to a cosine excitation force, and the one resulting from the imaginary parts corresponds to a sine excitation. Any of them can be expressed as

$$c(W, D, F, \theta) \cos(WT) + s(W, D, F, \theta) \sin(WT) = 0.$$

Since this equation has to be satisfied for any value of T , both $c(W, D, F, \theta)$ and $s(W, D, F, \theta)$ have to be separately equal to zero, providing two equations for D and θ . Elimination of θ leads to the following quadratic equation in D :

$$a_1(W)D + a_2(W)D\mu N + a_3(W)(\mu N)^2 = a_4(W) \quad (55)$$

where $a_j(W)$ ($j=1,4$) are frequency dependent coefficients.

After solving for D , θ is calculated with one of the two original equations. Then, (54), (46) and (47) are used

to compute \bar{F} , \bar{X}_1 and \bar{X}_2 .

An easier way to obtain (55) is to multiply (53) by its complex conjugate; the result is

$$\overline{DD} + \overline{DR} \bar{F} + \overline{D} \bar{R} F + \overline{RR} \bar{F} F = \overline{PP} \quad (56)$$

where the star denotes the complex conjugate.

From (50) and (54) we have:

$$\bar{D} = D \exp(-i\theta)$$

$$\bar{F} = -iF \exp(-i\theta)$$

and consequently

$$\overline{DF} = -iDF \exp(i\theta) \exp(-i\theta) = -iDF$$

$$\overline{D} \bar{F} = iDF \exp(i\theta) \exp(-i\theta) = iDF$$

$$\overline{DR} \bar{F} + \overline{D} \bar{R} F = -iDF \bar{R} + iDF \bar{R} = iDF[\bar{R} - R] = iDF[2i[\text{Imag}(\bar{R})]] = -2DF[\text{Imag}(\bar{R})] \quad (57)$$

where $\text{Imag}(\bar{R})$ denotes the imaginary part of \bar{R} . Recalling that the product of a complex quantity by its conjugate yields the square of its modulus we also have $\overline{DD} = D^2$, $\overline{RR} = R^2$, $\bar{F}F = F^2$, and $\bar{P}P = P^2$. Therefore, (56) becomes

$$D^2 - 2 \text{Imag}(\bar{R}) FD + R^2 F^2 = P^2 \quad (58)$$

which, as (55), is a quadratic equation for D.

4.2 Modified Harmonic Balance Methods

As it could be expected, the harmonic balance method yields very accurate results when the variation of the friction force with time is similar to the alternating square wave shown in Fig. 9. Larger errors occur when the joint is always locked (Fig. 7), because the force in the joint is actually harmonic and the value of its first and only nonzero Fourier coefficient is 1.0 and not $4/\pi$, or when slipping is prevented most of the time (Fig. 8), because such a coefficient will be closer to 1 than to $4/\pi$. Appreciable errors also occur when one or both of the displacements have significant components of higher frequencies, as in the example shown in Fig. 23.

Aiming to reduce the first of the above sources of error, some modifications to the method are proposed

here. They consist in estimating the first Fourier coefficient of the friction force with heuristic rules, instead of considering it always equal to $4/\pi$. Thus the amplitude of F , is now given by

$$F = C_f \mu N \quad (59)$$

where C_f is estimated with some rule satisfying the condition

$$1.0 \leq C_f \leq 4/\pi \quad (60)$$

The rules proposed here have the form

$$C_f = C_f(D) \quad (61)$$

which means that the coefficient is considered to be a function of the amplitude, D , of the relative displacement. Obviously, $C_f(D)$ is 1.0 when $D = 0$, and its maximum value is $4/\pi$.

The first rule is expressed in terms of a dimensionless parameter θ , and is called parametric. C_f is given by

$$C_f(\theta) = \left[\frac{\pi - 2\theta}{\cos \theta} + 2 \sin \theta \right] / \pi \quad (62)$$

θ is related to D by

$$D = D^1 (2\theta + \sin 2\theta) / \pi \quad (63)$$

where D^1 is obtained by substituting $F = \mu N$ into (58). The variation of $C_f(\theta)$ with D , according to this rule is shown in Fig 21.

The next step is to replace (59), (62) and (63) into (58) to obtain a nonlinear equation for θ . After solving numerically this equation, (59) and (63) are used to calculate D and F .

A second, simpler rule, also illustrated in Fig. 21, consists in assuming that C_f is a linear function of D , with values between 1.0 for $D = 0$ and $4/\pi = 1.2732$ for $D = D^1$, i.e.:

$$C_f = 1. + 0.2732 (D/D^1) \quad (64)$$

This rule has the advantage that substitution of F by $C_f \mu N$ into (58) yields another quadratic equation, without adding complexity to the algebraic problem. This approach is referred as the modified linear method.

A third rule, similar to the second one, consists in prescribing a parabolic variation for C_f within the interval 0 and D^1 , as it is also shown in Fig. 21. In this case

$$C_f = 1. + 0.2732 (D/D^1)^2 \quad (65)$$

Substitution into (58) produces this time a cubic real equation in D . This option will be called modified quadratic method.

A disadvantage of the preceeding rules is that equation (58) has to be solved twice for a given value of μN , first with $C_f = 1$, to compute D^1 , and then, for the corresponding estimate value of C_f . In the present study the additional numerical work is not excessive; but it can be very appreciable in problems with multiple joints.

Reductions in the numerical work when using the second and third rules can be obtained if D/D^1 is computed assuming that the variation of D with F is linear, as shown in Fig. 22. First, the value of μN corresponding to $D = 0$ is calculated taking into account that in this case the Fourier coefficient of the force in the friction joint is 1. From (58), this value is:

$$F = \mu N_0 = P/R \quad (66)$$

For any value of the amplitude of the friction force equal or greater than μN_0 the joint will be locked and the solution will remain the same. This provides an exact criterion to define the slip-stick limit for the joint because when the joint is locked the response is actually harmonic. It is important to take into account that it is possible to obtain physically acceptable solutions only for values of μN lower than μN_0 . Now, a linear variation of D with μN can be expressed as

$$D = D_0(1 - \mu N / \mu N_0) \quad (67)$$

where D_0 is the amplitude of the relative displacement corresponding to no friction force in the joint.

For the modified linear method, combining (64) and (67) we obtain

$$D/D^1 = 1/(1 + .2732\gamma) \quad (68)$$

where γ is a nondimensional parameter defined as

$$\gamma = (\mu N / \mu N_0) / [1 - \mu N / \mu N_0] \quad (69)$$

Therefore, we can compute C_f directly and then solve equation (58). Note that it is not necessary to compute the value of D_0 .

For the quadratic modification, from (65) and (67) we obtain

$$D/D^1 = (1 + 1.093\gamma - 1)/(.5465\gamma) \quad (70)$$

and we can proceed as in the previous case.

Again, the proposed modifications are intended to improve the performance of the harmonic balance method when higher frequencies do not play a significant role in the system response. If this is not the case, appreciable differences with exact results might be expected. For instance, Fig. 23 shows the variation with time of several response quantities for system II of Table 1, when the normalized excitation frequency is 0.5. Whereas x_1 and x_2 in Figs. 7 and 8 are essentially sinusoidal, x_2 in Fig. 23 is not, because the natural

frequency of the M_2 - K_2 system ($\Omega_2 = 1.29$) is close to the frequency of the second Fourier component of the friction force ($\omega = 3 \times 0.5 = 1.5$), which, as a consequence, has a significant participation in the motion of M_2 . It is clear that the approximate procedures for the dynamic analysis proposed in this section, which include the first harmonic component of the response only, cannot be expected to yield accurate results in cases such as this.

5 COMPARISON OF RESULTS OF DIFFERENT METHODS

In order to assess the accuracy and applicability of the different methods presented in this paper, results of the approximate methods are compared in this chapter with the corresponding exact results. Values of the parameters defining the system and the excitation forces selected to perform the comparisons are presented in Table 1. Cases of pure slip, partial slip and stuck conditions are included in this Table. The results are graphically presented in Figs. 24 through 38.

The exact displacements of the two masses obtained for Case III are presented in Fig. 24, in which they are identified by special symbols defined in the figure. Results obtained for this case with the harmonic balance method are indicated by a dashed line and those corresponding to the parametric modification of the harmonic balance method are shown by a continuous line. Good agreement between the exact values and those obtained with the parametric method can be appreciated for high values of the parameter $\mu N/Q_1$ (5 to 25). In these cases the harmonic balance method is less accurate. On the other hand, for low values of $\mu N/Q_1$ (1.7 and 2.5) the harmonic balance method yields more accurate results than its parametric modification. However, the errors of this method are moderate in any case.

For Cases IV to XVII of Table 1 we have obtained the exact values of the displacements of both masses and the corresponding approximate values with the parametric method. Approximate results from other proposed modifications of the harmonic balance method are in all cases very similar to those presented here. By examining these figures, it can be concluded that the parametric method provides good approximations to the exact results, with the exception of some values in the vicinity of the resonant frequency of the M_2 - K_2 system ($\Omega_2 = 0.577$) in cases X and XI (Figs. 31 and 32). The reason is that the natural frequency of the M_1 - K_1 system is in these cases exactly three times the previous frequency ($\Omega_1 = 3 \times 0.577 = 1.732$), and as a consequence the third Fourier component of the friction force has a significant participation in the response. A similar situation can be appreciated for Case II in time histories depicted in Fig. 23, which were obtained with numerical integration. It is evident that the higher frequency dominates in x_2 .

In order to assess the range of applicability of the approximate methods we have examined closely two particular cases. Results from all the methods considered in this report for case I, with $\omega = 1$, are presented

in Table 2. It can be appreciated that the modified parametric method provides approximate values very close to the exact ones in all cases. The quadratic method gives almost the same results as the parametric method. The errors of the linear modification are slightly greater than those of the previous methods. The larger discrepancies with exact results correspond to the classic harmonic balance method, the worst case being that in which $\mu N/Q_1$ is close to $\pi/4$ times the maximum value of that parameter ($10/12.96 = 0.772$). We can observe that the accuracy of the approximate results in Table 2 is in agreement with the precision found in estimating the first Fourier coefficient of the tangential force in the joint resulting from all the methods for the same values of the system and excitation parameters, as shown in Fig. 20.

The same type of results are presented in Table 3 and Fig. 19 for $\omega = 0.7071$. In this case, the harmonic balance method yields the most accurate results for all the values of $\mu N/Q_1$. Indeed, the modified methods provide acceptable results only for low values of $\mu N/Q_1$. By examining Fig. 19, we conclude that the reason is that in this particular case the joint is actually always sliding for almost all the values of $\mu N/Q_1$, conforming the assumptions of the classical harmonic balance method (see section 4.1).

In general, the modified methods yield accurate results in cases in which the slip-to-stuck (r_1) and the some-slip-to-pure-slip (r_2) limits of $\mu N/Q_1$ (see section 3.3 and Fig. 3) are far from each other. In the opposite case, the original method will provide better results. This emphasizes the importance of calculating those limits, as was done to construct Fig. 3. From this figure it is possible to affirm that the modified methods will be more accurate in the vicinity of the resonant frequency of the complete system ($\omega = 1$) where $r_2/r_1 = 0.07$. The classic method will be better when the mentioned limits have close values, for instance, for $\omega = 0.7071$, where $r_2/r_1 = 0.76$.

6 CONCLUDING REMARKS

Several methodologies to study the steady-state vibrations of the two-body system depicted in Fig. 1 have been presented. First, an efficient analytical exact solution was derived, which allows to calculate the actual values and characteristics of any response of interest. This method was used to obtain detailed results for a representative system.

The exact results show that the ratio of the normal force in the joint to the amplitude of the excitation forces, measured by the dimensionless parameter $\mu N/Q_1$, is a critical factor in the system response. For high values of this ratio the joint will be locked in most cases and the maximum values of the response will occur for the resonant frequency of the system vibrating as a unit ($\omega=1$ in the normalized system). However, if $\mu N/Q_1$ is small enough to allow some slipping in the joint, the corresponding energy dissipated will produce a significant reduction of the response amplitude.

For low values of the ratio $\mu N/Q_1$, the joint will be always sliding, and the peak responses will correspond to the natural frequencies of each mass-spring system vibrating independently of the other one. Again, even small values of forces in the joint will produce significant energy dissipation and a consequent reduction of the response.

An optimum value of the parameter $\mu N/Q_1$ can be calculated such that the maximum value of the response of interest is minimum, considering all the relevant frequencies. In general, the optimum $\mu N/Q_1$ will be small enough to reduce significantly the response at the resonant frequency of the whole system, and high enough to yield appreciable reduction of the response at the resonant frequencies of the bodies vibrating independently.

The analytical exact solution provides the means to compute the values of the ratios $\mu N/Q_1$ corresponding to the stick-slip transition in the joint. If $\mu N/Q_1$ is higher or equal to this limit, the joint will be locked, and slip can occur only for loads lower than the limit. Also the value of $\mu N/Q_1$ separating the region of pure-slip and partial slip can be calculated. The computation of these limits is important to obtain mathematical solutions consistent with the physical phenomena, and to determine the applicability of approximate procedures.

A complex variable version of the harmonic balance method also has been presented. It constitutes a simple way for deriving the algebraic real equations governing the problem, and seems to be the most appropriate approach to address multi-degree-of-freedom or multi-joint problems. An important feature of our formulation is that a criterion is proposed to exactly calculate the normal load corresponding to the slip-stick limit in the joint. Physically acceptable solutions are possible only for normal loads lower than this limit.

The comparisons of exact and approximate results show that methods based on considering only the first Fourier component of the tangential force in the friction joint, are very accurate, provided that the participation of higher Fourier components in the response is negligible. Such a participation can be prevented by designing systems in which the higher frequencies are not odd multiples of the lower ones.

Modifications to the harmonic balance method are also proposed. They consist in estimating the first Fourier coefficient of the tangential force in the joint with approximate heuristic rules. The improvement achieved in cases of partial slip with these modifications shows the relevance of a proper estimation of the first Fourier coefficient of the friction force. In cases in which the joint is sliding during an entire cycle the classical assumption that such a coefficient is equal to $4/\pi$ will provide the best results. If the slipping is only partial, the rules proposed in the modified harmonic balance methods will produce better results. The quadratic rule seems to be, in these cases, a good compromise between simplicity and accuracy.

The agreement of most of the exact results with the approximate ones supports the assumption that the

actual response of the two-body system studied in this work is nearly harmonic. This behavior can also be expected in multi-joint and multi-body systems, provided the effect of high frequencies is reduced to a minimum by means of an appropriate design of the system. This would allow the application of the approximate methods presented here to the analysis of such systems, resulting in a substantial simplification of the mathematical problem.

REFERENCES

1. Den Hartog, J. P. "Forced Vibrations with Combined Coulomb and Viscous Friction," *Trans. ASME AMP-53-9*, 1931, pp. 107-115.
2. Den Hartog, J. P., *Mechanical Vibrations*, 3th ed. McGraw-Hill New York, 1947.
3. Plunkett, R. "Friction Damping" *Damping Applications for Vibration Control, AMD*, Vol. 38, edited by P. J. Torvik, ASME, New York, 1980.
4. Griffin, J. H., "Friction Damping Of Resonant Stresses in Gas Turbine Airfoils," *ASME Journal of Engineering for Power*, Vol. 102, April 1980, pp. 329-333
5. Sinha, A. and Griffin, J. H., "Friction Damping of Flutter in Gas Turbine Engine Airfoils", *AIAA Journal of Aircraft*, Vol. 20, No. 4, April 1983, pp. 372-376
6. Chia-Hsiang, M. and Griffin, J. H. "A Comparison of Transient and Steady State Finite Element Analyses of Forced Response of a Frictionally Damped Beam," *ASME 83-DET-24*, presented at the Design and Production Engineering Technical Conference, Sep. 11-14, 1983, Dearborn, Mich. 7 pp.
7. Muszynska, A. Jones, D. I. G., Lagnese, T., and Whitford, L., "On Nonlinear Response of Multiple Blade Systems," *Shock and Vibration Bulletin*, Vol. 51, Part 3, May 1981, pp. 88-110.
8. Srinivasan, A. V., Cutts, D. G., and Shidhar, S., "Turbojet Engine Blade Damping," *NASA Contract Report 165406*, July 1981.
9. Dominic, R. J., Graf, P., and Raju, B. B., "Analytical and Experimental Investigation of Turbine Blade Damping," *University of Dayton Publication UDR-TR-82-39*, Aug. 1982.
10. Soni, M. L. and Bogner, F. K., "Finite Element Vibration Analysis of Damped Structures," *AIAA Journal*, Vol. 20, No 8, pp. 700-707, 1982.
11. Bathe, K-J. and Wilson, E. L., *Numerical Methods in Finite Element Analysis*, Prentice Hall, Englewood Cliffs, New Jersey, 1976.
12. Newmark, N. M. and Rosenblueth, E., *Fundamentals of Earthquake Engineering*, Prentice Hall, Englewood Cliffs, New Jersey, 1971.
13. Dickens, J. M. and Wilson, E. L., "Numerical Methods for Dynamic Substructure Analysis," *Report UCB/EERC-80/20*, University of California, Berkeley, June 1980.
14. Hilber, H. M., Hughes T. J. R. and Taylor, R. L., "Improved Numerical Dissipation for the Integration Algorithms in Structural Mechanics," *Int. J. Numer. Methods in Eng.*, Vol. 5, pp. 283-292, 1977.
15. Bazzi, G. and Anderheggen, E., "The p-Family of Algorithms for Time-step Integration with Improved Numerical Dissipation," *Earthquake Eng. Struct. Dyn.*, Vol. 10, No 4, pp. 537-550, 1982.
16. Zienkiewicz, O. C., Wood, W. L., Hine, N. H. and Taylor, R. L., "A Unified Set of Single Step Algorithms. Part 1: General Formulation and Applications," *Int. J. Numer. Methods Eng.*, Vol. 20, No 8, pp. 1529-1552, 1984.
17. Caughey, T. K., "Sinusoidal Excitation of a System with Bilinear Hysterisis," *ASME, Journal of Applied Mechanics*, Vol. 27, pp. 640-643, 1960.

18. Spanos, P-T. D. and Iwan, W. D., "On the Existency and Uniqueness of Solutions Generated by Equivalent Linearization", *Int. J. Non-Linear Mechanics*, Vol. 13, pp. 71-78, 1978.

TABLE I
NUMERICAL RESULTS

Case	System parameters			Excitation parameters			
	m	k	ζ_1	ζ_2	α	β	$\mu N/Q_\xi$
I	0.50	0.75	1.00	1.00	0	0	variable
II	0.12	0.47	1.00	1.00	0	0	0.10
III	0.50	0.25	0.82	1.41	1	0	variable
IV	0.50	0.25	0.82	1.41	1	0	variable
V	0.50	0.75	1.41	0.82	0	0	variable
VI	0.50	0.25	0.82	1.41	1	180	variable
VII	0.25	0.50	0.82	1.41	1	0	variable
VIII	0.50	0.50	1.00	1.00	1	90	variable
IX	0.50	0.50	1.00	1.00	1	180	variable
X	0.75	0.25	1.15	1.15	1	0	variable
XI	0.75	0.25	1.15	1.15	0	0	variable
XII	0.25	0.25	0.67	2.00	1	90	variable
XIII	0.50	0.50	1.00	1.00	0	0	variable
XIV	0.50	0.50	1.00	1.00	2	0	variable
XV	0.25	0.25	0.67	2.00	1	0	variable
XVI	0.50	0.25	0.82	1.41	2	0	variable
XVII	0.50	0.25	0.82	1.41	1	90	variable

Note: Angle β is in degrees and ζ_1 and ζ_2 are in percentage.

TABLE 2
COMPARISON OF RESULTS FROM DIFFERENT METHODS

Case I $\omega = 1.00$						
$\frac{\mu N}{a_1}$	result	exact	harmonic balance	modified harmonic balance		
				parametric	quadratic	linear
1.00	x_1	5.35	6.38	6.33	6.34	6.36
	x_2	5.17	5.09	5.02	5.04	5.06
	E	13.61	14.41	14.25	14.29	14.35
	C_1	1.273	1.273	1.257	1.261	1.267
2.40	x_1	10.93	12.73	12.31	12.46	12.58
	x_2	12.01	12.20	11.76	11.93	12.06
	E	26.46	29.33	28.58	28.86	29.08
	C_1	1.237	1.273	1.227	1.244	1.257
6.91	x_1	30.49	35.24	32.08	32.54	33.45
	x_2	31.32	35.15	31.96	32.44	33.35
	E	37.72	35.45	38.45	38.07	37.28
	C_1	1.135	1.273	1.158	1.175	1.208
10.0	x_1	42.61	50.87	44.04	44.34	45.65
	x_2	42.98	50.87	44.01	44.30	45.63
	E	22.78	2.67	20.68	20.03	16.97
	C_1	1.080	1.273	1.101	1.109	1.142
12.5	x_1	50.93	51.76	51.20	51.21	51.55
	x_2	50.96	51.76	51.20	51.21	51.55
	E	2.50	0.00	1.76	1.73	0.6
	C_1	1.042	1.273	1.025	1.025	1.032

x_1 = normalized displacement of mass M_1 of Fig. 1.
 x_2 = normalized displacement of mass M_2 of Fig. 2.
 E = energy dissipated per cycle
 C_1 = First Fourier coefficient of the friction force

TABLE 3
COMPARISON OF RESULTS FROM DIFFERENT METHODS

Case I $\omega = 0.7071$						
$\frac{\mu N}{a_1}$	result	exact	harmonic	modified harmonic balance		
			balance	parametric	quadratic linear	
0.20	x_1	149.0	149.1	151.1	150.4	149.8
	x_2	0.56	0.51	0.50	0.50	0.50
	E	119.2	119.2	116.1	117.3	118.2
	C_1	1.273	1.273	1.223	1.241	1.256
0.39	x_1	100.6	100.7	107.5	105.9	103.9
	x_2	1.09	0.99	0.92	0.94	0.96
	E	156.8	157.0	156.1	156.5	156.8
	C_1	1.273	1.273	1.185	1.206	1.233
0.60	x_1	46.93	47.23	62.74	60.98	56.76
	x_2	1.68	1.53	1.37	1.39	1.43
	E	112.5	113.2	135.2	133.0	127.6
	C_1	1.273	1.273	1.144	1.159	1.193
0.74	x_1	11.75	11.70	35.69	34.39	29.30
	x_2	2.06	1.88	1.64	1.66	1.71
	E	32.83	34.10	92.00	89.30	78.40
	C_1	1.273	1.273	1.110	1.119	1.154
0.90	x_1	1.89	2.00	9.87	9.52	6.11
	x_2	2.05	2.00	1.90	1.91	1.94
	E	1.05	0.00	28.85	27.83	17.57
	C_1	1.119	1.273	1.057	1.059	1.079

x_1 = normalized displacement of mass M_1 of Fig. 1.
 x_2 = normalized displacement of mass M_2 of Fig. 2.
E = energy dissipated per cycle
 C_1 = First Fourier coefficient of the friction force

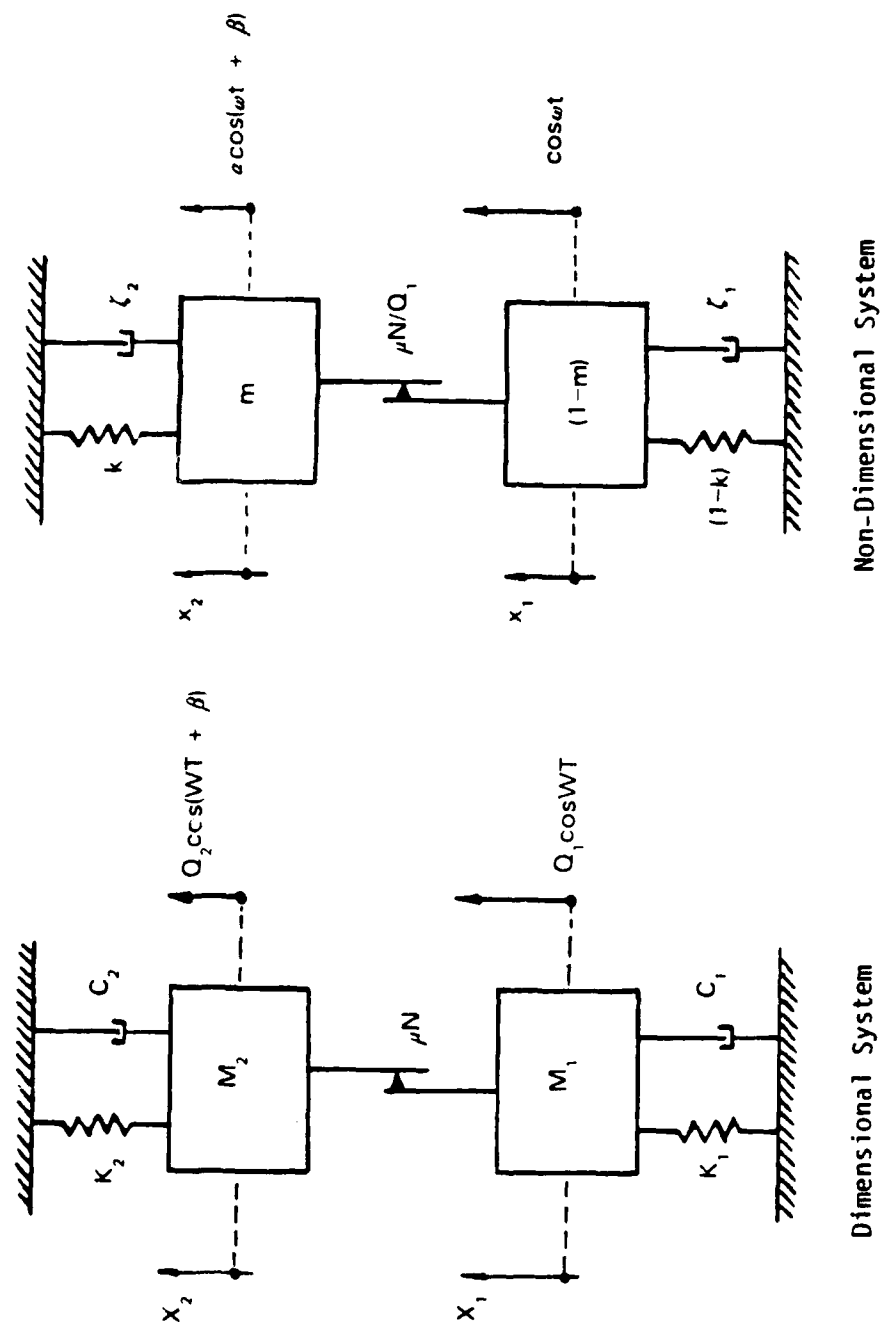


Fig. 1: Two-Body System with a Frictional Interface

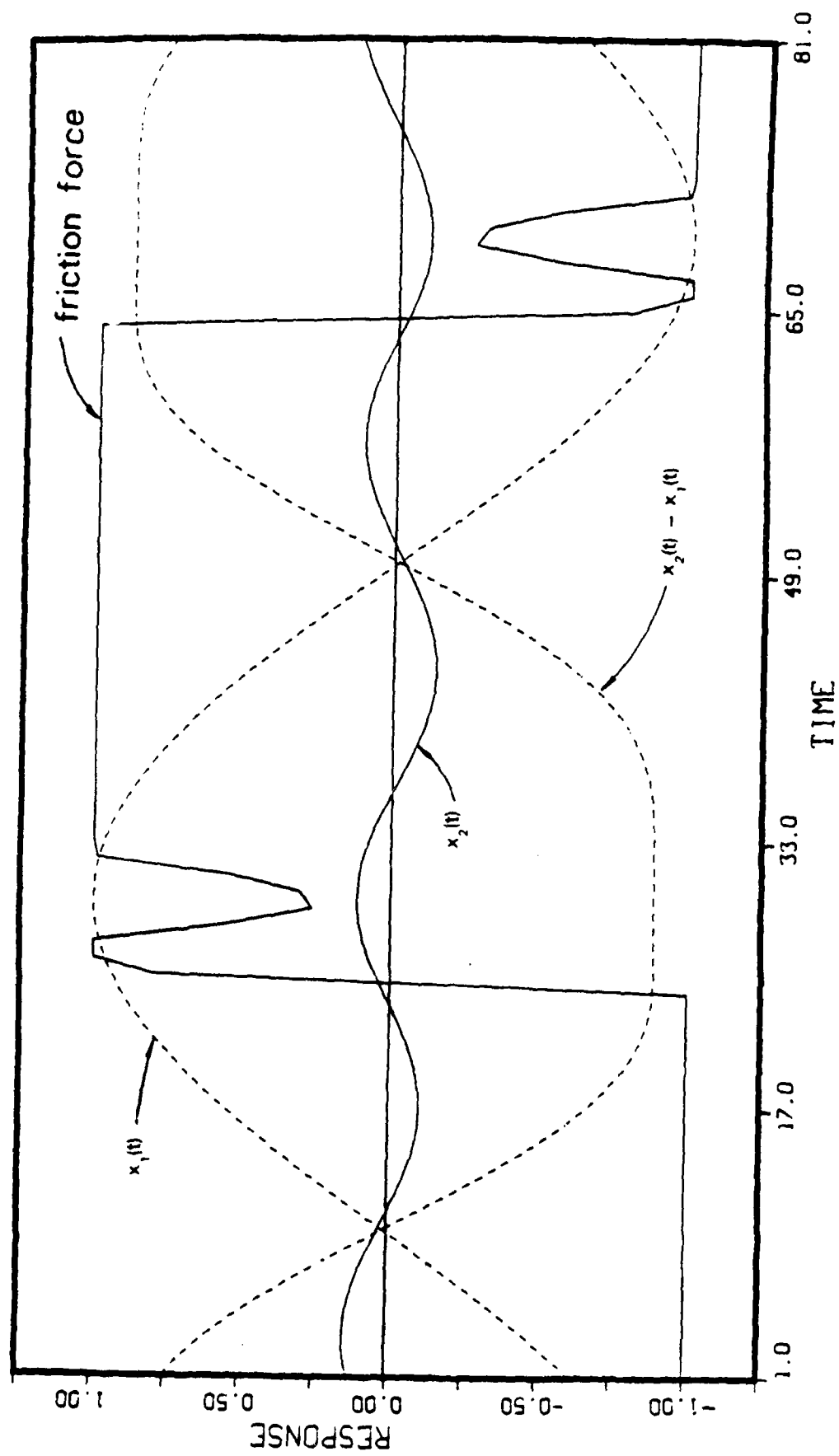


Fig. 2: Exact Response Time Histories for Case XI, $\mu N/Q_1 = 0.5$, $\omega = 0.59$

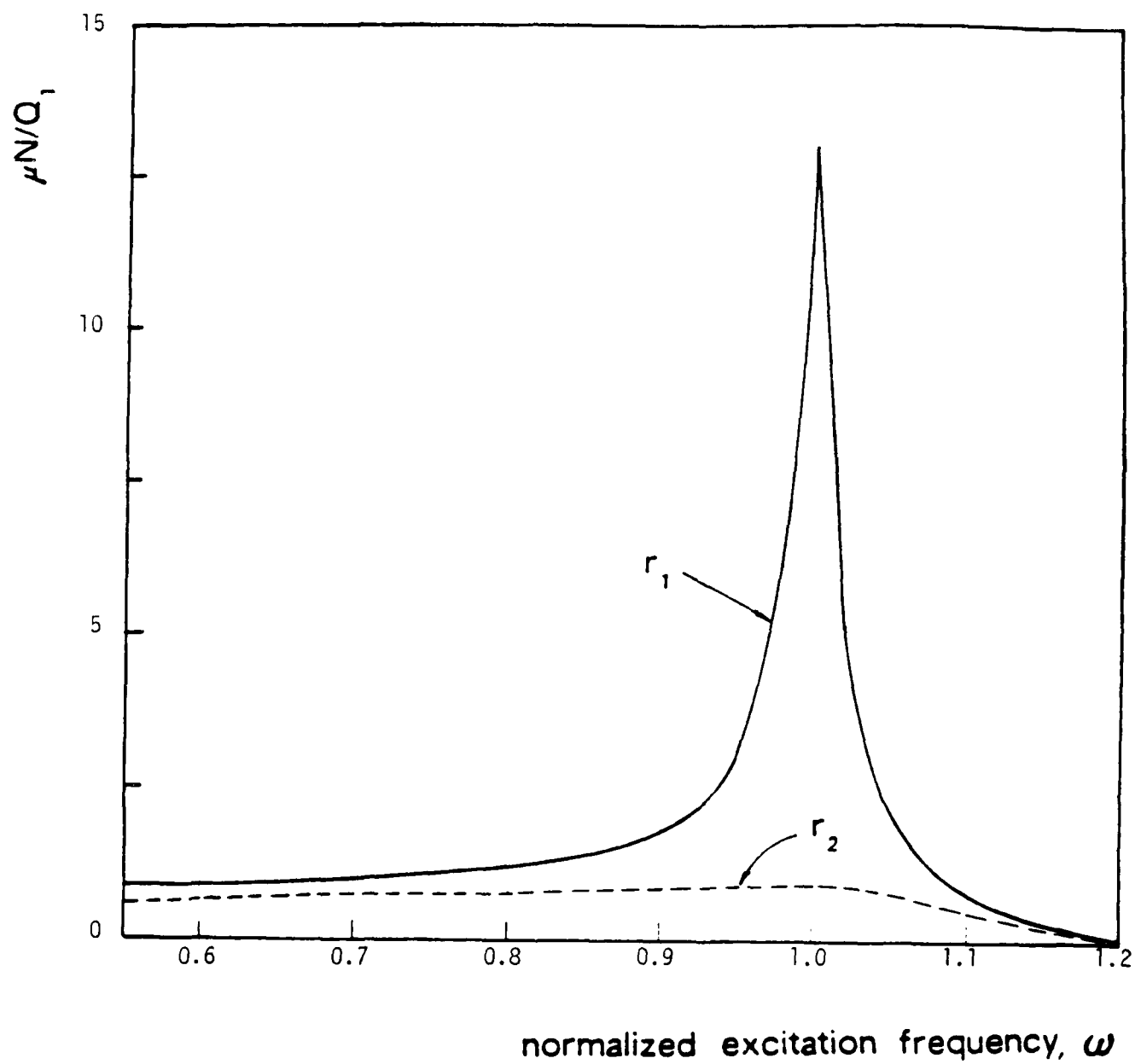


Fig. 3: Slip-Stick and Partial-Slip-Pure-Slip Limits for Case 1 of Table 1.

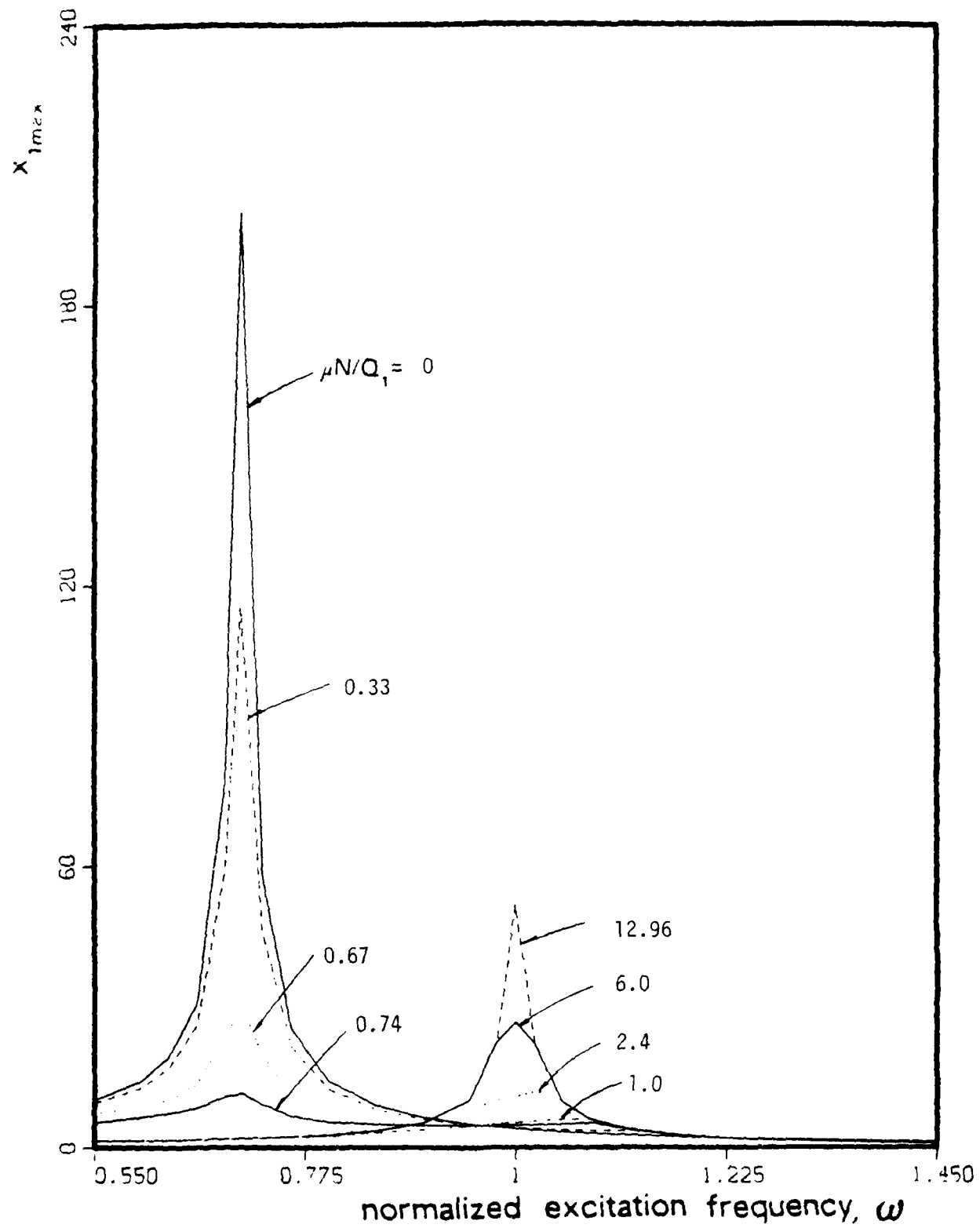


Fig. 4: Maximum Exact Displacement of Mass M_1 of Fig. 1.

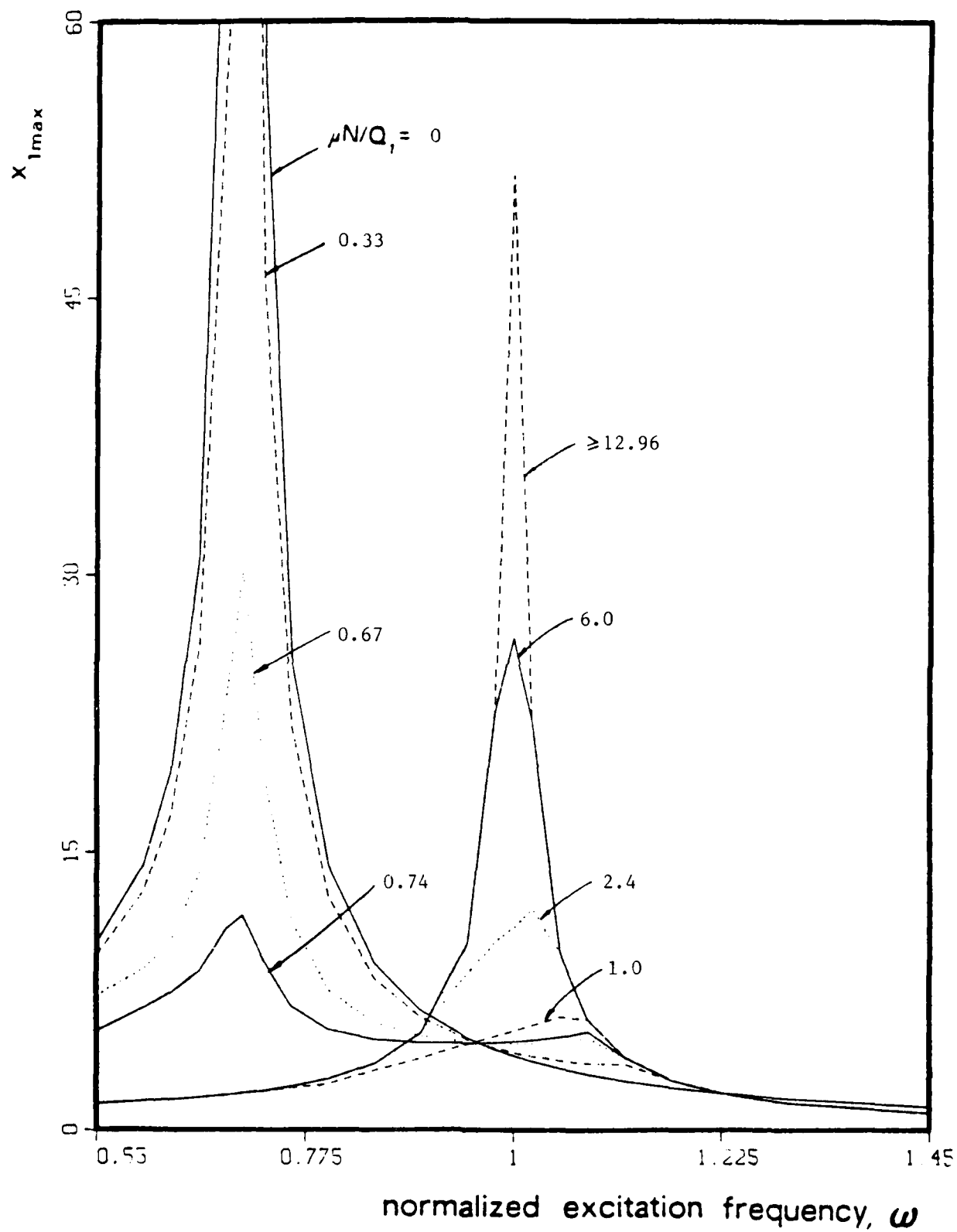


Fig. 5: Maximum Exact Displacement of Mass M_1 of Fig. 1. (amplified)

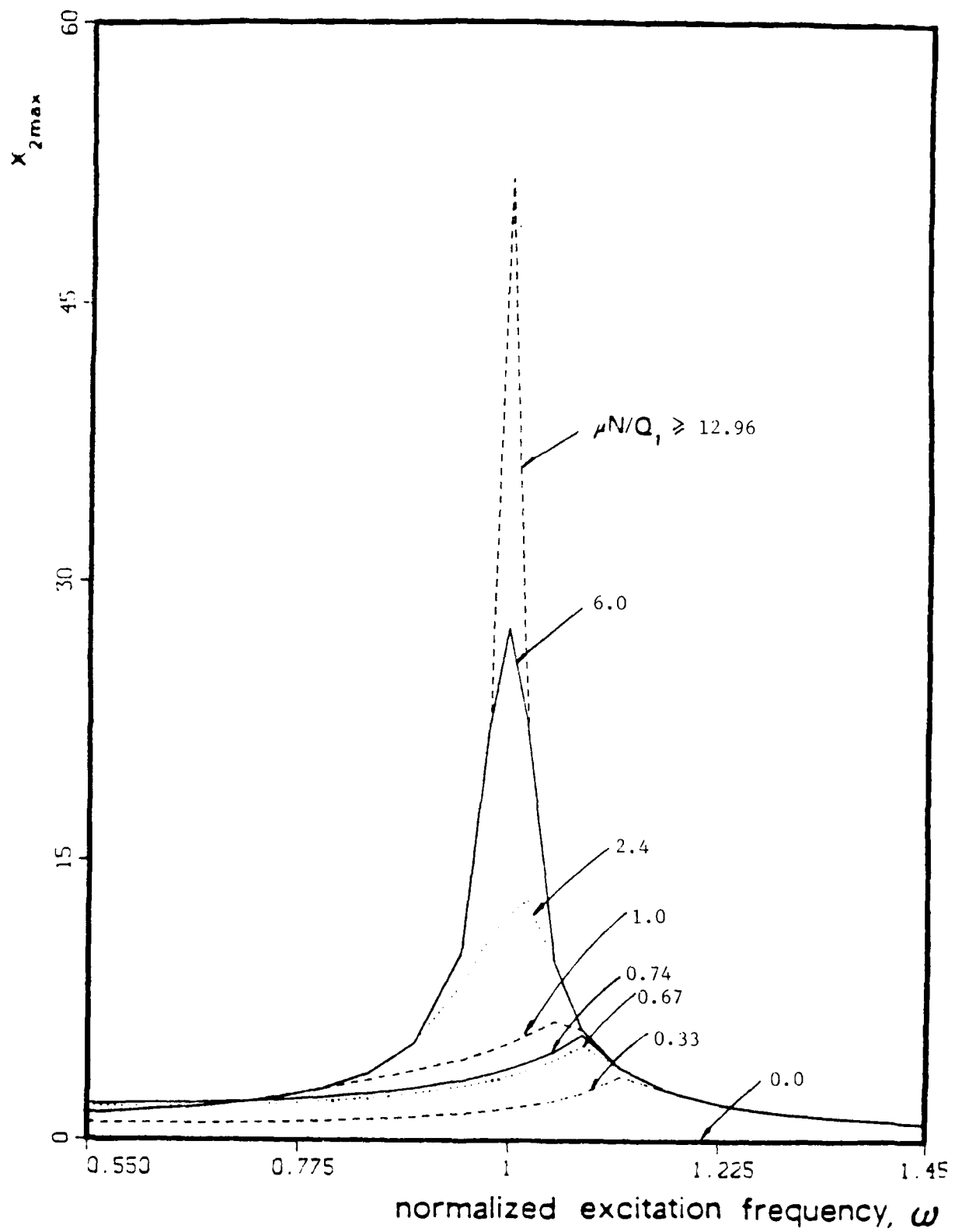


Fig. 6: Maximum Exact Displacement of Mass M_2 of Fig. 1.

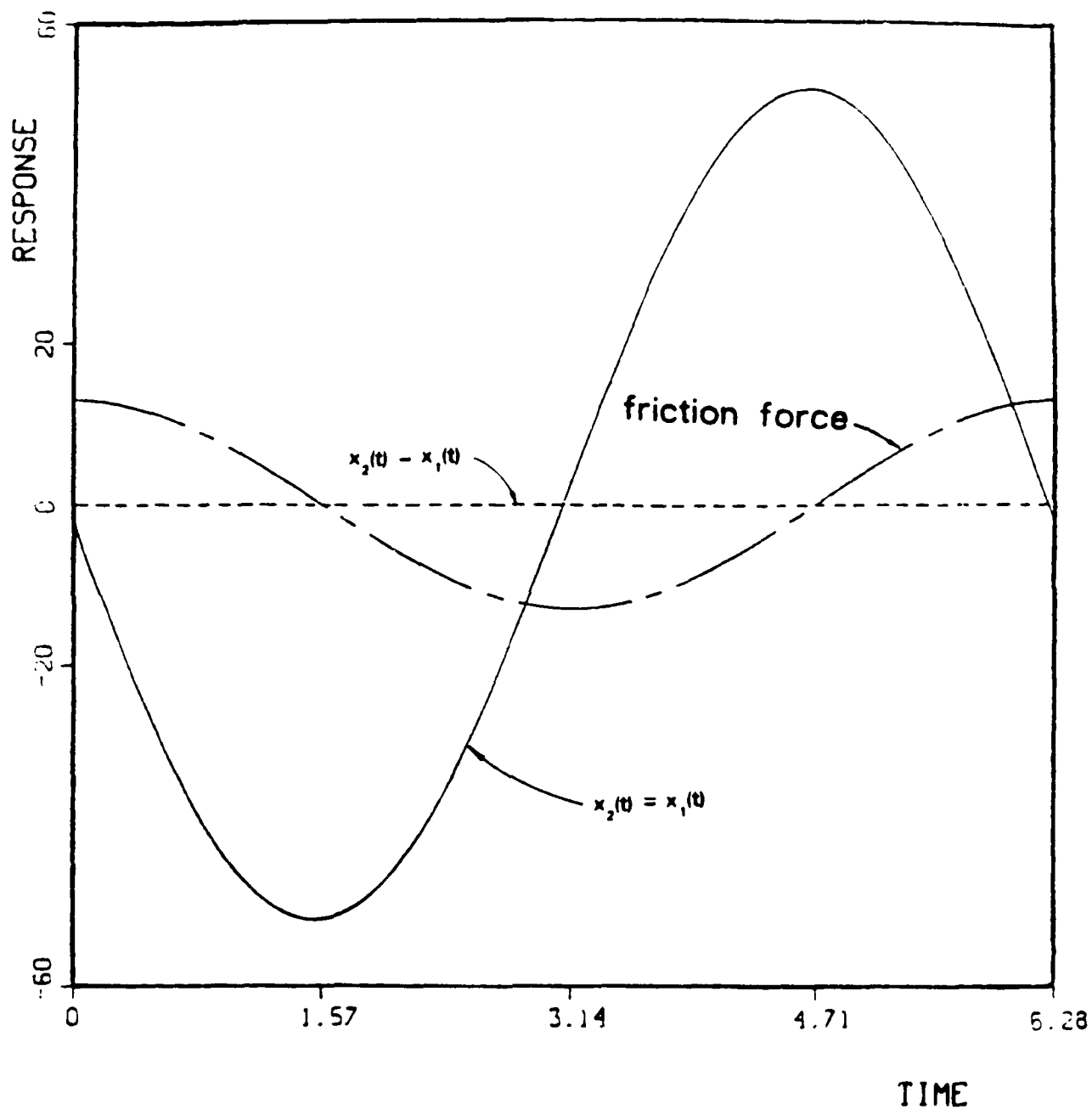


Fig. 7: Exact Response Time Histories for a Case with the Joint Stuck
(Case I of Table 1. $\mu N/Q_1 \geq 12.96$, $\omega=1.0$)

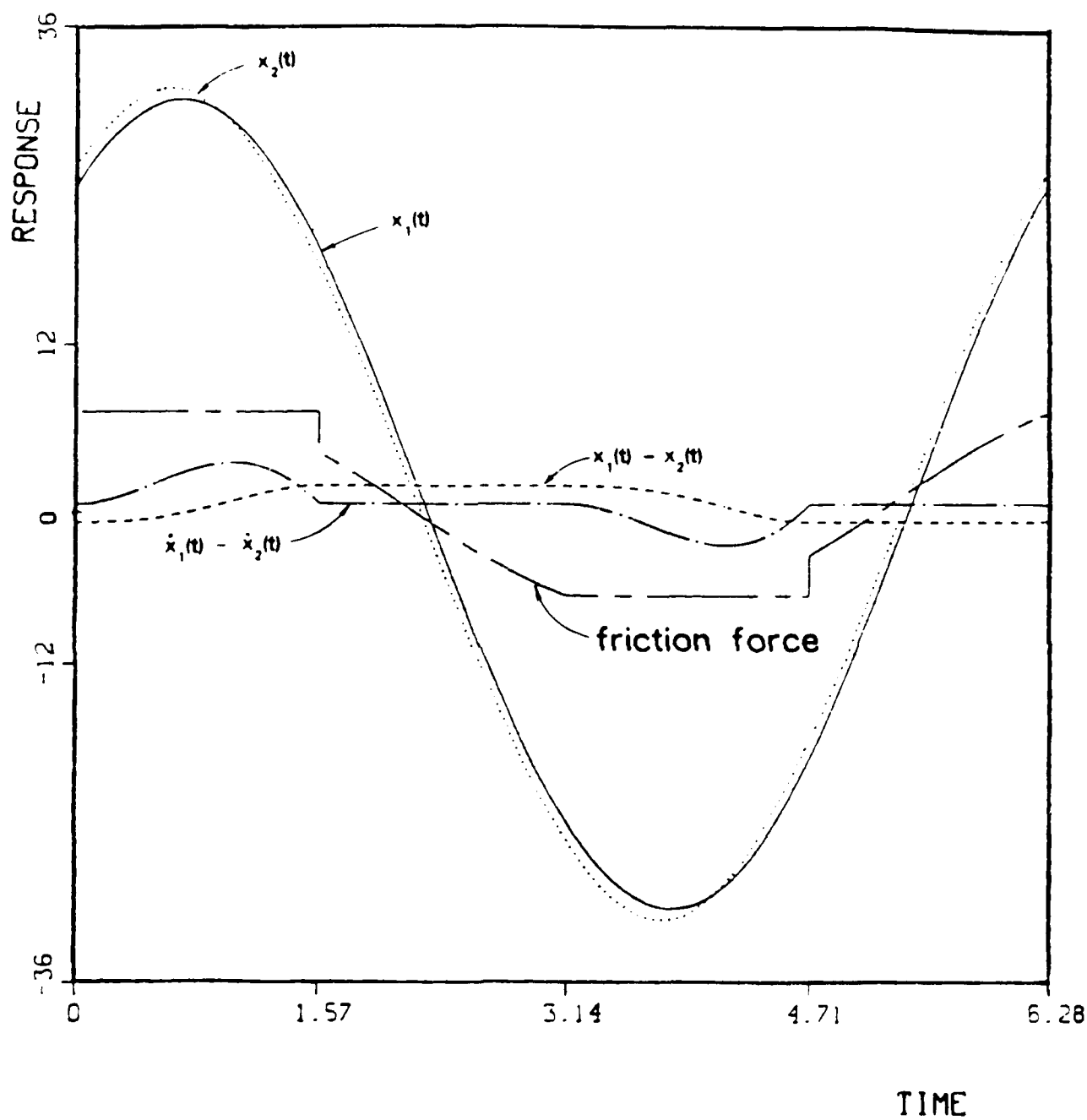


Fig. 8: Exact Response Time Histories for a Partial-Slip Case.
(Case I of Table 1, $\mu N/Q_1 = 6.91$, $\omega = 1.0$)

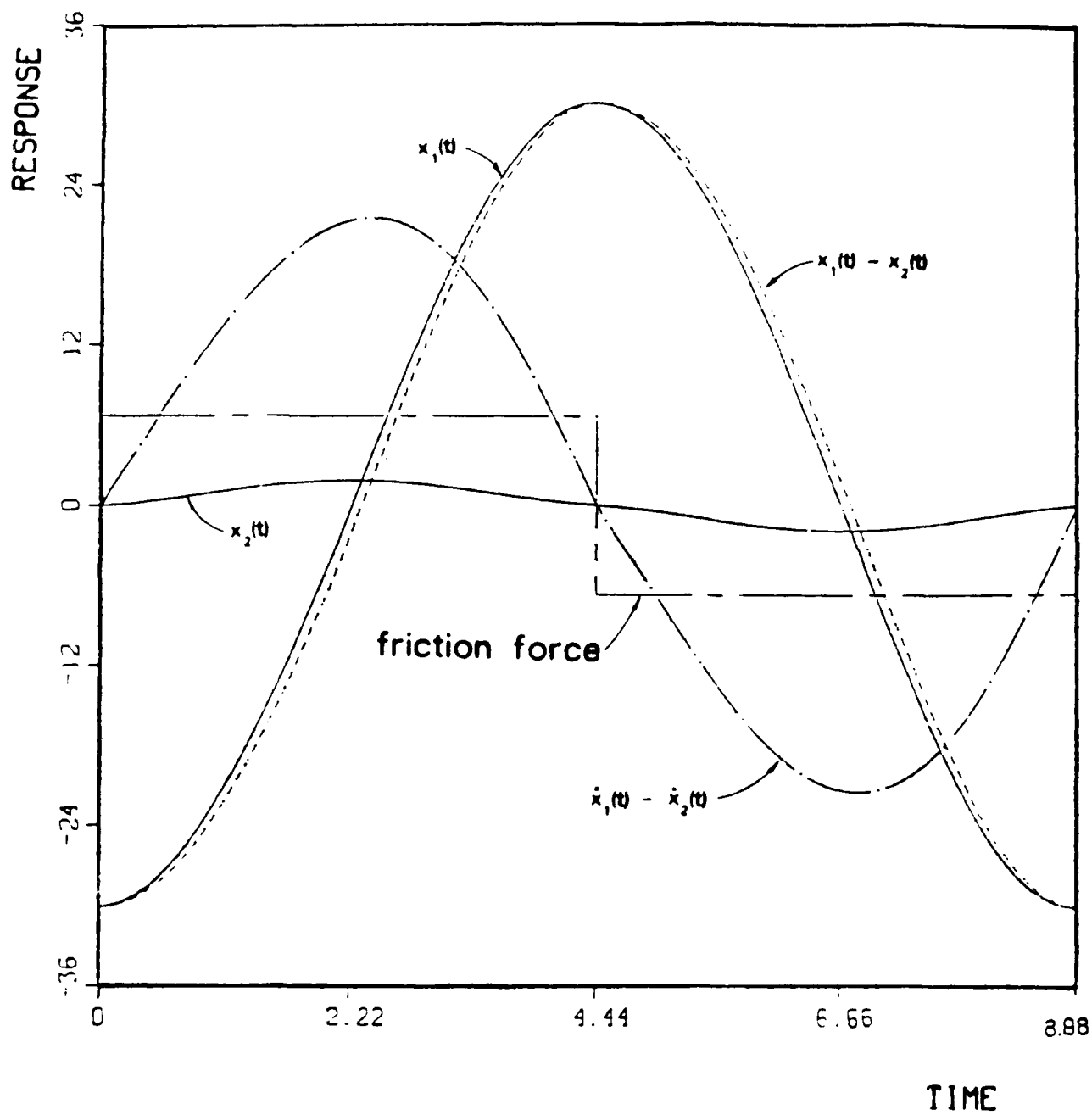


Fig. 9: Exact Response Time Histories for a Pure-Slip Case.
(Case I of Table 1, $\mu N/Q_1 = 0.67$, $\omega = 1.41$)

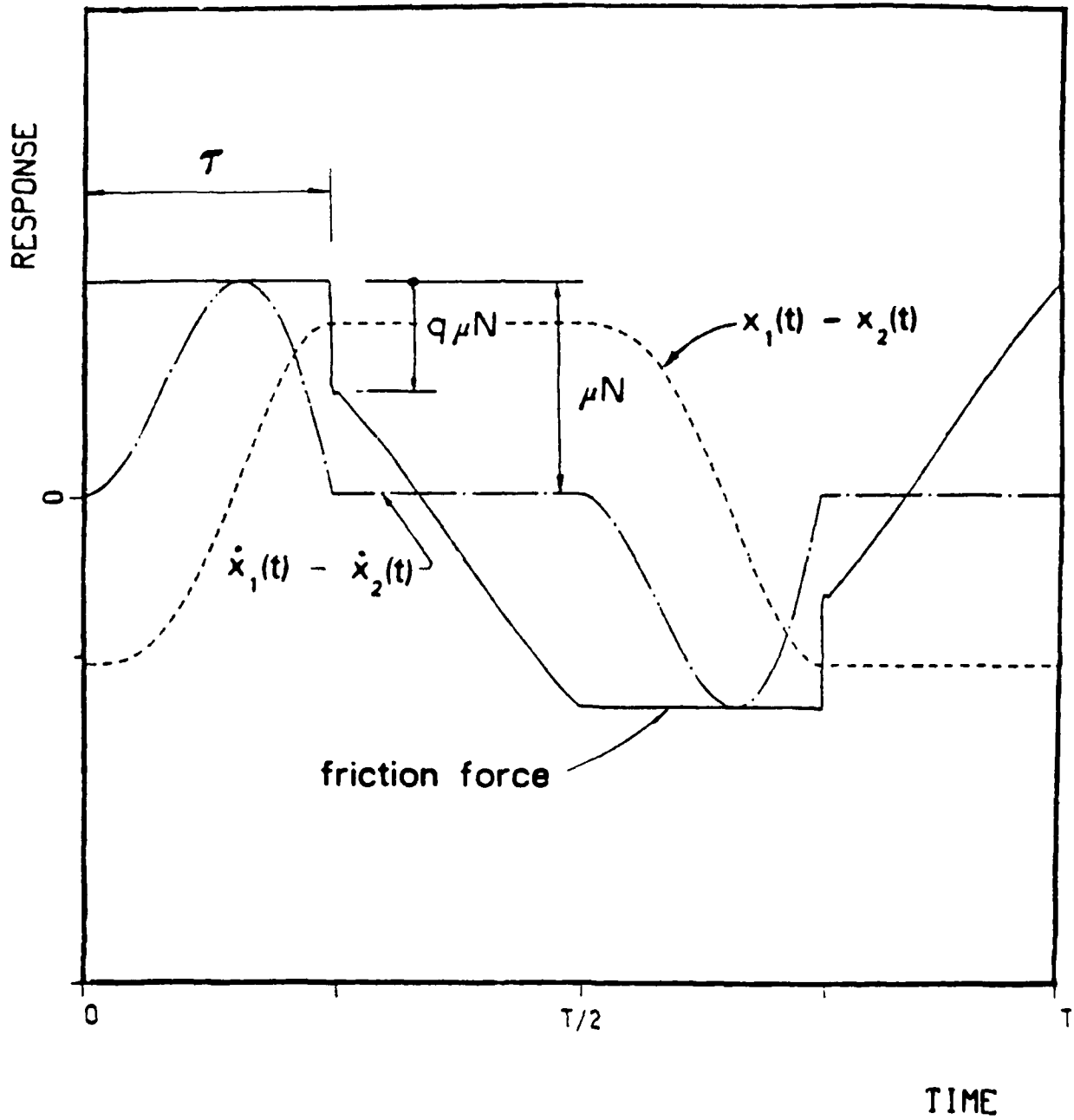


Fig. 10: Discontinuities in Response Functions in a Case of Partial Slip in the Joint.

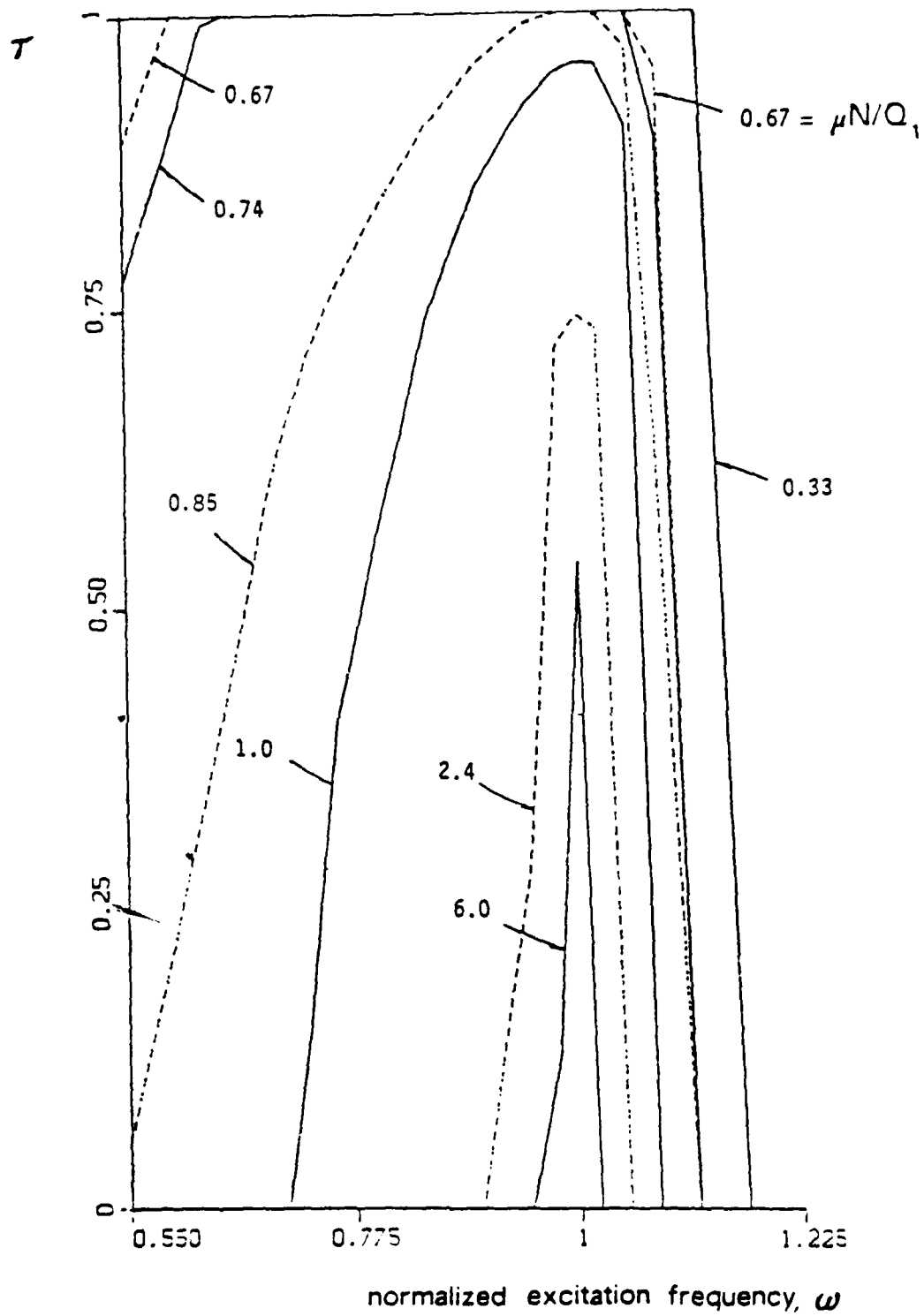


Fig. 11: Normalized Slipping Time for Case I of Table 1.
(τ is defined in Fig. 10.)

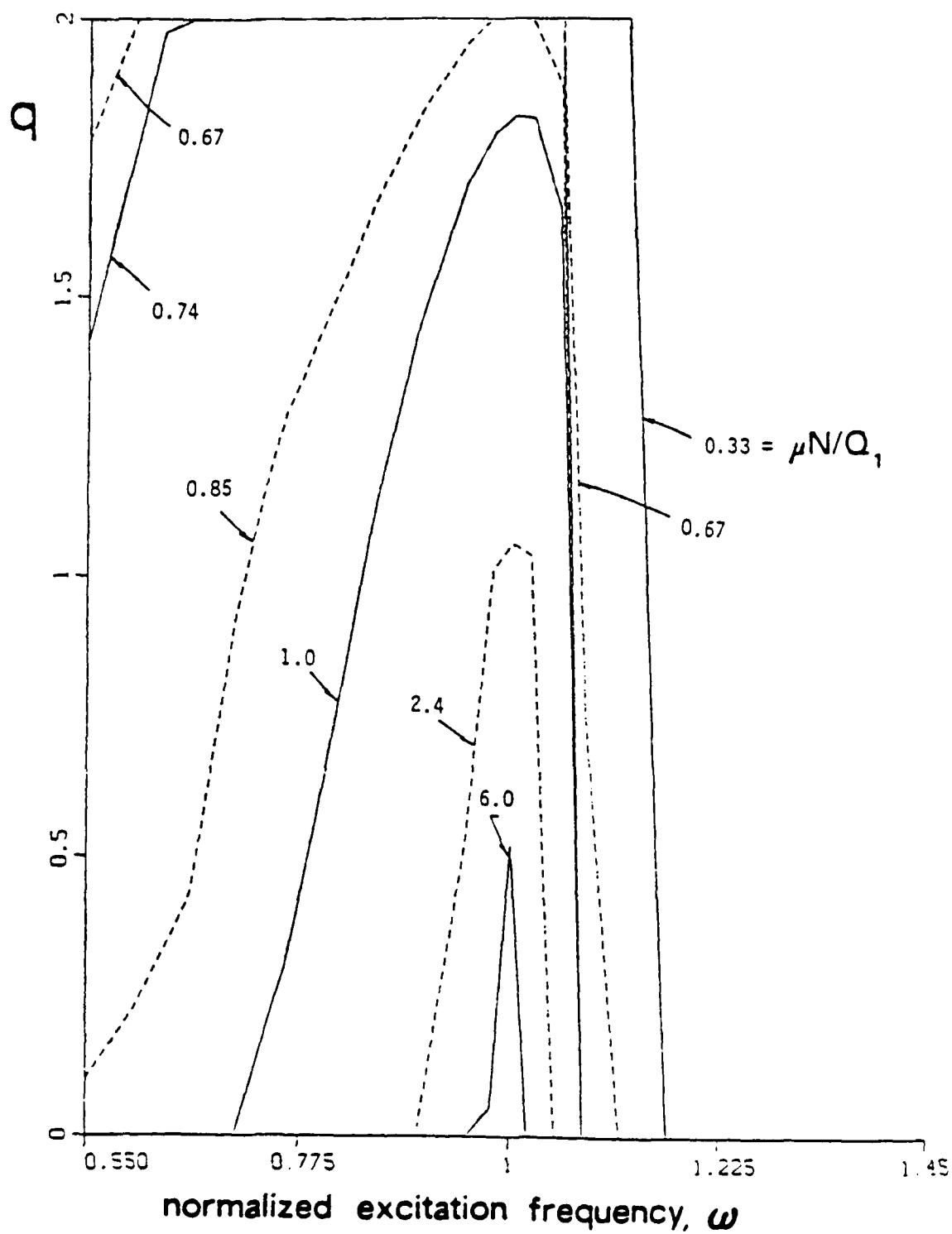


Fig. 12: Discontinuity in the Slip Force in a Case of Partial Slip.
(q is defined in Fig. 10)

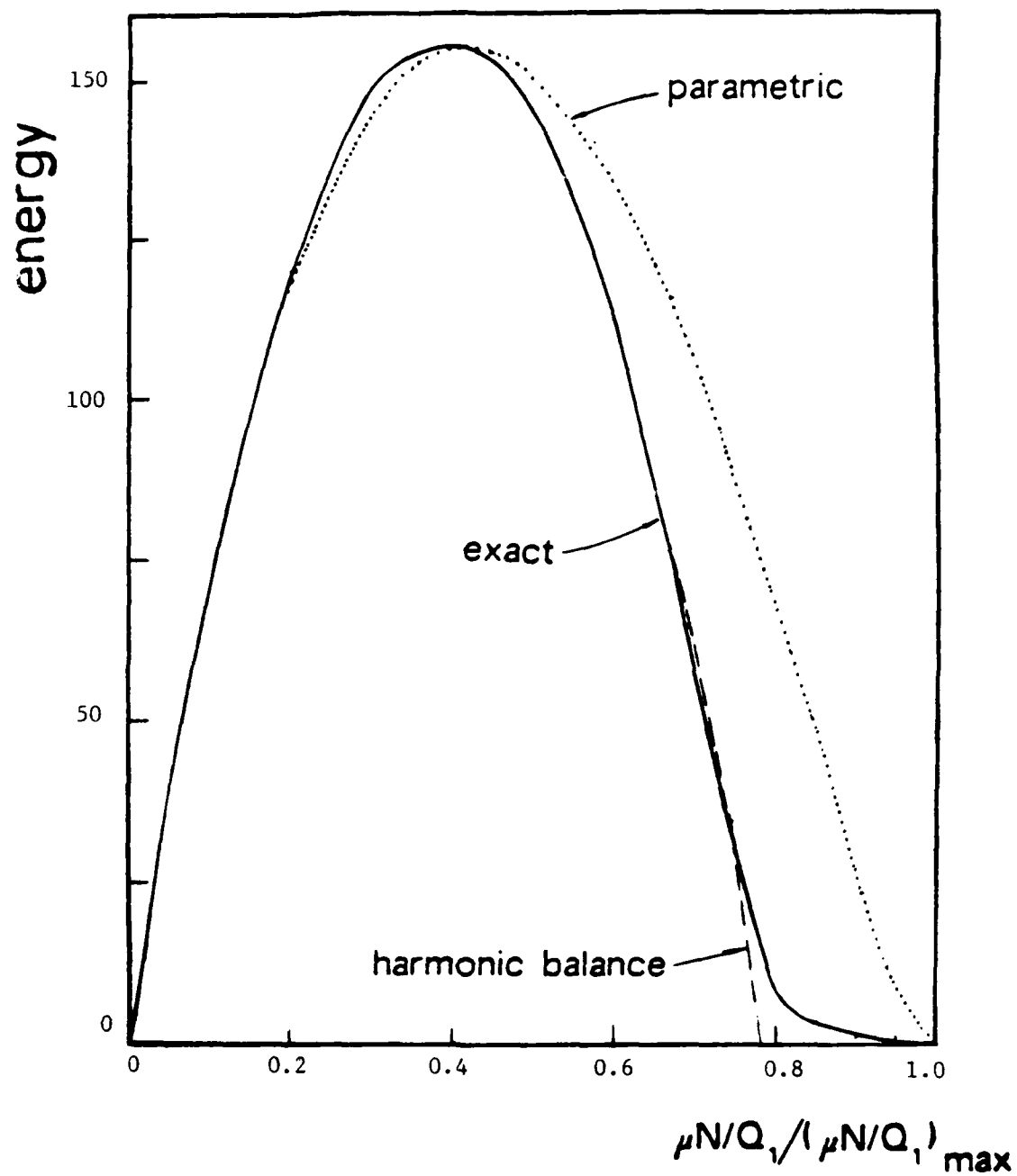


Fig. 13: Energy Dissipated per Cycle. Case 1 of Table 1, $\omega=0.7071$.

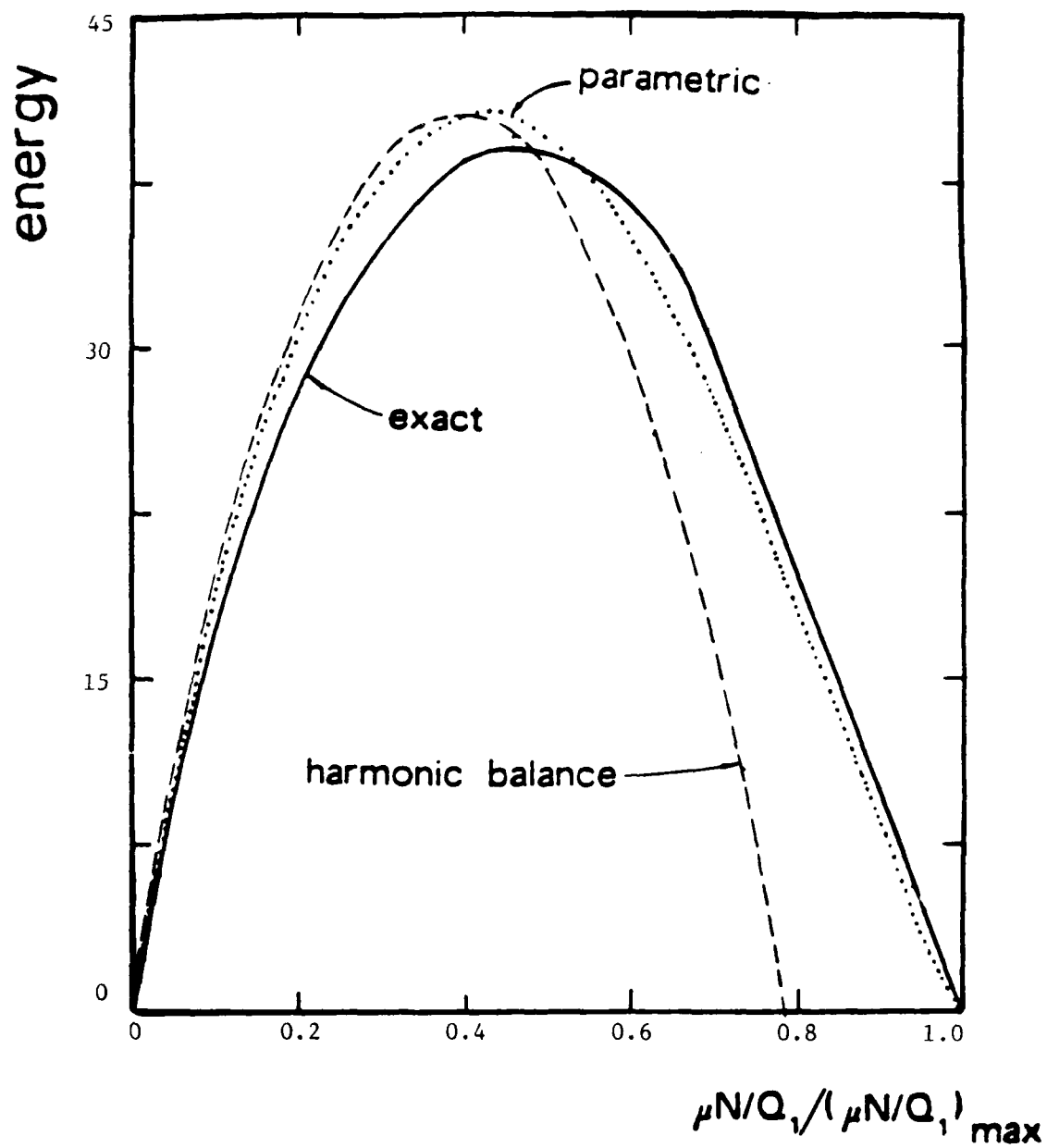


Fig. 14: Energy Dissipated per Cycle. Case I of Table 1, $\omega=1.0$.

energy

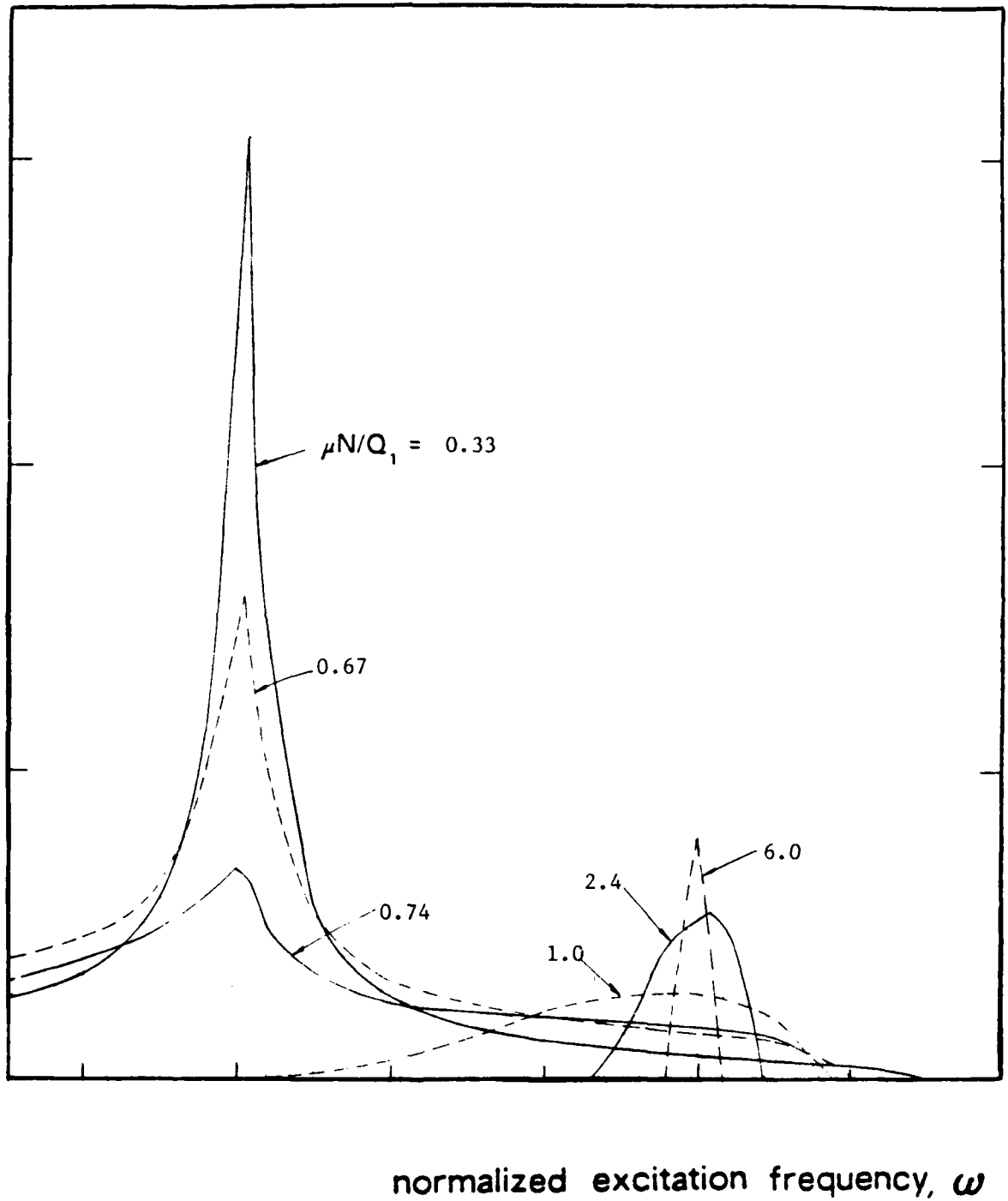


Fig. 15: Variation with Frequency of the Energy Dissipated per Cycle for Case I of Table 1.

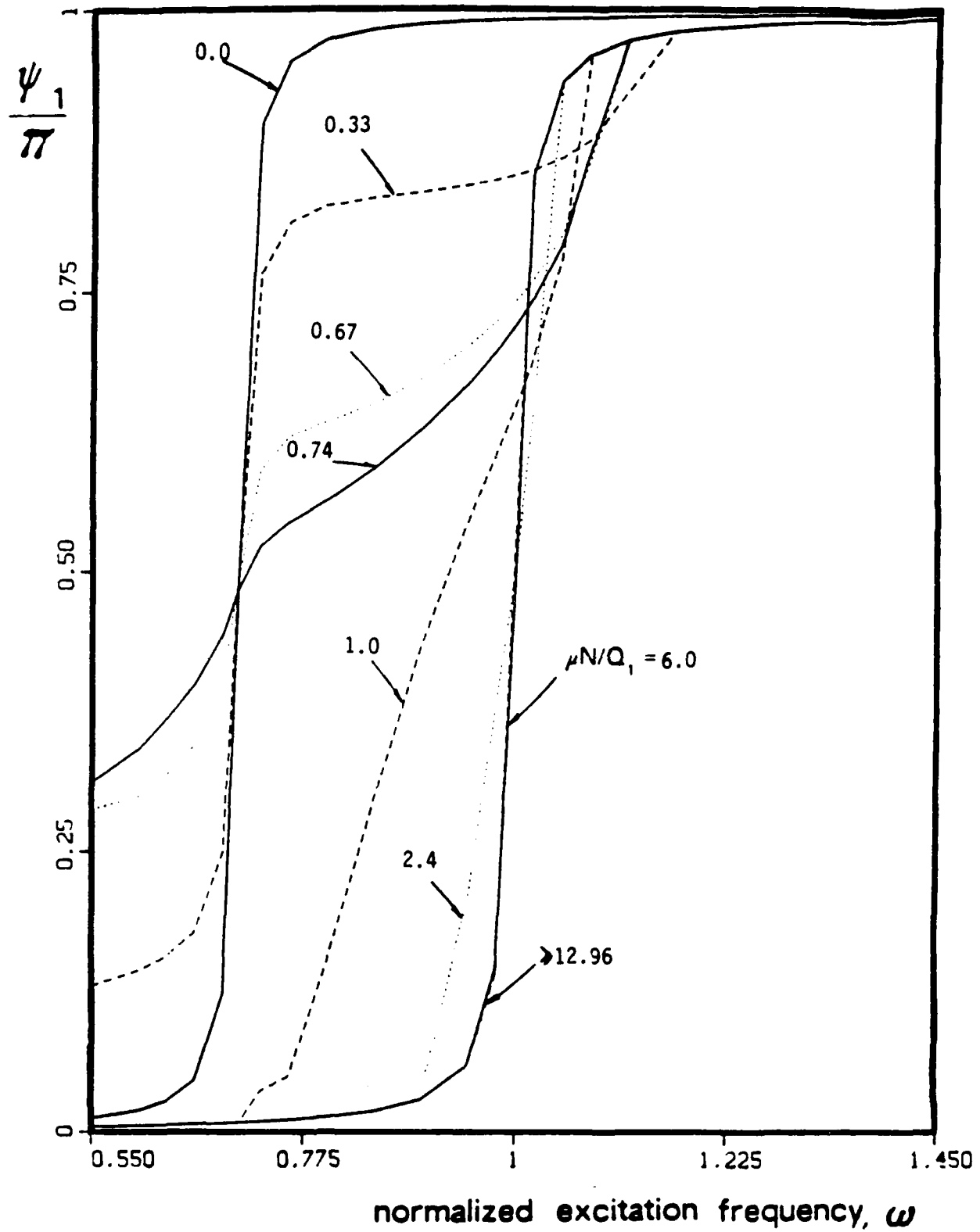


Fig. 16: Phase Angle of the Displacement of Mass M_1 of Fig. 1.

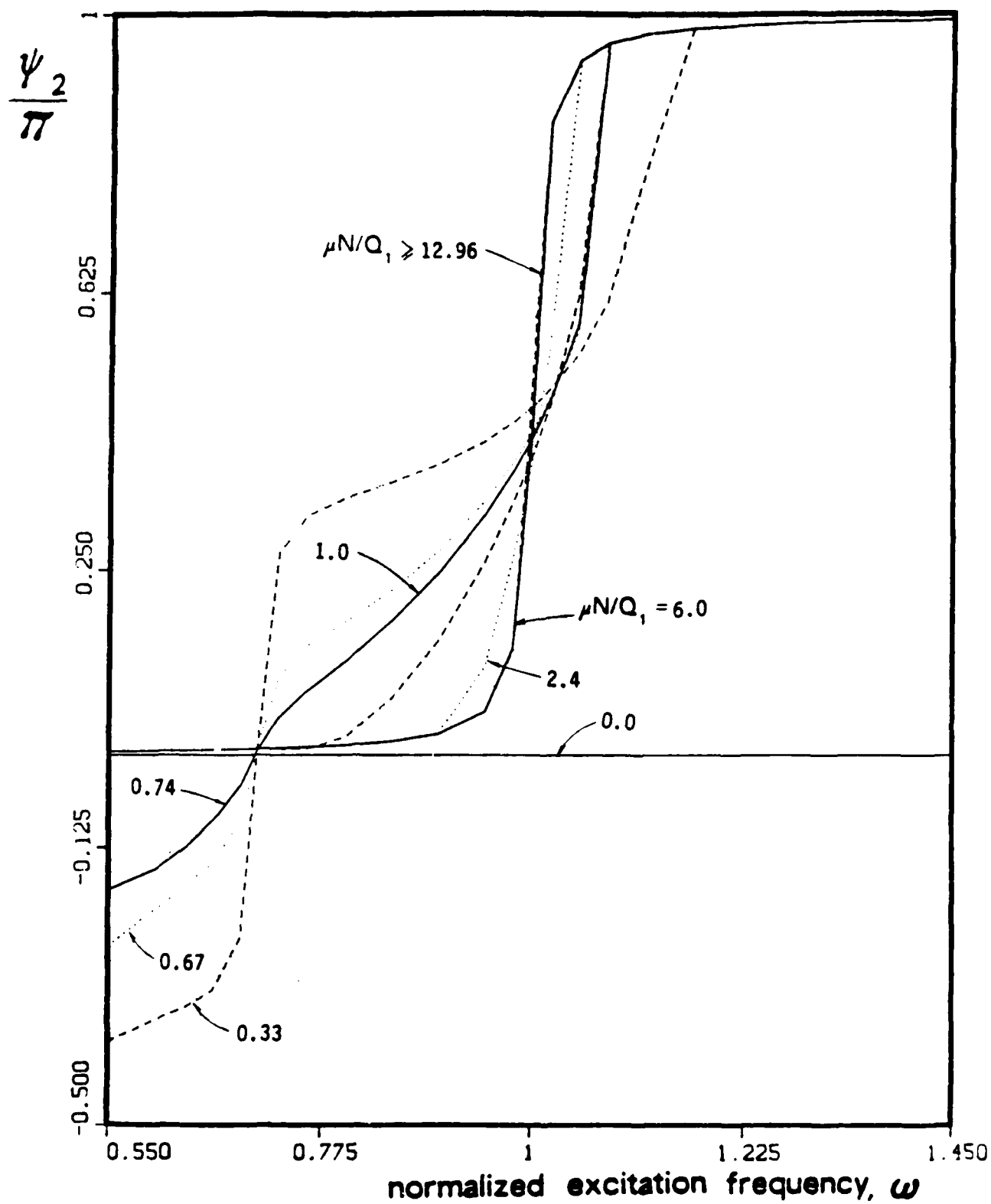


Fig. 17: Phase Angle of the Displacement of Mass M_2 of Fig. 1.

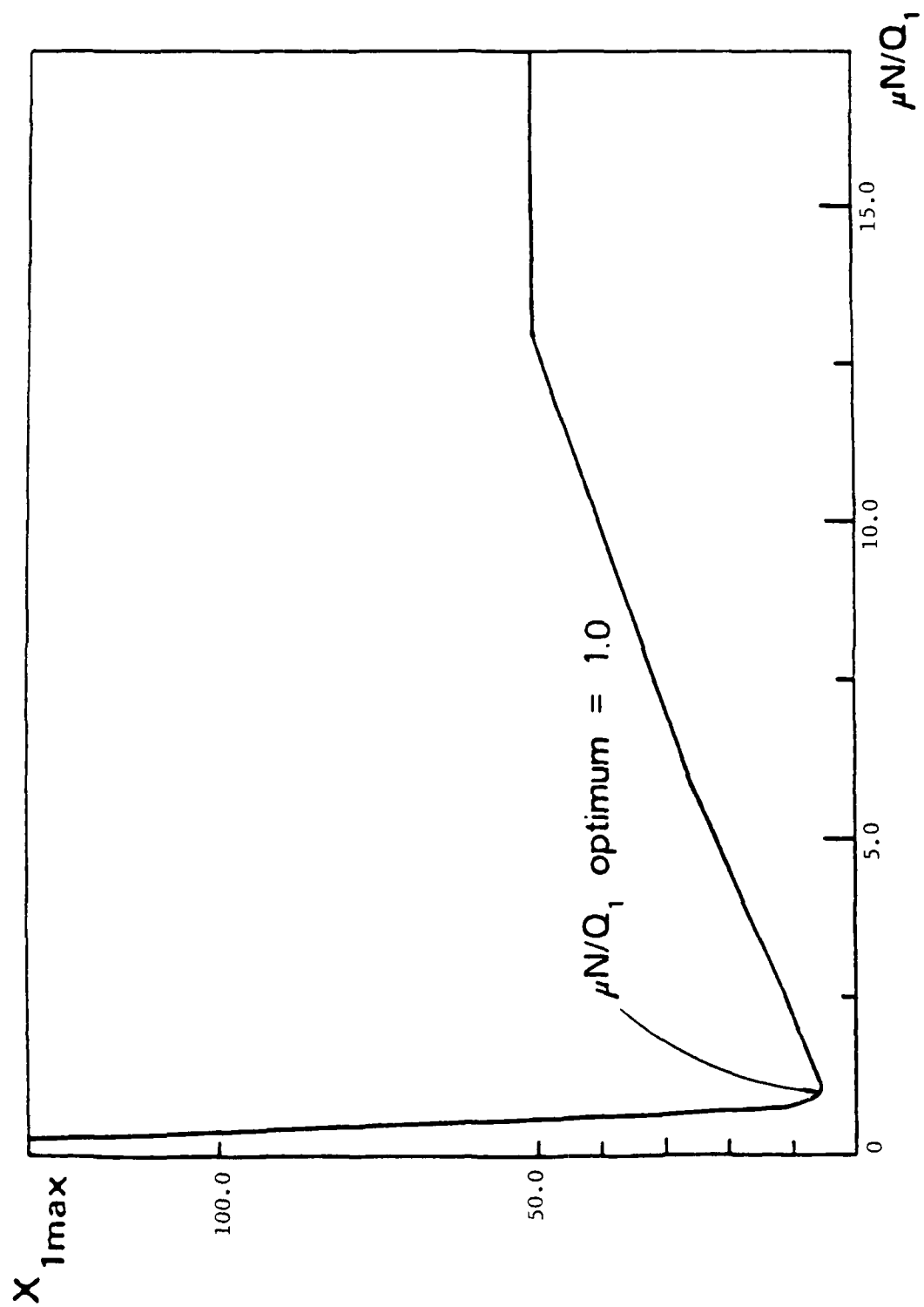


Fig. 18: Optimization Curve for Case 1 of Table 1.

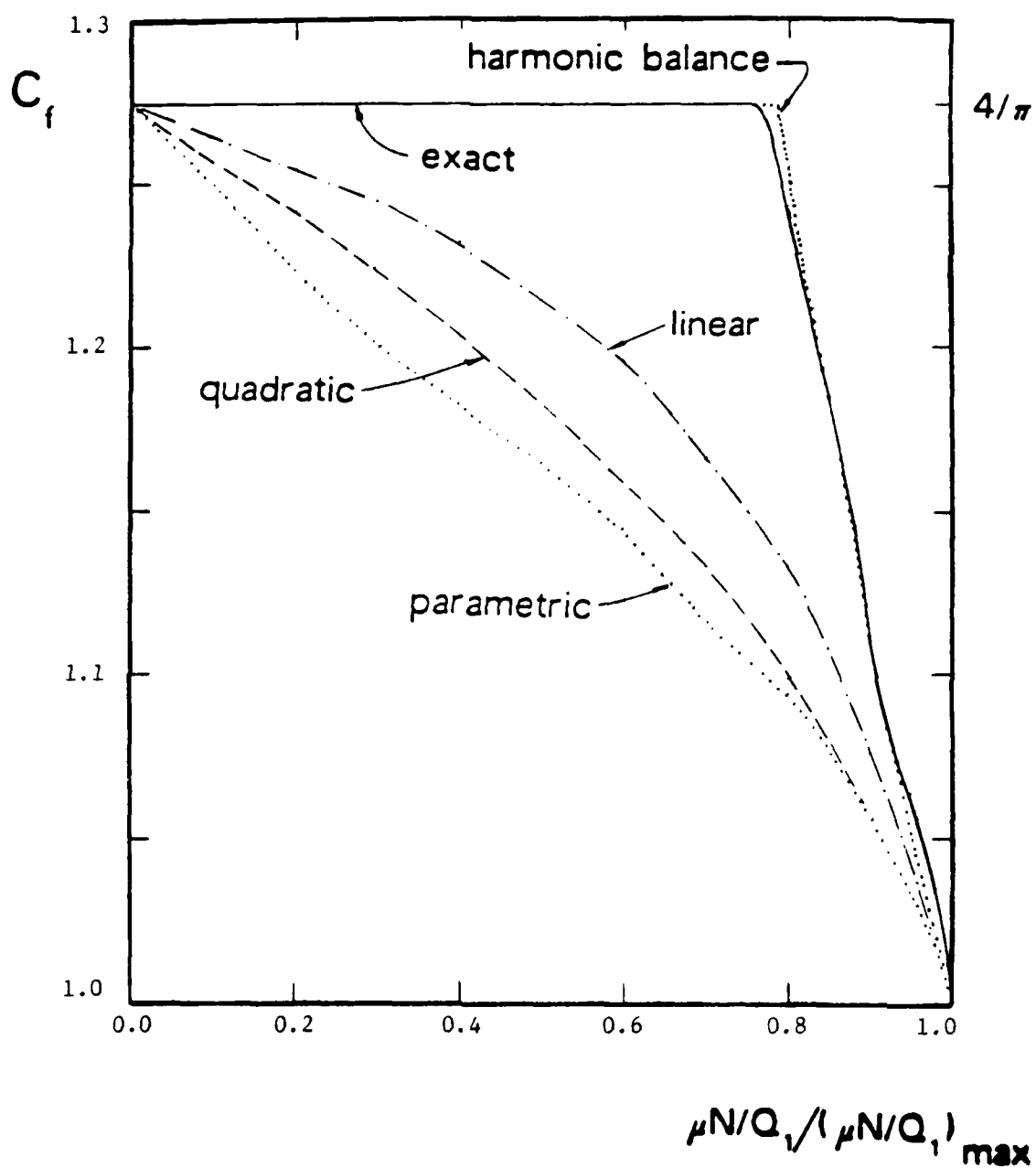


Fig. 19: First Fourier Coefficient of the Friction Force.
Case I of Table 1, $\omega=0.7071$.

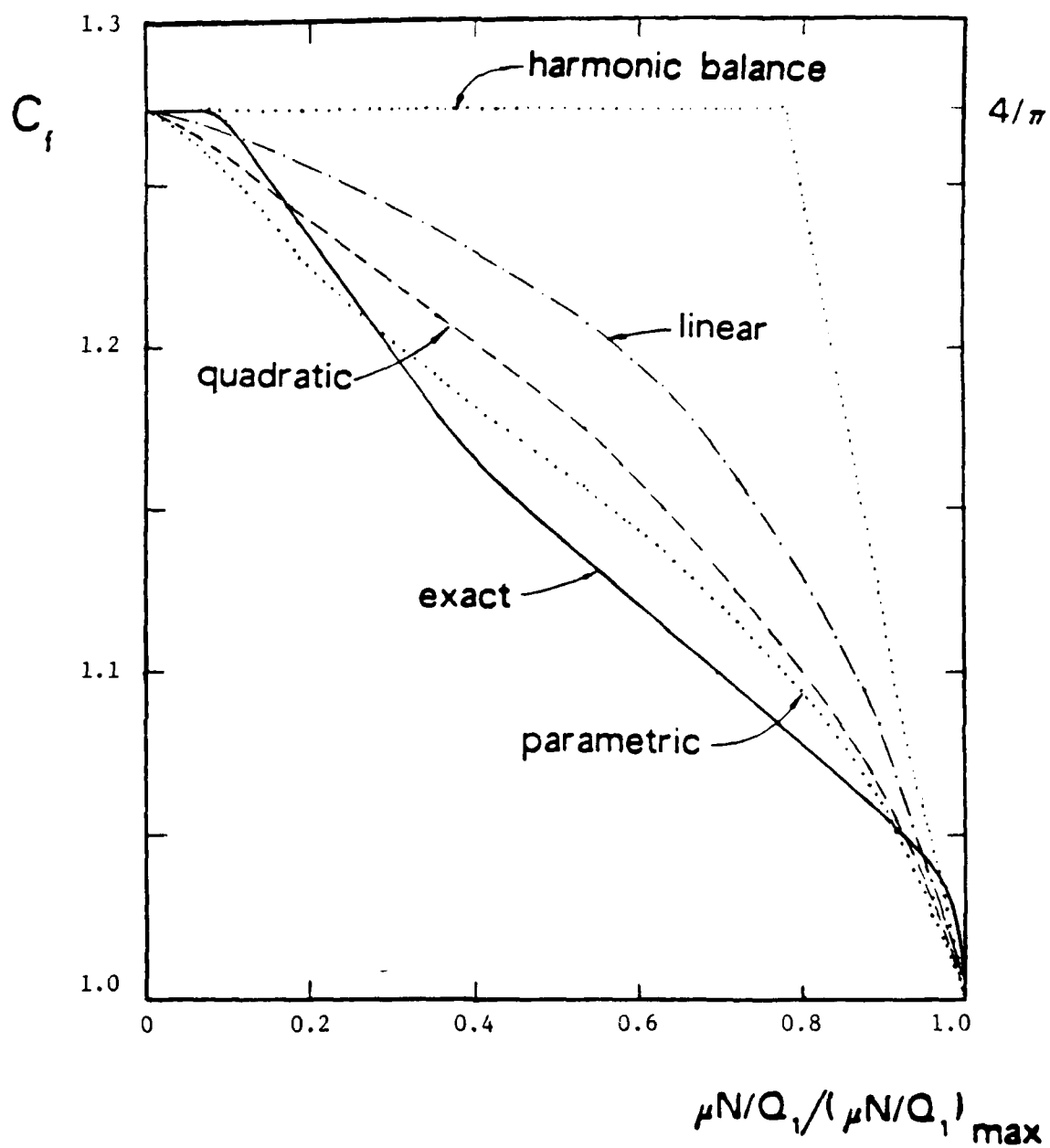


Fig. 20: First Fourier Coefficient of the Friction Force.
Case I of Table 1, $\omega=1.0$.

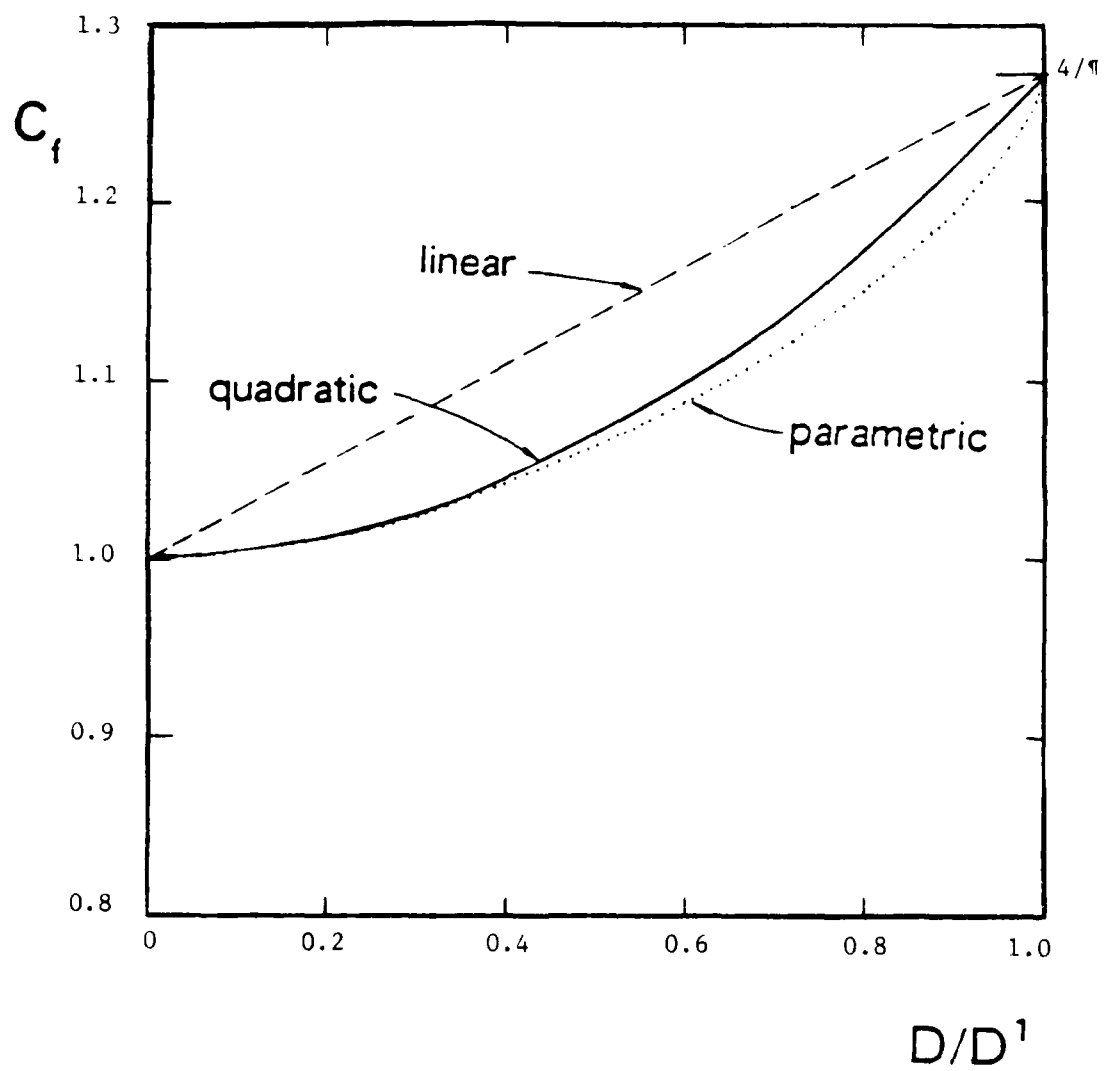


Fig. 21: Variation of C_f with D in the Approximate Harmonic Balance Methods

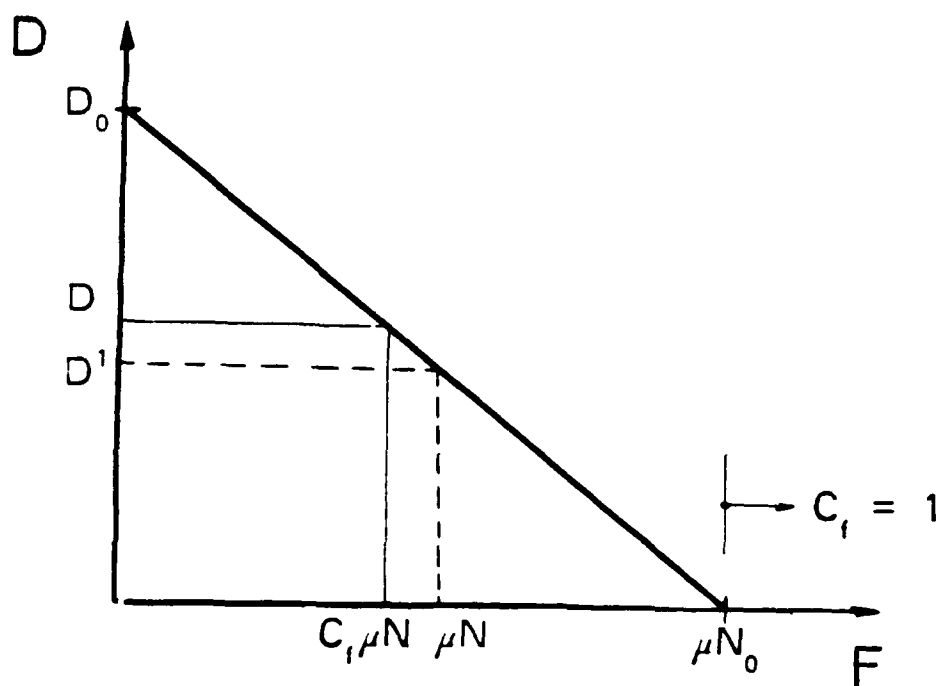


Fig. 22: Assumed D-F Curve to Compute D/D'

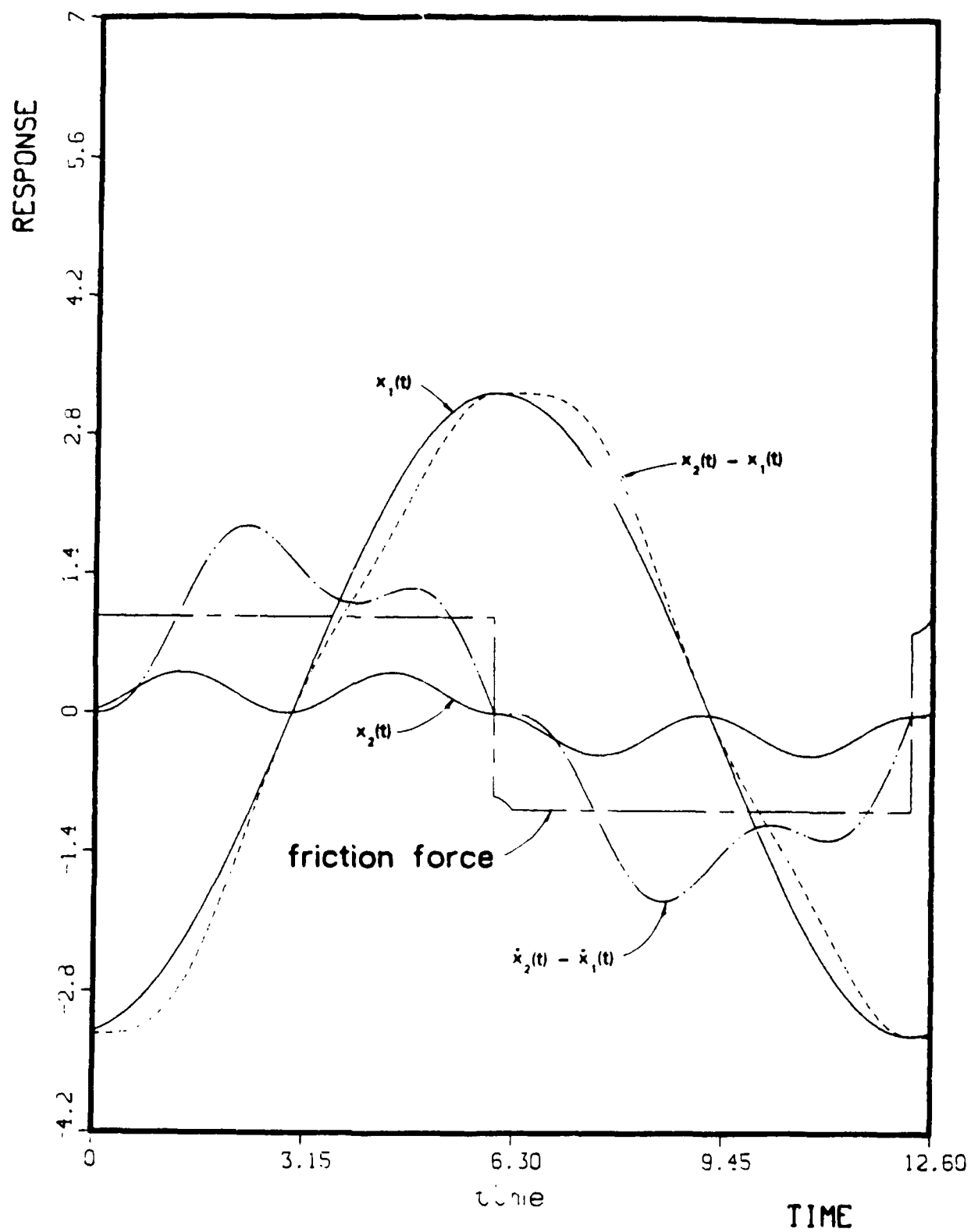


Fig. 23: Response Time Histories for Case II of Table 1.

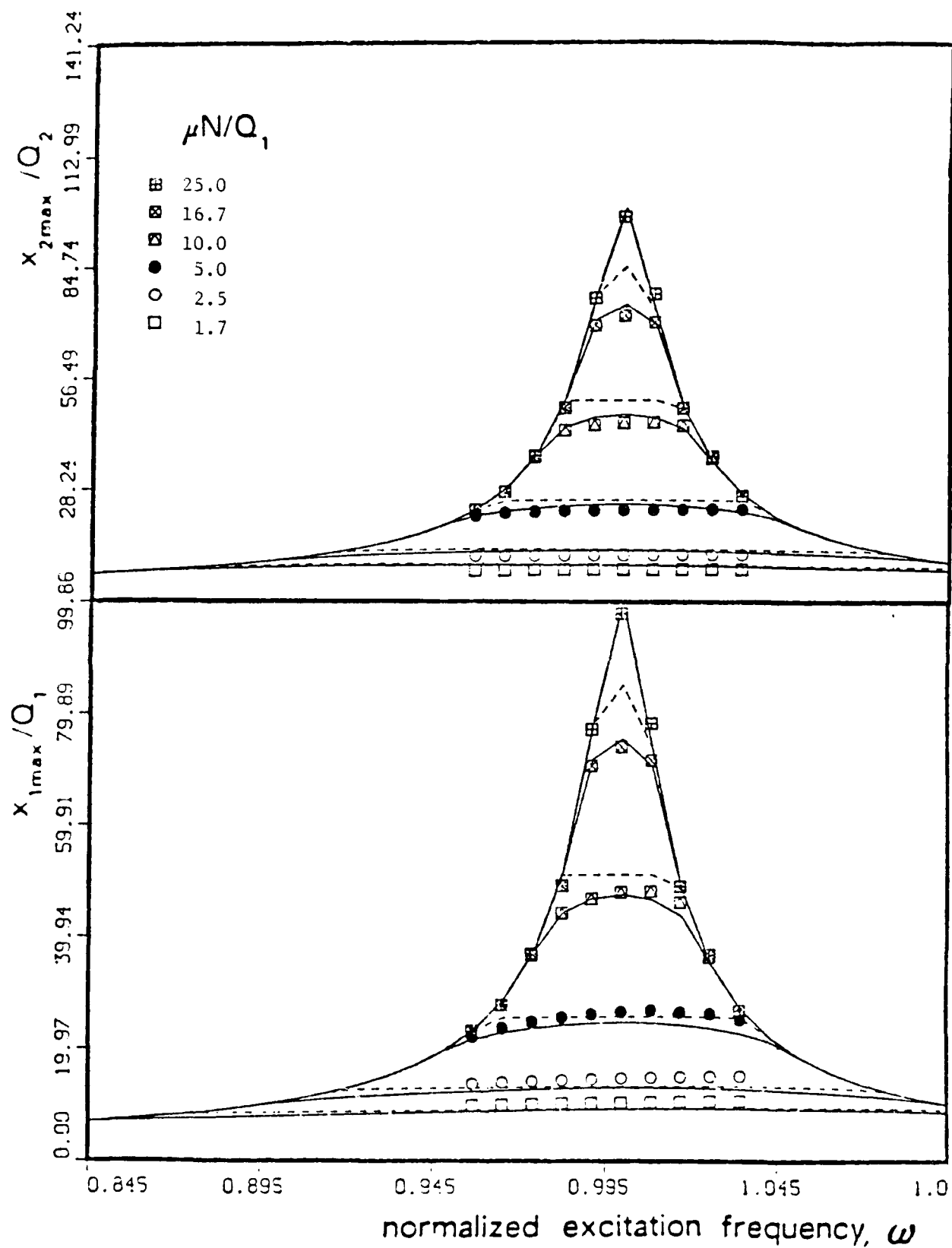


Fig. 24: Comparison of Exact and Approximate Results. Case III of Table 1.

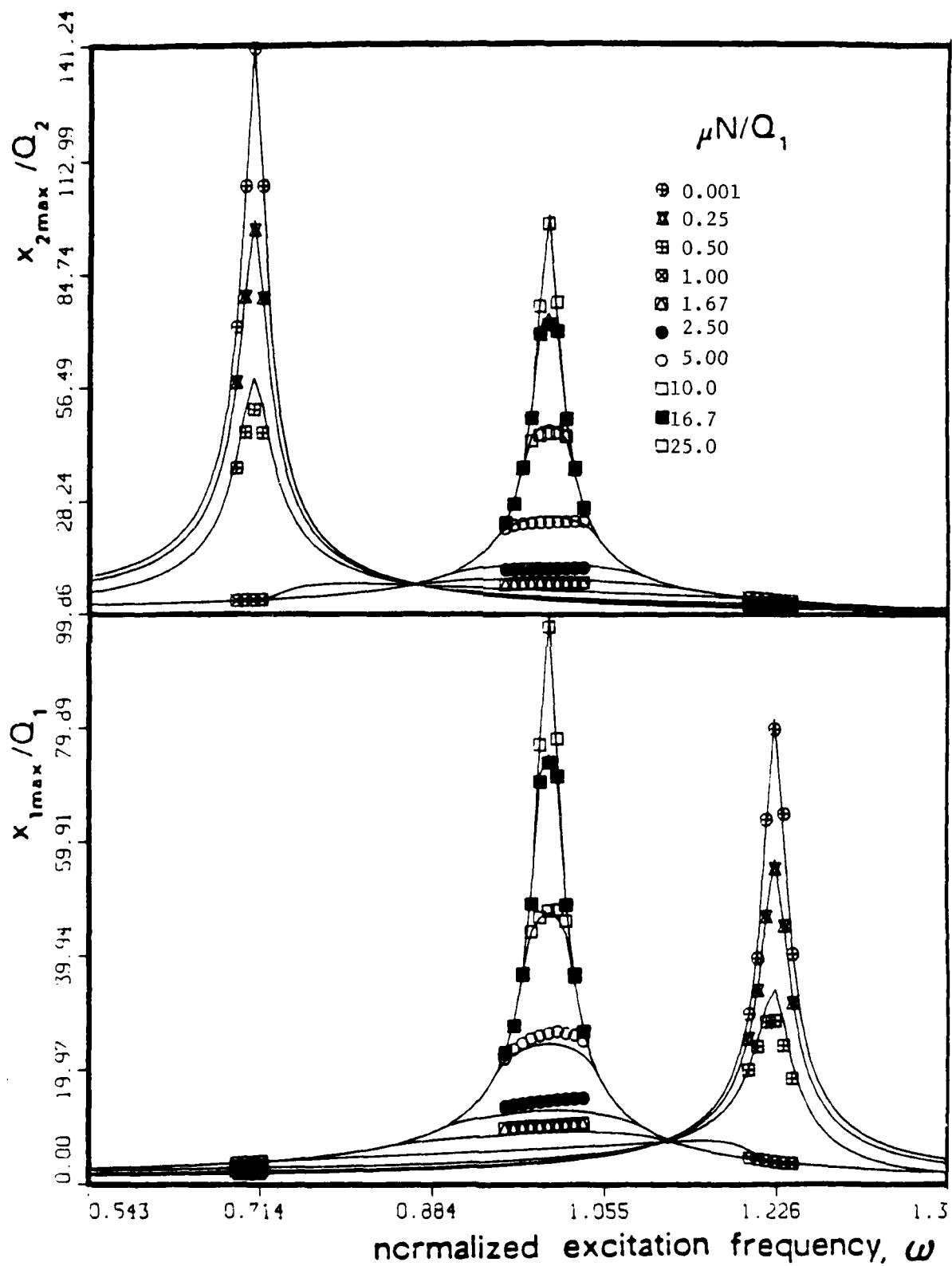


Fig. 25: Comparison of Exact and Approximate Results. Case IV of Table 1.

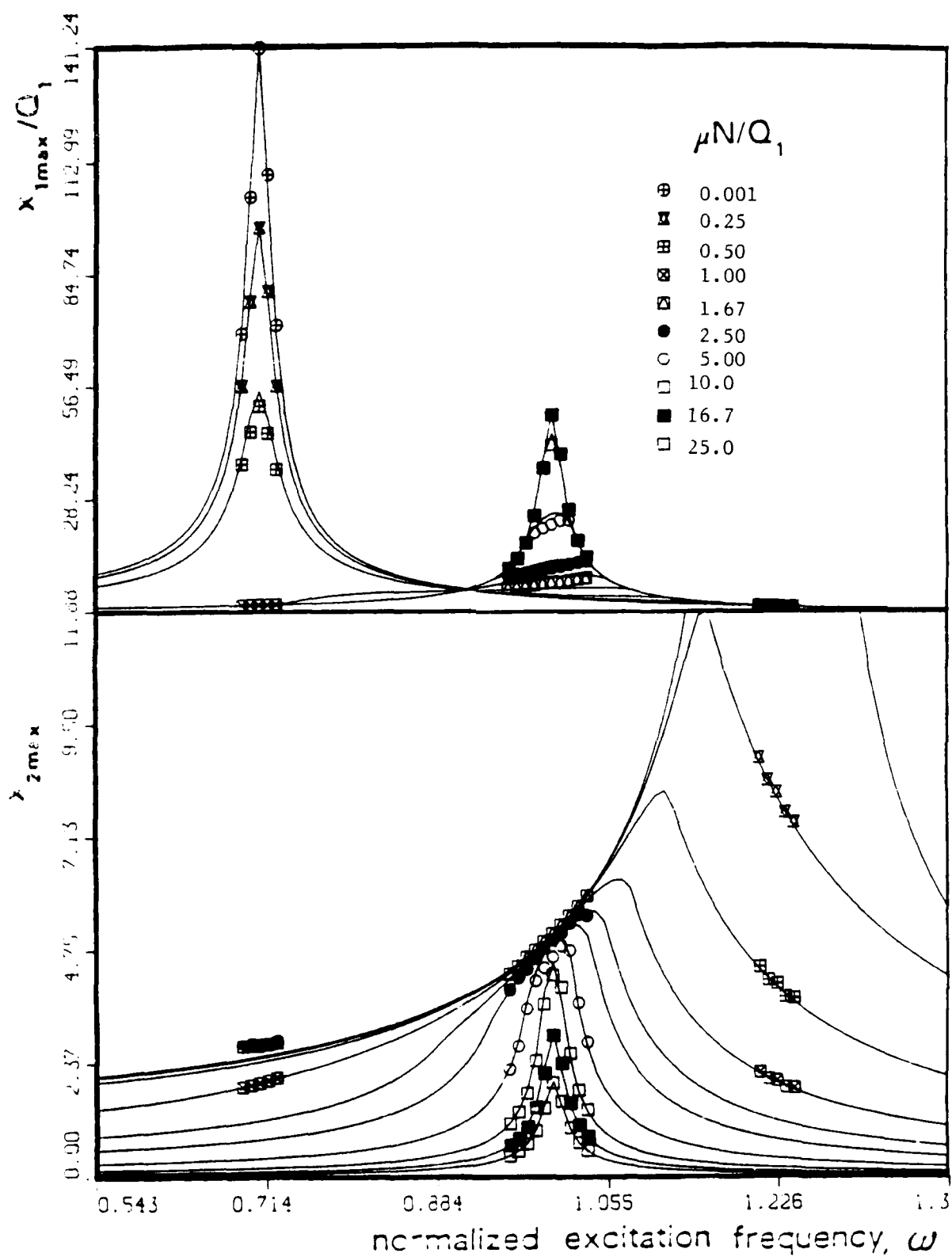


Fig. 26: Comparison of Exact and Approximate Results. Case V of Table 1.

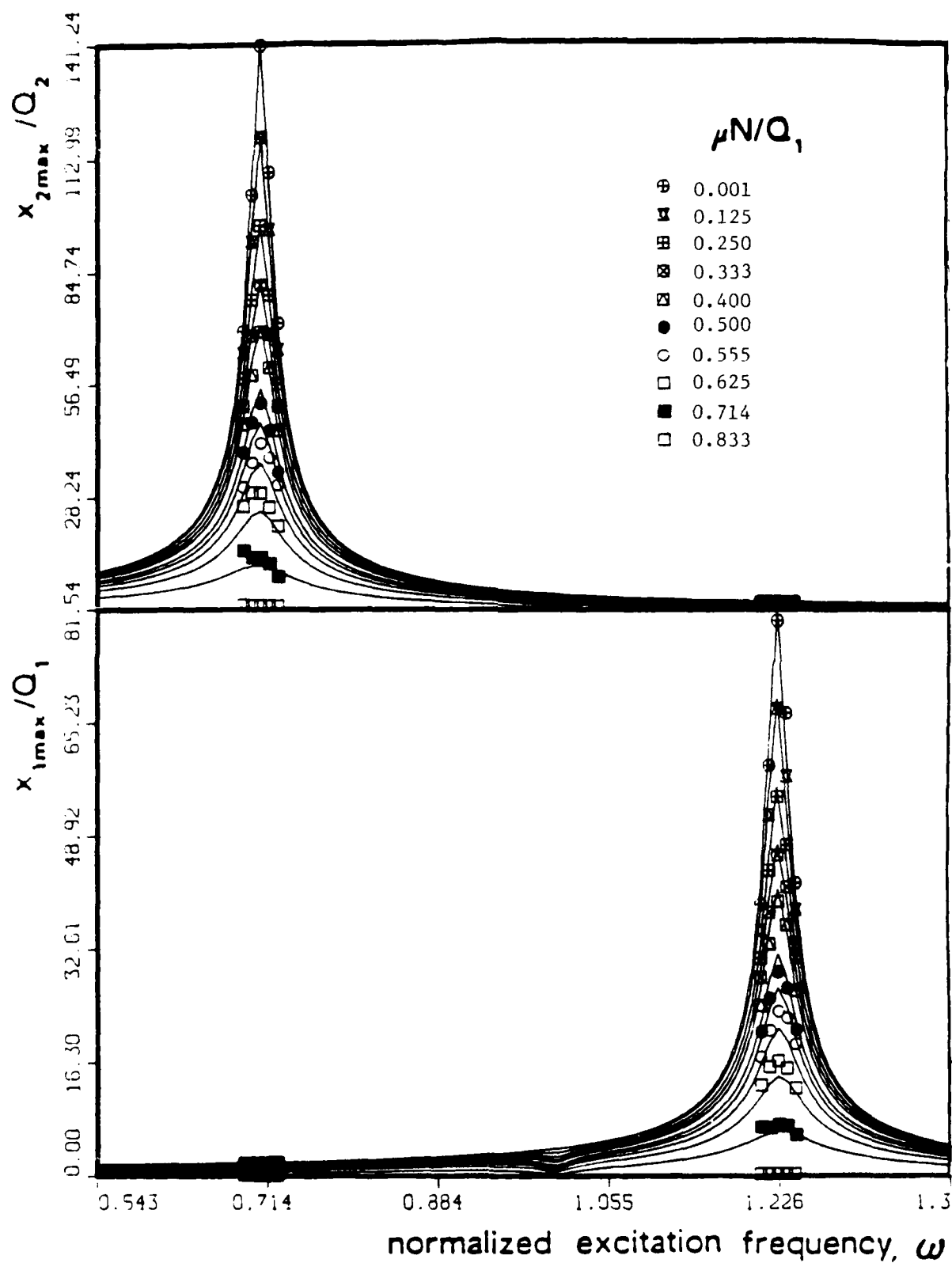


Fig. 27: Comparison of Exact and Approximate Results. Case VI of Table 1.

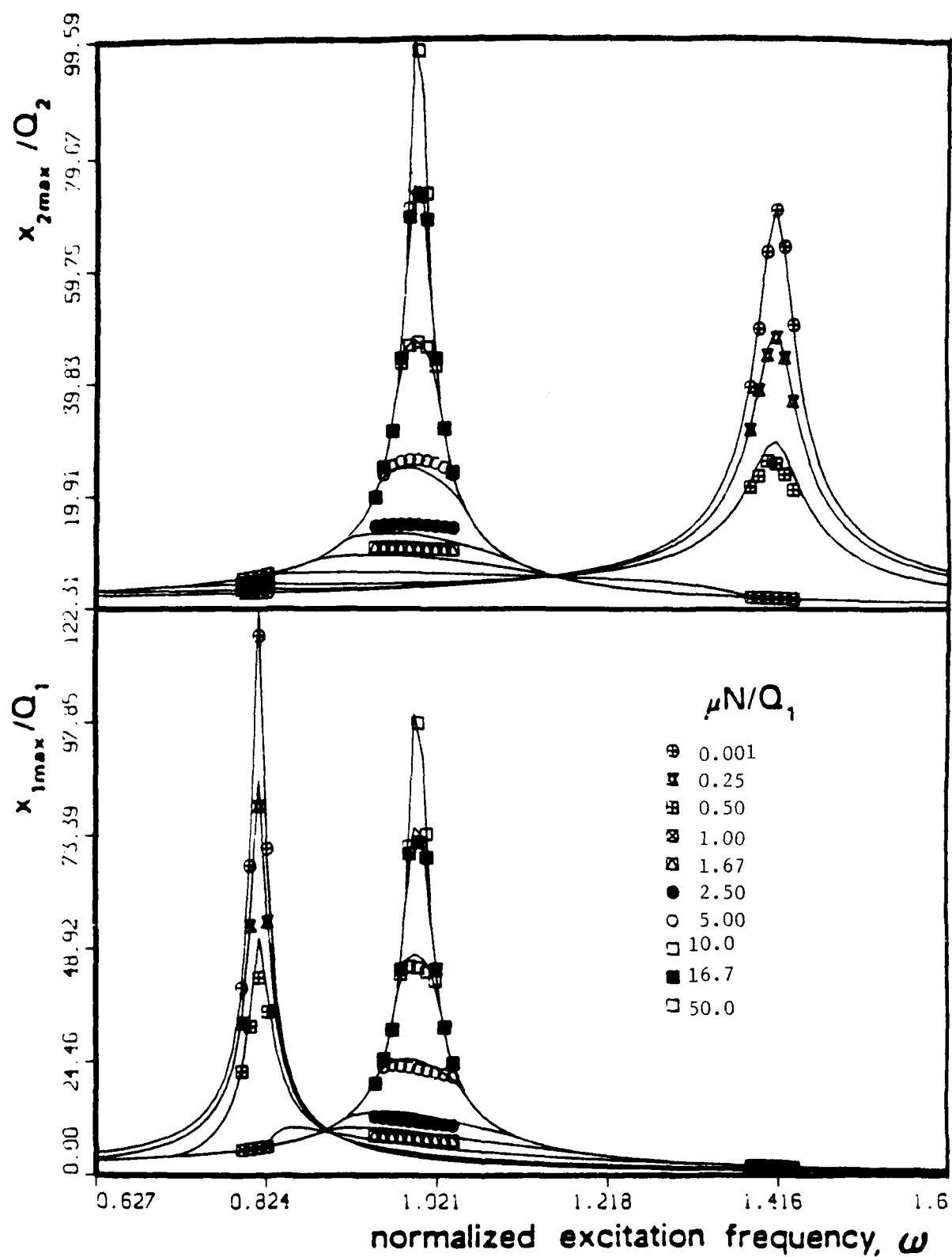


Fig. 28: Comparison of Exact and Approximate Results. Case VII of Table 1.

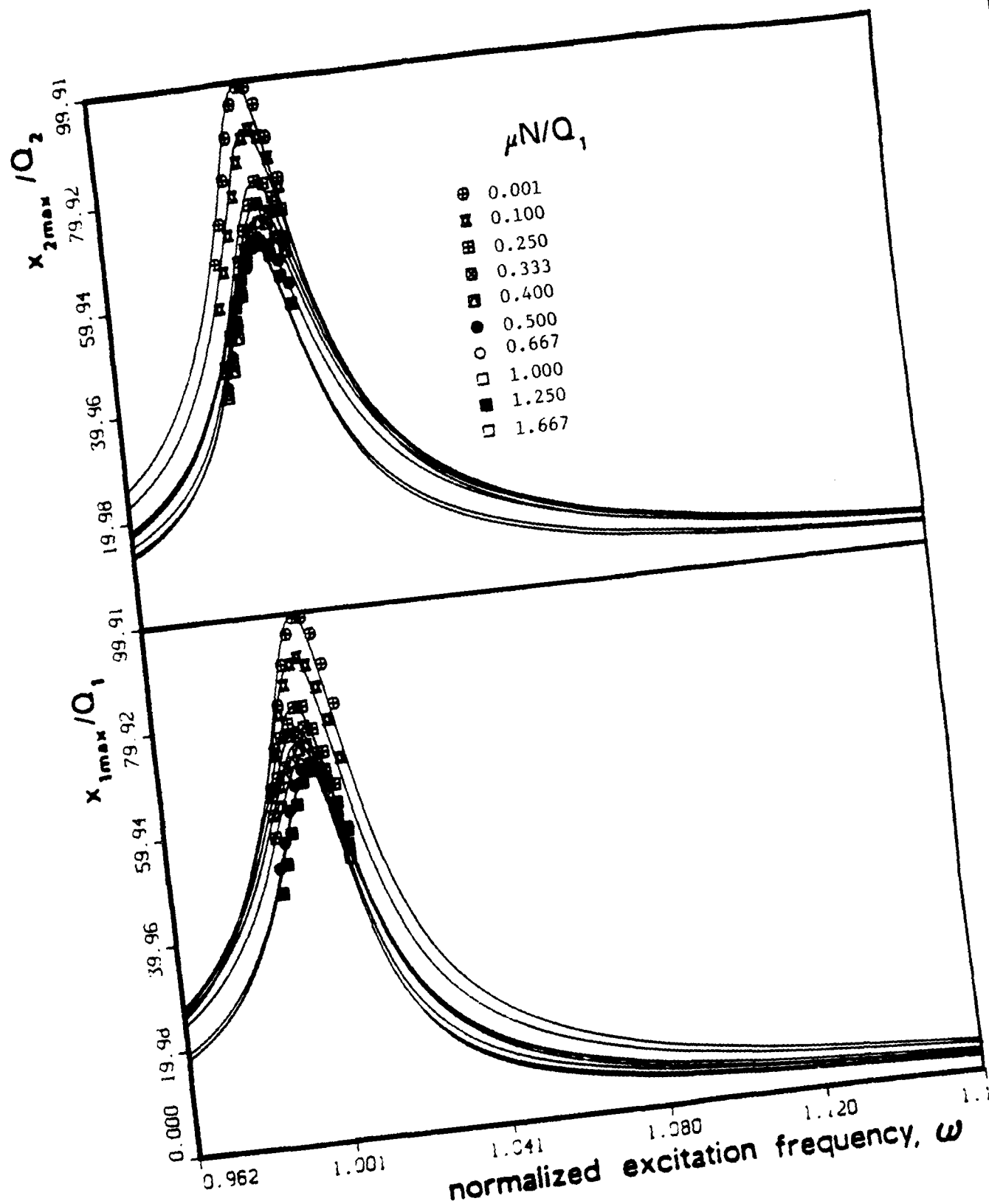


Fig. 29: Comparison of Exact and Approximate Results. Case VIII of Table 1.

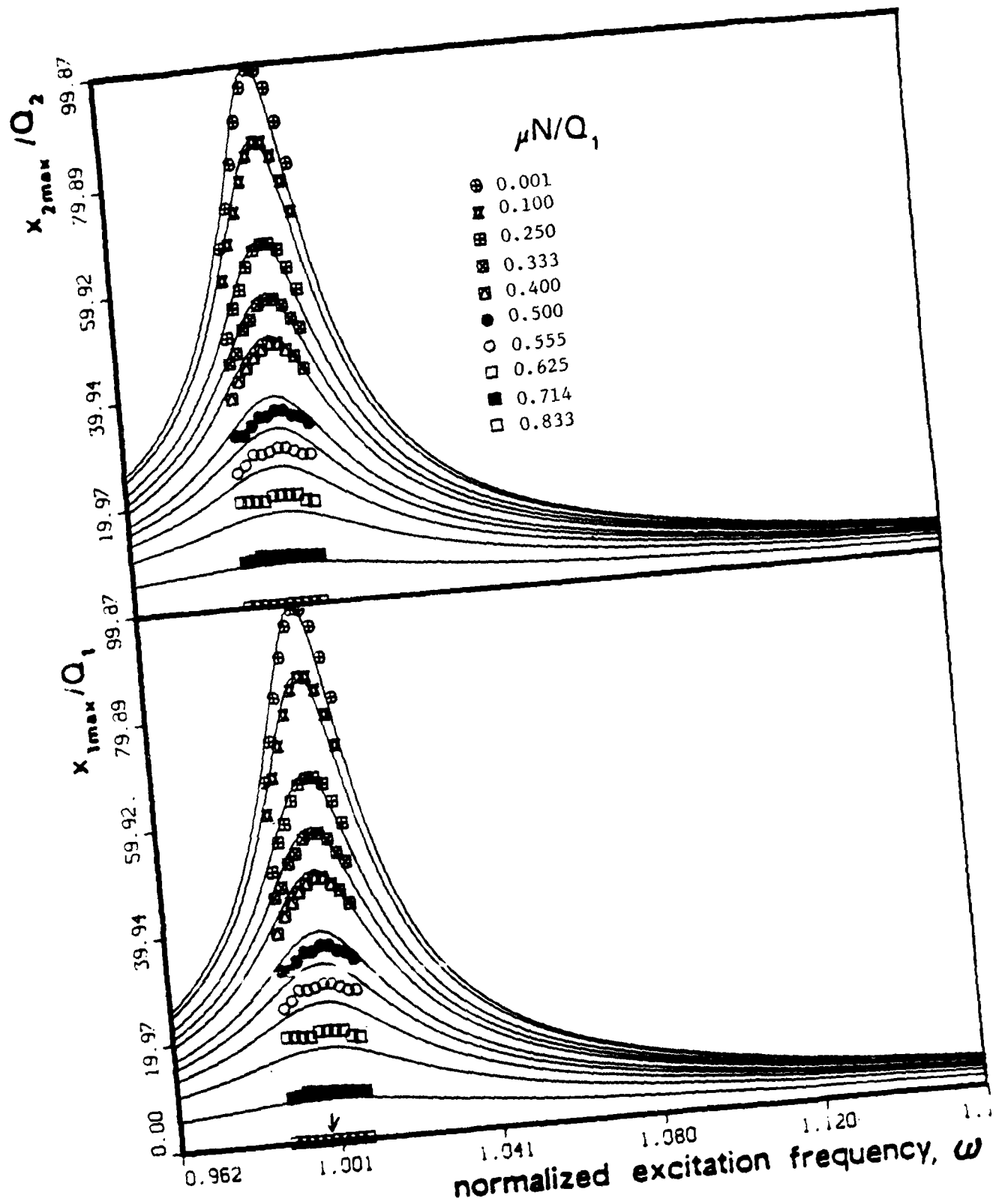


Fig. 30: Comparison of Exact and Approximate Results. Case IX of Table 1.

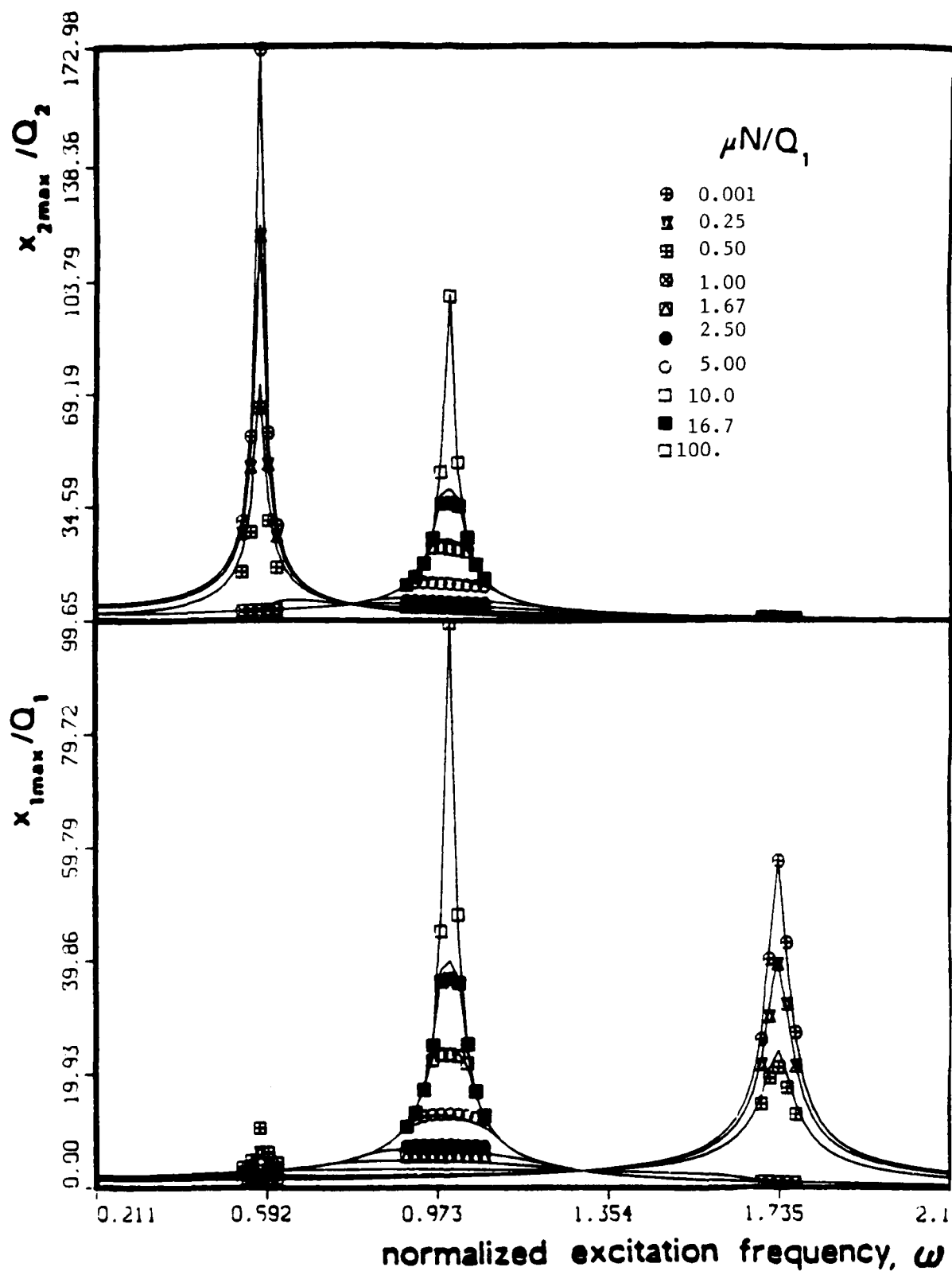


Fig. 31: Comparison of Exact and Approximate Results. Case X of Table 1.

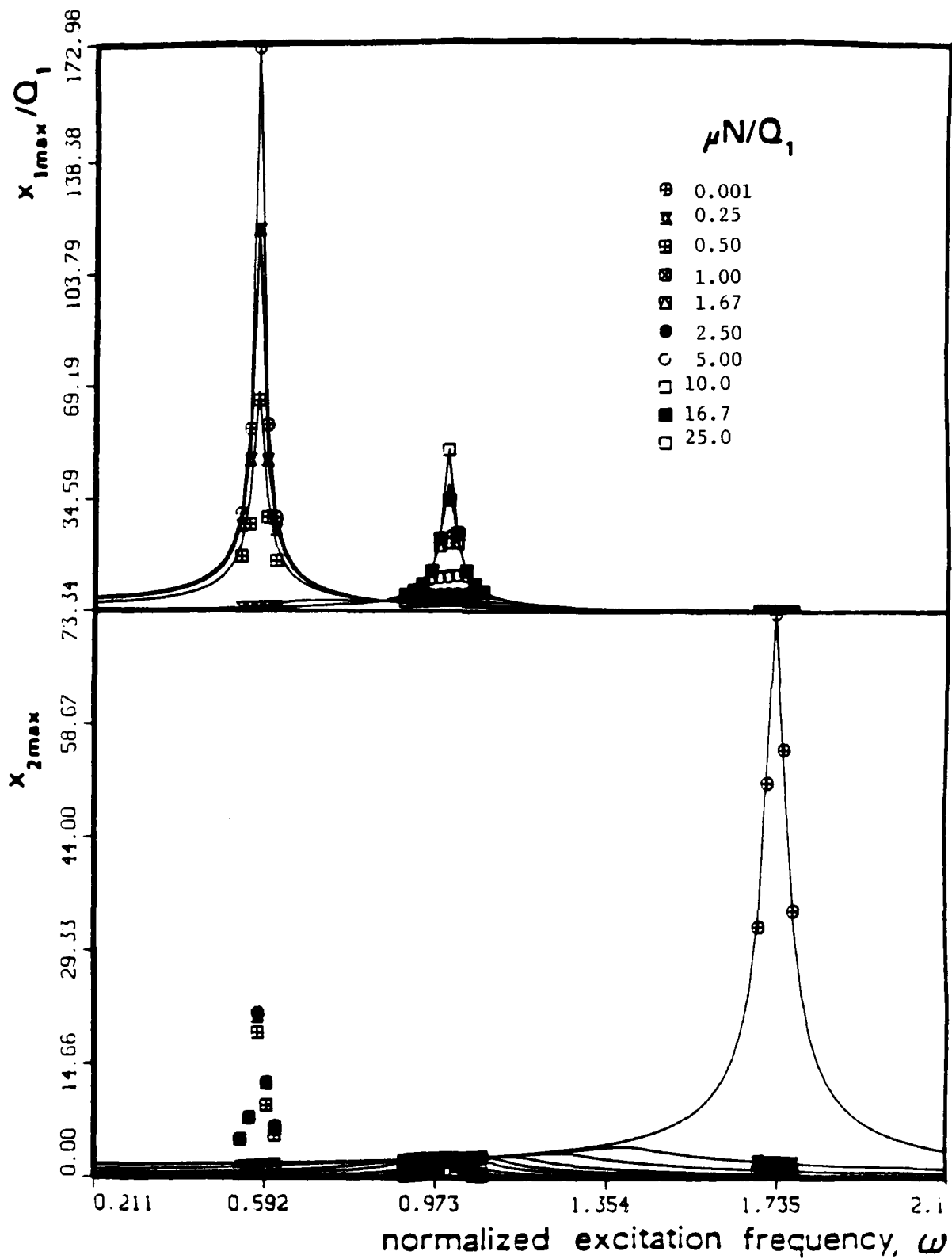


Fig. 32: Comparison of Exact and Approximate Results. Case XI of Table 1.

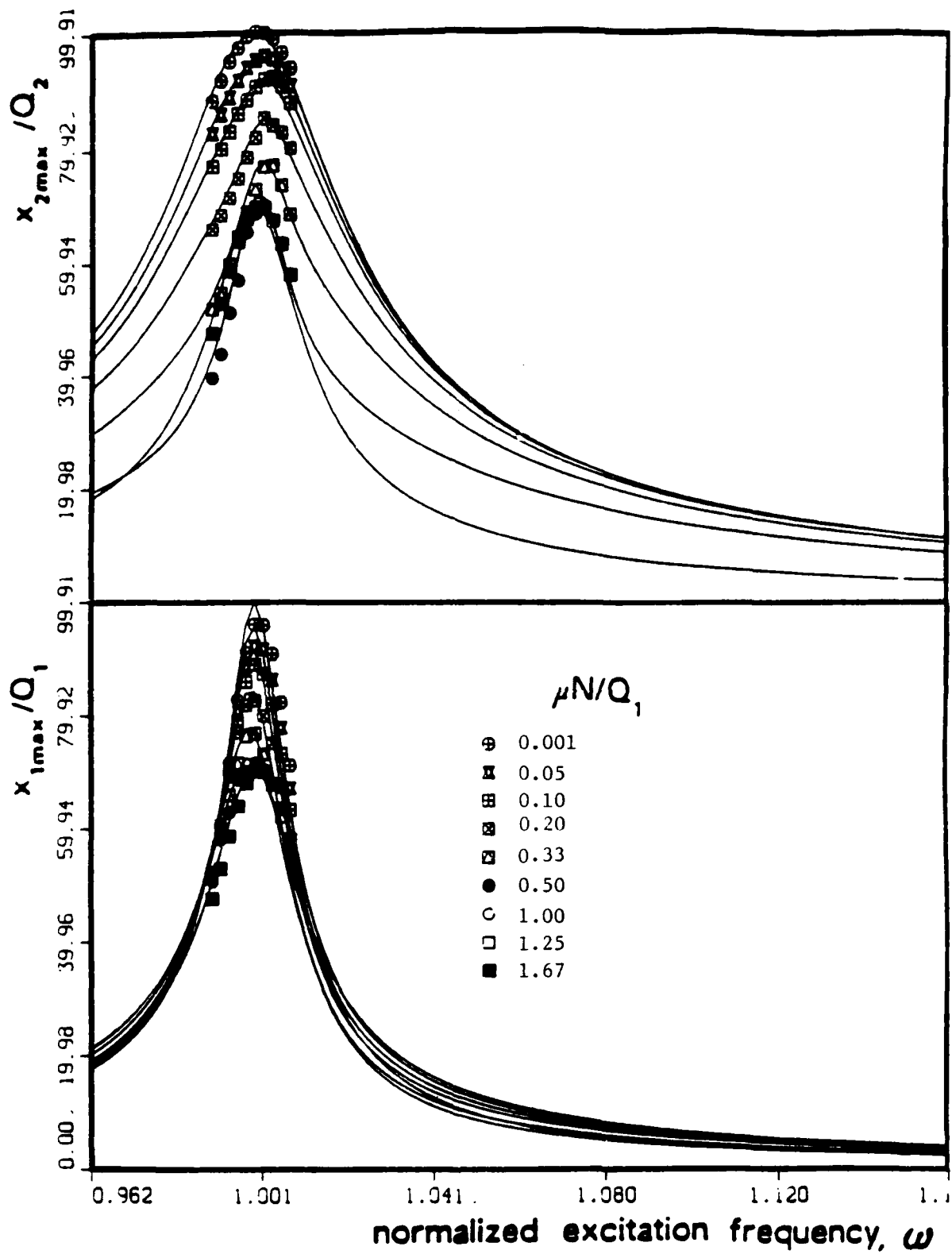


Fig. 33: Comparison of Exact and Approximate Results. Case XII of Table 1.

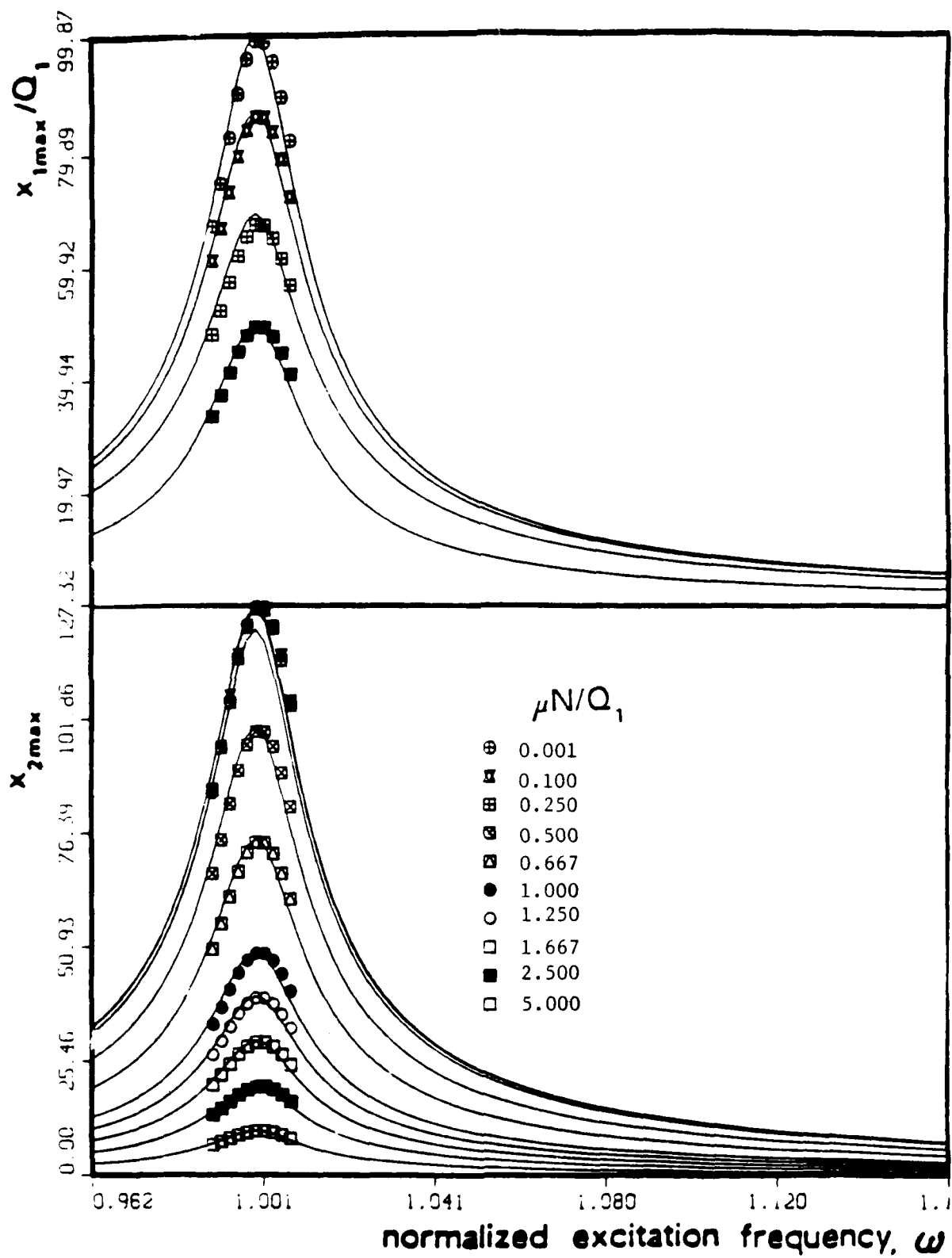


Fig. 34: Comparison of Exact and Approximate Results. Case XIII of Table 1.

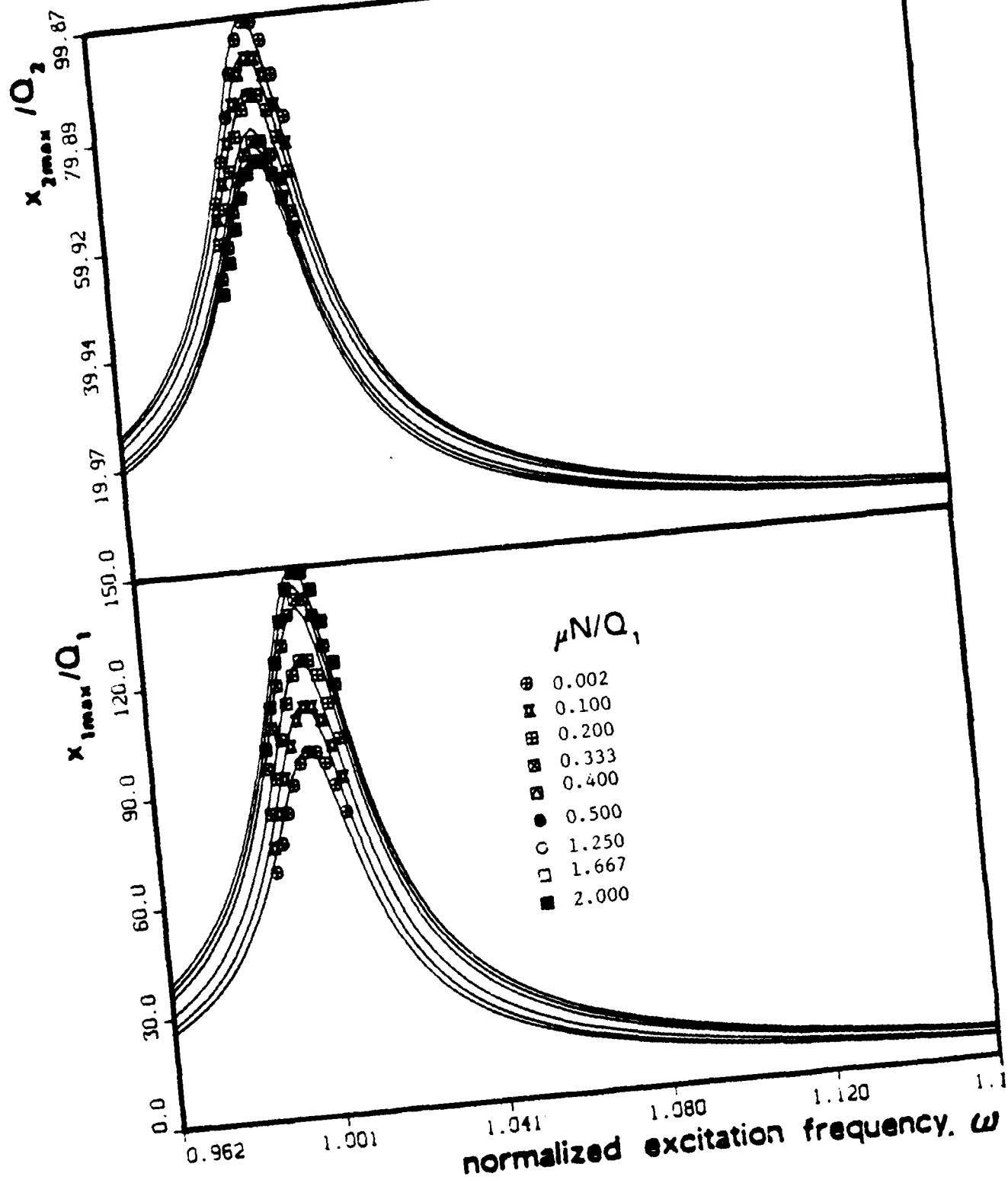


Fig. 35: Comparison of Exact and Approximate Results. Case XIV of Table 1.

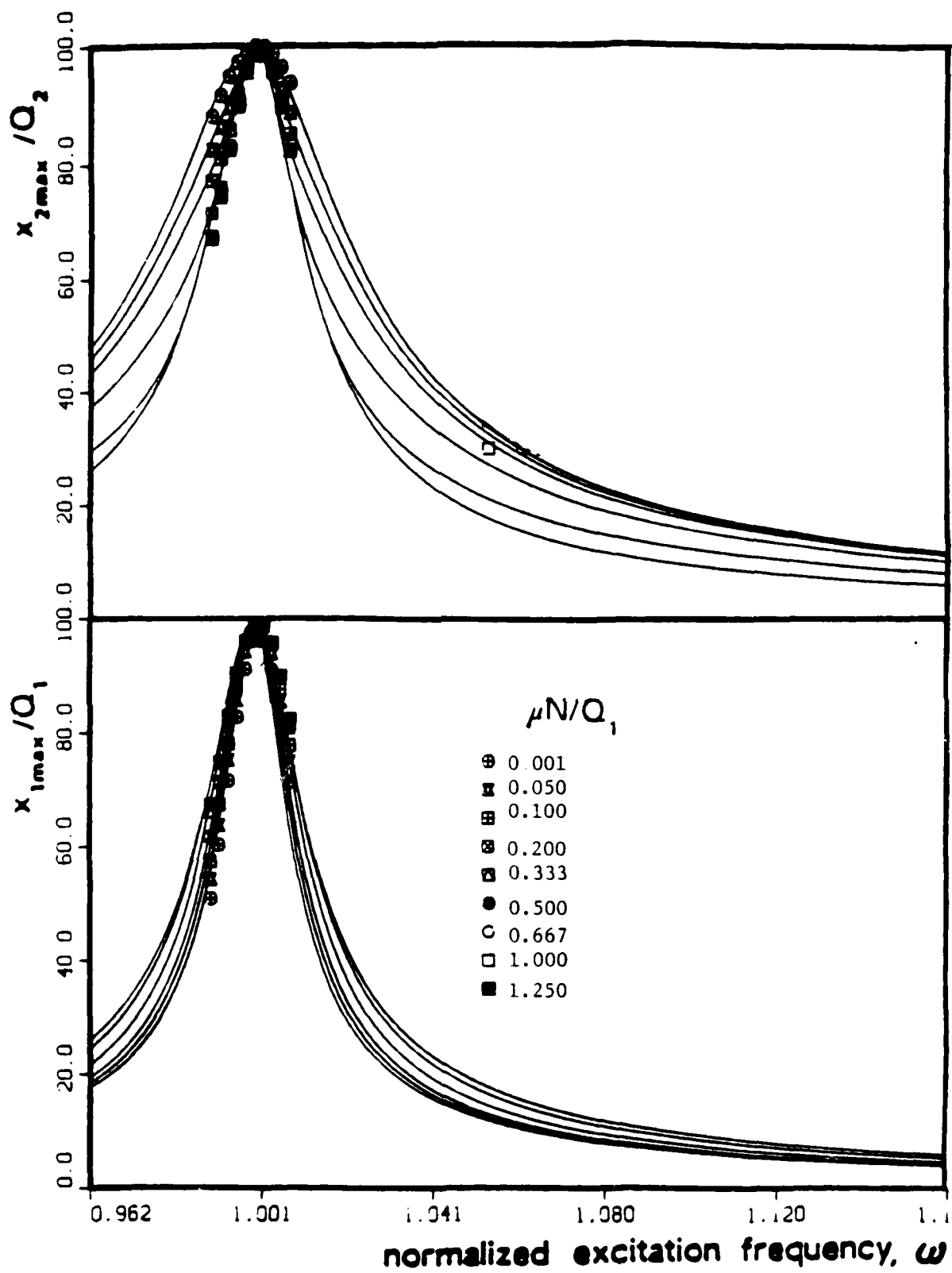


Fig. 36: Comparison of Exact and Approximate Results. Case XV of Table 1.

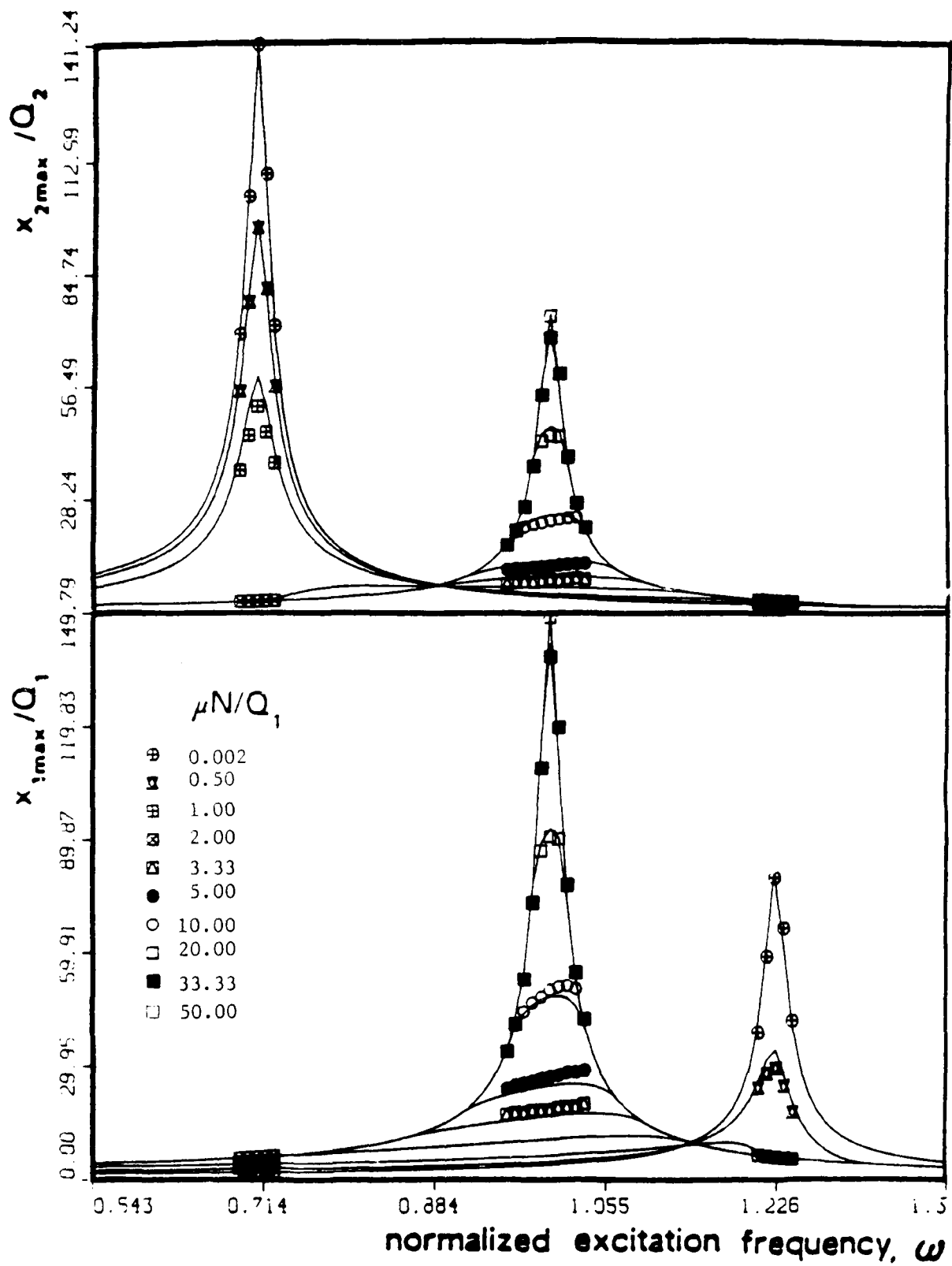


Fig. 37: Comparison of Exact and Approximate Results. Case XVI of Table 1.

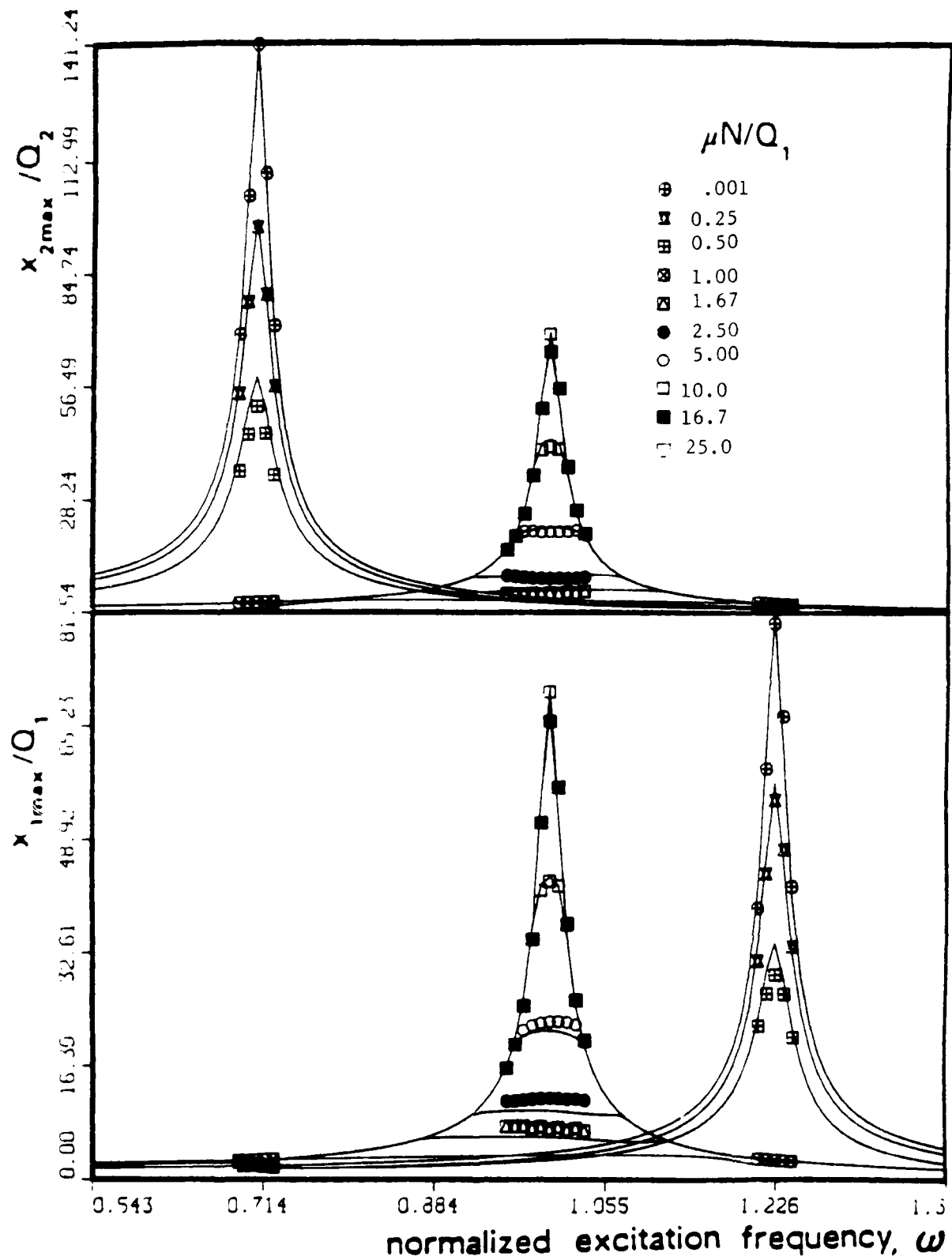


Fig. 38: Comparison of Exact and Approximate Results. Case XVII of Table 1.

APPENDIX A

a) Functions defining the solution of equations (5) and (6)

The following functions are used in expressions (9) and (10)

$$f_1(t) = \exp(-\zeta_1 \Omega_1 t) \sin \Omega_1' t \quad A.1$$

$$f_2(t) = \exp(-\zeta_1 \Omega_1 t) \cos \Omega_1' t \quad A.2$$

$$f_3(t) = \exp(-\zeta_2 \Omega_2 t) \sin \Omega_2' t \quad A.3$$

$$f_4(t) = \exp(-\zeta_2 \Omega_2 t) \cos \Omega_2' t \quad A.4$$

$$\text{where } \Omega_j' = \sqrt{1 - \zeta_j^2} \Omega_j, \quad j=1,2$$

and

$$g_j(t, \phi) = [B_j \sin(\omega t + \psi_j) + D_j \cos(\omega t + \psi_j)] \quad A.5$$

$$\text{where } B_j \equiv (2\zeta_j \omega / \Omega_j) \lambda_j$$

$$D_j \equiv (1 - \omega^2 / \Omega_j^2) \lambda_j, \quad j=1,2$$

$$\lambda_1 = 1 / [(1 - k) \sqrt{B_1^2 + D_1^2}]$$

$$\lambda_2 = a / [k \sqrt{B_2^2 + D_2^2}]$$

$$\psi_1 = \phi$$

$$\psi_2 = \phi + \beta$$

b) Algebraic transformation of the second member of equation (13)

From A5 we can write

$$\dot{g}_j(0, \phi) = [B_j \cos \psi_j - D_j \sin \psi_j] \omega \quad A.6$$

Considering that

$$\sin(\phi + \beta) = \cos \beta \sin \phi + \sin \beta \cos \phi$$

$$\cos(\phi + \beta) = -\sin \beta \sin \phi + \cos \beta \cos \phi$$

Substitution of ψ_1 and ψ_2 into 1.6 yields

$$\dot{g}_1(0, \phi) = [B_1 \cos \phi - D_1 \sin \phi] \omega$$

$$\dot{g}_2(0, \phi) = [(B_2 \cos \beta - D_2 \sin \beta) \cos \phi - (B_2 \sin \beta + D_2 \cos \beta) \sin \phi] \omega$$

Define

$$q_1 = [B_1 - (B_2 \cos \beta - D_2 \sin \beta)] \omega \quad A.7$$

$$p_1 = [-D_1 + (B_2 \sin \beta + D_2 \cos \beta)] \omega \quad A.8$$

From 1.1 to 1.4 we can also define

$$b_{11} = \dot{f}_1(0) = \Omega_1' \quad A.9$$

$$b_{12} = \dot{f}_2(0) = -\zeta_1 \Omega_1 \quad A.10$$

$$b_{13} = \dot{f}_3(0) = \Omega_2' \quad A.11$$

$$b_{14} = \dot{f}_4(0) = -\zeta_2 \Omega_2 \quad A.12$$

Expression (14) follows from substitution of A.7 to A.12 into expression (13).

c) Functions defining the solution of equation (8)

The following functions appear in expression (17)

$$f_5(t) = \exp(-\zeta t) \sin(\sqrt{1-\zeta^2} t)$$

$$f_6(t) = \exp(-\zeta t) \cos(\sqrt{1-\zeta^2} t)$$

$$g_3(t, \phi) = 2\zeta \omega [\sin(\omega t + \phi) + \sin(\omega t + \phi + \pi)]/L + (1 - \omega^2) [\cos(\omega t + \phi) + \cos(\omega t + \phi + \pi)]/L$$

where

$$\zeta = \zeta_1 \sqrt{(1-k)(1-m)} + \zeta_2 \sqrt{km}$$

$$L = (1 - \omega^2)^2 + (2\zeta\omega)^2$$

APPENDIX B. Derivation of equations (22) to (24)

Equation (22) is obtained by subtracting (20) from (19). From (21), E_2 can be expressed as

$$E_2 = [A_1 \dot{f}_1(t_1) + A_2 \dot{f}_2(t_1) + \dot{g}_1(t_1, \phi) - \dot{g}_3(t_1, \phi) - E_1 \dot{f}_5(t_1)] / \dot{f}_6(t_1) \quad B.1$$

Substituting this result and equation (22) into (19) and solving for E_1 , we obtain

$$E_1 = A_1 f_7(t_1) + A_2 f_8(t_1) + A_3 f_9(t_1) + A_4 f_{10}(t_1) + g_4(t_1, \phi) + c_1 f_0 \quad B.2$$

where the following definitions have been adopted

$$f_7(t_1) = (1-k)f_1(t_1) - \dot{f}_1(t_1)f_6(t_1)/\dot{f}_6(t_1)$$

$$f_8(t_1) = (1-k)f_2(t_1) - \dot{f}_2(t_1)f_6(t_1)/\dot{f}_6(t_1)$$

$$f_9(t_1) = kf_3(t_1)$$

$$f_{10}(t_1) = kf_4(t_1)$$

$$g_4(t_1, \phi) = (1-k)g_1(t_1, \phi) - \dot{g}_1(t_1, \phi)f_6(t_1)/\dot{f}_6(t_1) - g_3(t_1, \phi) + \dot{g}_3(t_1, \phi)f_6(t_1)/\dot{f}_6(t_1) + kg_2(t_1, \phi)$$

$$c_1 = (1-k)/(1-m) + k/m$$

Backsubstitution of E_1 into E_2 yields equation (24) with the following definitions

$$f_{11}(t_1) = [\dot{f}_1(t_1) - f_7(t_1)\dot{f}_5(t_1)] / \dot{f}_6(t_1)$$

$$f_{12}(t_1) = [\dot{f}_2(t_1) - f_8(t_1)\dot{f}_5(t_1)] / \dot{f}_6(t_1)$$

$$f_{13}(t_1) = -f_9(t_1)\dot{f}_5(t_1) / \dot{f}_6(t_1)$$

$$f_{14}(t_1) = -f_{10}(t_1)\dot{f}_5(t_1) / \dot{f}_6(t_1)$$

$$g_5(t_1, \phi) = [\dot{g}_1(t_1, \phi) - \dot{g}_3(t_1, \phi) - g_4(t_1, \phi)\dot{f}_5(t)]/\dot{f}_6(t_1)$$

$$c_2(t_1) = -\dot{f}_5(t_1)c_1/\dot{f}_6(t_1)$$

Note that $g_4(t_1, \phi)$ and $g_5(t_1, \phi)$ are eventually linear combinations of the harmonic functions $g_j(t, \phi)$ ($j = 1, 2, 3$) defined in Appendix A. Consequently they can be expressed in the form $p(t_1)\sin\phi + q(t_1)\cos\phi$ that is used in equation (29).